UNCLASSIFIED

AD 286 075

Reproduced
by the

ARMED SERVICES TECHNICAL INFORMATION AGENCY
ARLINGTON HALL STATION
ARLINGTON 12, VIRGINIA

UNCLASSIFIED

STUDY OF THE PROPAGATION
AND DISSIPATION OF "ELASTIC"
WAVE ENERGY IN GRANULAR SOILS

F. E. Richart, Jr.
J. R. Hall, Jr.
J. Lysmer

STUDY OF THE PROPAGATION AND

DISSIPATION OF "ELASTIC" WAVE ENERGY

IN GRANULAR SOILS

F. E. Richart, Jr
J. R. Hall, Jr.
J. Lysmer

September, 1962

Department of Civil Engineering
Engineering and Industrial Experiment Station
University of Florida

for

ABSTRACT

Laboratory tests were conducted on selected granular materials to determine the velocities of propagation of the shear and compression waves and to evaluate the internal damping. Test variables included the confining pressure, amplitude of vibration, void ratio of the material, saturation, and grain size. Resonant column tests were used for wave velocity evaluation, and the vibration decay method and static torsion tests were used to determine damping. The granular materials used were Ottawa standard sand, two sizes of glass spheres, and a crushed quartz.

Confining pressure had the most significant effect on velocities of wave propagation, with velocities increasing about with the 1/4 po r of the confining pressure. The effect of more than 200 times increase in amplitude caused a reduction of wave velocity of only 10 to 15 per cent. The same order of reduction of wave velocity resulted from an increase of void ratio from the minimum to maximum value.

Damping determined from the decay of steady state vibrations behaved like viscous damping. The values of logarithmic decrement varied from about 0.02 to 0.20 for these materials and test conditions. Higher values of logarithmic decrement were found in the static torsion tests because stresses up to 75 per cent of the failure conditions were used.

A brief review of the literature is included and a method is indicated for evaluating the relative importance of damping through dissipation of energy by elastic waves and damping due to internal friction within the material.

TABLE OF CONTENTS

TABLE OF CONTENTS (Continued)

TABLE OF CONTENTS (Continued)

DISTRIBUTION LIST

Addresses	No. of Copies
Bureau of Mines, Washington, D. C., ATTN: J. E. Crawford	1
Chief, Bureau of Yards and Docks, ND, Washington 25, D. C., ATTN: D-440	1
Chief, Defense Atomic Support Agency, Washington 25, D. C., ATTN: Document Library	12
Chief of Engineers, Department of the Army, Washington 25, D. C., ATTN: ENGRD-S	3
ATTN: ENGMC-EB	2
Chief of Naval Operations, ND, Washington, D. C., ATTN: Op-75	1
Chief of Research and Development, DA, Washington 25, D. C., ATTN: Atomic Division	1
Commander, Air Force Ballistic Missile Division, Air Research and Development Command, ATTN: WDFN, P. O. Box 262, Inglewood 49, California	1
Commander, Armed Services Technical Information Agency (ASTIA), Arlington Hall Station, Arlington 12, Virginia	20
Commander, Air Force Special Weapons Center, Kirtland Air Force Base, Albuquerque, N. M., ATTN: SWRS	4
Commander, Wright Air Development Center, Wright-Patterson Air Force Base, Ohio, ATTN: WCOSI	1
Commanding Officer and Director, U. S. Naval Civil Engineering Laboratory, Port Hueneme, California	2
Director, Weapons Systems Evaluation Group OSD, Room 1E880, The Pentagon, Washington 25, D. C.	1
Director, U. S. Army Engineer Waterways Experiment Station, P. O. Box 631, Vicksburg, Mississippi	25
Director of Civil Engineering, Headquarters, U. S. Air Force, Washington 25, D. C., ATTN: AFOCE	1
Director of Defense Research and Engineering, Washington 25, D. C., ATTN: Technical Library	1

Addresses	No. of Copies
Headquarters, U. S. Air Force, Washington 25, D. C., ATTN: AFTAC, C. F. Romney	2
Space Technology Laboratory, Inglewood, California, ATTN: B. Sussholz	1
U. S. Coast and Geodetic Survey, Washington, D. C., ATTN: D. S. Gardner	1
U. S. Coast and Geodetic Survey, San Francisco, California, ATTN: W. K. Cloud	1
U. S. Geological Survey, Washington, D. C., ATTN: J. R. Balsley	1
California Institute of Technology, Pasadena, California, ATTN: F. Press	1
ATTN: R. Benioff	1
Columbia University, New York, N. Y., ATTN: J. E. Oliver	1
Pennsylvania State College, Atomic Defense Engineering Dept., State College, Pa., ATTN: Professor Albright	1
Stanford Research Institute, Physical Sciences Division, Menlo Park, California, ATTN: Dr. R. B. Vaile, Jr.	2
American Machine and Foundry, 7501 North Natchez Avenue, Niles 48, Illinois, ATTN: Mr. Tom Morrison	1
Barry Wright Corporation, 700 Pleasant Street, Watertown 72, Mass., ATTN: Mr. Cavanaugh	1
Holmes and Narver, Los Angeles, California, ATTN: S. B. Smith	1
Dr. Harold Brode, RAND Corporation, 1700 Main Street, Santa Monica, California	1
Dr. N. M. Newmark, Civil Engineering Hall, University of Illinois, Urbana, Illinois	1
Dr. T. H. Schiffman, Armour Research Foundation, Illinois Institute of Technology, Technology Center, Chicago 16, Illinois	1
Professor H. O. Ireland, Dept. of Civil Engineering, Talbot Laboratory, University of Illinois, Urbana, Illinois	1
Professor Robert L. Kondner, The Technological Institute, Northwestern University, Evanston, Illinois	1

Addresses	No. of Copies
Professor Gerald A. Leonards, School of Civil Engineers, Purdue University, Lafayette, Indiana	1
Professor H. Bolton Seed, Dept. of Civil Engineering, University of California, Berkeley, California	1
Professor H. Neils Thompson, Civil Engineering Dept., University of Texas, Austin 12, Texas	1
Professor R. V. Whitman, Room 1-343 Massachusetts Institute of Technology, Cambridge 39, Massachusetts	1
Dr. Grover L. Rogers, Recon, Incorporated, Box 3622 MSS, Tallahassee, Florida	1
Mr. Kenneth Kaplan, Broadview Research Corporation, 1811 Trousdale Drive, Burlingame, California	1
Mr. W. R. Perret, 5112, Sandia Corporation, Sandia Base, Albuquerque, N. M.	1
Mr. Fred Sauer, Physics Department, Stanford Research Institute Menlo Park, California	1
Mr. A. A. Thompson, Terminal Ballistics Laboratory Aberdeen Proving Ground, Aberdeen, Maryland	1

TOTAL · 106

INTRODUCTION

The object of this investigation was to evaluate the influence of important variables on the "elastic" wave propagation and damping in sands Thus, it is a study of material properties alone. The results of this type of tests provide information of the variations to be introduced into theories of soil-structure interaction to account for the behavior of real sands. Thus, the test data represent fundamental information which may be applied to many types of design considerations.

The methods for evaluating internal damping in the material require calculations based on theory. The general theories available are described in Section I under Review of Previous Work and the details of the particular theories and definitions to be utilized in connection with the test program are given in Section II.

The terms used for damping are applied to specify behavior of the sand material alone. Because the dynamic behavior of a soil-structure system is sometimes defined by fitting it into the one-degree-of-freedom system with viscous damping, there have been numerous attempts to determine a damping constant for the whole system. The damping constant thus determined includes both the internal damping in the sands as well as a dissipation of energy by propagation of elastic waves developed by the structure moving against the soil. Both forms of damping are developed whether a single impulsive load is applied or whether repeated loads occur. In order to evaluate the dissipation damping which is principally a function of geometry, the theory of an oscillator resting on an elastic semi-infinite

body is reviewed briefly. From this example and the test data on internal damping, an estimate can be made of the significance of each. It is important to maintain the distinction between damping which occurs as energy losses within the soil, and dissipation of energy through geometrical distribution of wave energy propagation.

In order to evaluate the variables which influence the "elastic" wave propagation and damping in sands, tests were made using a procedure based on steady state vibrations. A column of sand encased in a rubber membrane was placed in a triaxial cell and excited into either longitudinal or torsional oscillations. Measurements of the amplitude of vibration resulting from changes of frequency and input force permitted an evaluation of the wave propagation and internal damping in the specimen under the particular test conditions. The effects of amplitude of resonant oscillation, confining pressure, saturation, and grain characteristics were studied.

The resonant column method was chosen in preference to the single pulse method for this study in order to obtain both the longitudinal and shear wave propagation velocities in the soil structure under controlled amplitude conditions. In a saturated soil, longitudinal waves are propagated both in the fluid and in the soil structure and some of the test data previously reported in the literature have indicated that difficulties arise in separating the two effects when only transmitted pulses were used In the resonant column method control and evaluation of the amplitude of oscillation for both longitudinal and torsional modes of oscillation is relatively easy.

The studies of damping were carried out using the resonant column apparatus by measuring the decay of amplitude of oscillation after the driving

power was turned off. Values of the damping quantities were measured for the same series of variables used for the wave propagation studies. A separate series of torsion tests using repeated static loads on a specimen of dense Ottawa sand was conducted for the purpose of evaluating the effects of pre strain and stress history on damping.

The amplitudes of motion considered in the resonant vibration tests varied from about 1×10^{-5} in. to 1×10^{-3} in. double amplitude in longitudinal oscillation and from about 1×10^{-5} to 2.5×10^{-3} rad. double amplitude in torsional oscillation. For the lower confining pressures, the average stresses developed by these motions amounted to about 20 per cent of the ultimate shear stress. The amplitudes were restricted to this magnitude to ensure that the grain structure was not altered significantly during the course of the test and that the wave propagation and damping values corresponded to the "elastic" range. However, in the repeated static torsion tests the maximum stress in a few tests reached 75 per cent of the ultimate stress. In the test program proposed for the continuing work it is planned to use amplitudes which definitely cause a breakdown of the grain structure and compaction of the sample during vibratory or impact loads.

I. REVIEW OF PREVIOUS WORK ON
WAVE PROPAGATION AND DAMPING IN SOILS

A. THEORIES OF ELASTIC WAVE PROPAGATION

Elastic waves in ideal elastic solids

In an infinite, elastic isotropic, homogeneous body a disturbance
may be propagated by waves of volume change, designated as the compression
wave, push wave, or P-wave, and by waves of distortion at constant volume
designated as the shear wave, transverse wave, or S-wave. The compression
and shear waves also transmit disturbances throughout the interior of a
semi-infinite elastic, isotropic, homogeneous body, but because of the free
surface a third type of wave appears (Rayleigh, 1885). This surface wave
has been designated as the Rayleigh wave or R-wave. A comprehensive study
of the development and propagation of the surface Rayleigh wave caused by
an impulse applied at the surface or at a point below the surface of an
elastic, isotropic, homogeneous body was given by Lamb (1904). This classic
paper by Lamb is the starting point for many theories which have been
developed during the past half century for treating impulsive loadings
acting on various segments of the surface of the semi-infinite body. The
relationship between the velocities of the P-wave, S-wave, and R-wave has
been given by Knopoff (1952) as a function of the Poisson's ratio, μ ,
of the elastic material. The velocity of the S-wave is given by

$$\mathcal{N}_s = \sqrt{\frac{G g}{\gamma}} = \sqrt{\frac{G}{\rho}}$$

in which G is the shear modulus of elasticity, γ is the unit weight, and ρ is the mass density of the elastic material. Table I gives the ratio of the velocities of the P-wave and R-wave as a function of ν_s and μ.

TABLE I

Poisson's Ratio μ	$\dfrac{\nu_R}{\nu_s}$	$\dfrac{\nu_P}{\nu_s}$
0	0.875	1.418
0.1	0.893	1.493
0.2	0.911	1.626
0.3	0.927	1.869
0.4	0.942	2.439
0.5	0.955	∞

Additional waves appear in non-isotropic or layered materials and these are described by Leet (1950), and treated extensively in the book by Ewing, Jardetzky, and Press (1957). The mathematical theories which treat the reflection, refraction, and propagation of waves into and through elastic solids have been highly developed by mathematicians and seismologists, and are now being applied to the study of blast effects within a semi-infinite elastic body. (See, for example, Miles (1960), Serbin (1960), and Baron and Matthews (1961).)

Dissipation of wave energy in elastic solids

Theoretical treatments of elastic wave energy dissipation in elastic bodies have also developed from Lamb (1904). Miller and Pursey (1955) determined analytically the distribution of energy between the compression, shear and Rayleigh waves caused by a single, or a group of single loads, acting on the surface of a semi-infinite solid. When the solid has a Poisson's ratio of 0.25, they found for the case of a single source of vertical

loading on the free surface that 67 per cent of the energy was dissi-
pated as a Rayleigh (surface) wave, 26 per cent as the shear wave,
and 7 per cent as a compression wave. Reissner (1937) showed that
when purely torsional oscillations were applied at the surface of a
semi-infinite, homogeneous, isotropic. elastic body, no surface waves
(Rayleigh waves) were developed, but that all the wave energy was
directed downward into the body. Sato (1951) determined theoretically
the combination of vertical and horizontal pulsating forces acting
along the perimeter of a circle at the surface of a semi-infinite
elastic body to produce a system of waves giving no Rayleigh waves.
This treatment is of academic interest only, while Reissner's results
may have practical significance.

The dispersion of energy by the propagation of elastic waves out-
ward from the source establishes a quantity which may be termed a geo-
metrical or dispersion type of damping. This occurs in structure-
elastic body systems in which there is no loss of energy through internal
damping within the elastic material. The concept of energy losses
through radiation by elastic waves applies equally well to the cases of
impulsive or repeated loadings on footings supported by an elastic body,
or for the supporting portion of buried structures.

In order to illustrate the characteristics of this geometrical
type of damping, the theory for oscillators resting on the surface of
an elastic semi-infinite body is described in Section II-D. This treat-
ment is based on the theories developed by Reissner (1936) and Sung (1953)
and includes recent elaborations prepared by Hsieh (1962).

Elastic waves in porous elastic solids

A closer approximation to the treatment of elastic waves in soils has been made by investigators who consider the behavior of a porous elastic solid in which the pores were filled with a viscous fluid, either air or water. Morse (1952) considered a medium consisting of solid granular materials and fluid which filled the voids. Then he assumed the grains to be motionless and incompressible, thereby restricting his analysis to the wave propagated in the fluid, and evaluated the dissipation of the wave energy by viscous flow through the pores. Sato (1952) treated a sphere of material which contained a spherical hole full of fluid. Then he replaced this system by a sphere of different radius (but with the original compressibility) of homogeneous material and determined the elastic wave velocities from this adjusted structure. Thus he ignored the fluid motion. Kosten and Zwikker (1949), Paterson (1955), Brandt (1955), and Biot (1956) studied the elastic waves propagated in saturated porous materials. Expressions for the compression waves propagated in the fluid, and the compression and shear waves propagated in the solid structure as well as the coupling between the pore and frame waves were presented. Paterson included his test results obtained for longitudinal waves in saturated sand with various confining pressures, and Brandt demonstrated the correlation between his theoretical results and previously published data.

The theories of waves propagated in porous elastic solids represent the best approximation to granular solids when the rigidity of the structural framework of the soils is analyzed by considering it as an aggregate of elastic spheres. This was done first by Hara (1935). Gassman (1951) obtained a solution for the propagation of elastic waves in a fluid saturated and dry hexagonal packing of spheres. However, he treated only the cases

of no coupling and perfect coupling between spheres and he considered
only the normal contact forces between the spheres as given by the Hertz
theory. More recently, Duffy and Mindlin (1957) have derived the differential
stress-strain relations and have considered the wave propagation in a face-
centered cubic array of elastic spheres in contact. They considered both
the normal and tangential contact forces. The work of Kosten and Zwikker
with modifications by Paterson, and that of Brandt, Biot, and Duffy and
Mindlin were analyzed and evaluated for an example corresponding to Ottawa
standard sand by Hardin (1961).

For the problem of a fluid-saturated aggregate of spherical particles,
the theoretical treatment indicates that the disturbed fluid wave has a
velocity slightly higher than the velocity of sound in water. This is due
to the coupled motions of the frame and the fluid. Both the rigidity of
the frame and the smaller compressibility of the solid material cause this
increase in velocity. This disturbed fluid wave is nearly independent of
the pressure in the ranges normally considered in soil mechanics. Both of
the frame waves, the compression and shear waves, were found to vary with
the 1/6 power of the confining pressure, which is in accordance with the
theory of elastic spheres in contact.

B. TESTS OF ELASTIC WAVE PROPAGATION

Field data

The science of seismology includes methods for evaluating the
effective elastic constants of the materials which form the earth. The
major part of this work has been concerned with large volumes of materials
or distances measured in thousands of feet or miles. Hvorslev (1948) has
given a concise review of seismic methods and has compiled a diagram which

shows the variation of the compression wave velocity for soils and rocks.
Tables which give these variations in wave velocities for materials
grouped into rather loose categories have also been given by Murphy (1958),
Leet (1950), and numerous other authors. For the purpose of illustration
Table II reproduces the data given by Leet.

TABLE II

Material	Velocity (ft/sec)
Sand	650-6500
Loess	1000-2000
Artificial Fill	1000-2000
Alluvium	1600-6500
Loam	2600-5900
Clay	3300-9200
Marl	5900-12,500
Salt	15,000
Sandstone	4600-14,100
Limestone	5600-21,000
Slate and Shale	7500-15,400
Granite	13,000-18,700

The values of velocity given in Table II represent the range of observed
values for the materials which fall under the general categories noted.
As a result, these values have use only as a very crude first approxi-
mation to the compression wave velocity in a particular volume of soil.

        In order to determine the velocities of propagation of "elastic"
waves in soils within localized zones, Ramspeck and Muller (1936) (DEGEBO)
made extensive field tests on different soils by using a rotating mass type
oscillator to excite steady state waves in the soil. Their test results
have been reproduced repeatedly in papers written by other authors since
that time, often without a satisfactory reference given to the source of
the information. Table III is a reproduction, once more, of the summary

table from Ramspeck and Muller (with the compression wave velocity con-
verted to ft/sec).

TABLE III

Material	Compression Wave Velocity (ft/sec)	Resonant Frequency of the DEGEBO OSCILLATOR cps	Allowable Bearing Capacity of the Soil (kg/cm^2)
3 m thick swamp over sand	260	4	0
Flour sand	360	19.3	1
Tertiary clay-damp	430	21.8	-
Loamy fine sand	460	20.7	-
Damp medium sand	460	21.8	2
Jura clay, damp	490	-	-
Old piled sand-slag	530	-	-
Medium sand and water	530	-	2
Dry medium sand	530	22	2
Loamy sand over marl	560	22.6	2.5
Gravel with stones	590	23.5	2.5
Damp loam	620	23.6	-
Rocky marl	620	23.8	3
Fine sand + 30% med. sand	620	24.2	3
Dry sand + lime fragments	660	25.3	-
Med. sand-undisturbed	720	-	4
Marl	720	25.7	4
Gravel under 4 m sand	1080	-	4.5
Large gravel, com- pact	380	30	4.5
Mixed sandstone	1640	32	-
Medium hard red marl	2130	-	-
Mixed sandstone	3600	-	-

Because a single value of velocity was given for each type of material,
the information in Table III has often been used with considerably more
confidence than is justified.

Members of the Earthquake Research Institute in Japan have also
made many outstanding contributions to the study of elastic wave propagations in soils. For instance, Nasu (1949) used a steady state oscillator to determine the velocities of the compression and shear waves i
loam in Tokyo and from these measured velocities he computed the elastic
soil constants. The velocities were determined between the soil surface
and a depth of 10 meters. For this material he found that the computed
shear modulus of elasticity, G, and the Poisson's ratio varied from 670 psi
and 0.38 at the surface to 8900 psi and 0.43 at a depth of 10 meters, respectively. This is one of the many illustrations from field measurements
that even for cohesive materials the wave velocities and elastic constants
vary markedly with depth, or overburden pressure.

The use of pulse techniques or steady state vibrations for purposes
of evaluating the properties of soil in a particular locality has been
termed "Microseismics" by Bernhard (1957) to designate the propagation and
evaluation of elastic waves in soils within a distance of a few hundred
feet. He has described numerous evaluations of soil properties determined
from the elastic waves generated by his specially designed mechanical oscillator. The use of steady state vibrations for field evaluations of subbase conditions of highways and airports has become fairly common during the
past decade. [Van der Poel (1948, 1953), Bergstrom and Linderholm (1946),
Jones (1958)] Papers presented at the Symposium on Vibration Testing of
Roads and Runways, Amsterdam (1959), and Heukelom and Foster (1960), for
example, all described the techniques and significance of the results which
have been obtained by this method. It appears that the vibration test
represents a non-destructive dynamic equivalent of the plate bearing test,
with the added advantage that by changing the frequency, different depths

soil can be brought into the range of the test.

Techniques for evaluating soil properties by analyzing the elastic waves generated by a single impulse have, of course, been used extensively in seismological prospecting. See, for example, Domzalski (1956). Usually, a small explosion is used to generate the impulse. Reflection and refraction techniques have also been used for localized zones, particularly in highway work, in which the impulse is generated by a hammer blow on the surface. The purpose of this type of survey is usually to locate the interfaces between different soil types or to determine the surface elevation of rock. Another variation of this concept of evaluating soil constants by a pulse technique involves pulsing between small transducers placed on or slightly into the soil. Hamilton, Shumway, Menard, and Shipek (1956) have used this technique to measure the sound velocities of sediments on the sea bottom. By this method, they have determined the velocity of the coupled fluid wave. The transducers were set into the sea bottom by divers.

At the present time, the use of steady state oscillators on the ground surface appears to be developing into a standard tool for a localized evaluation of the dynamic soil constants. The procedure described by Heukelom and Foster (1960) for determining the interfaces between layers in the soil appears to work, but the theoretical justification of the reason for plotting the measured velocity against a depth corresponding to one-half the wave length does not appear to be readily available. The method of pulsing between probes also has interesting possibilities, but for evaluation of the frame waves, some alternate procedure should be developed to produce and detect shear waves.

Laboratory data

Two methods are often used in the laboratory to measure the dynamic properties of materials. In the first method a cylindrical column of the material is set into resonance by a variable frequency exciter, and the wave velocities and elastic properties are computed from the dynamic response of the sample to changes in frequency. The equations for computing the elastic constants from the resonant column tests were given by Pickett (1945). Both longitudinal and torsional modes of oscillation are used. In the second method a pulse is sent through the sample and the time delay is measured. A review of the sonic methods for determining the mechanical properties of materials is given by Kessler and Chang (1957).

Birch and Bancroft (1938, 1938, 1940) made extensive use of the resonant column method for evaluating the elastic constants of rocks under variable temperatures and pressures up to 9000 kg/cm^2. They found an appreciable increase in shear wave velocity with pressure. In tests to evaluate the effects of frequency, they found an influence of less than 1 per cent on the wave velocities within a frequency range of 140-4500 cps. Peselnick and Outerbridge (1961) also found the effect of frequency to be unimportant. For a range from 4 to 10^7 cps the shear modulus of Solenhofen limestone varied less than 2 per cent.

Iida (1939) also determined the elastic constants of rock by the resonance method, then ran extensive tests on sands (Iida 1938, 1939, 1940). Primarily he determined the longitudinal wave velocities but he included some tests for the torsional wave velocities on dry and saturated sands. He used vertical cylinders of sand retained only by thin cellophane shells such that the only confining pressure of the material at any depth was produced by the overburden. In his tests to evaluate the effects of change of

water content, he found that by increasing the water content, the shear modulus was drastically reduced. as might be anticipated for sands under conditions of low confining pressures. He found that for a particular water content, the wave velocities increased approximately in proportion to the 1/6 power of the height of the specimen.

The results of the tests by Matsukawa and Hunter (1956), Duffy and Mindlin (1957), Shannon, Yammane, and Dietrich (1959), and Taylor and Whitman (1954) were summarized in Fig. 6 of the paper by Richart (1960). From this group of test results on granular materials, it is seen that the wave velocities increase at a rate between the 1/4 and 1/6 power of the confining pressure. Further test data by Hardin (1961) on Ottawa sand also shows this behavior. However, for materials designated as granular materials, Smoots, Stickel and Fischer (1961) report a much wider variation in the effect of confining pressure on the wave velocities. Wilson and Miller (1961) give results for materials ranging from "medium fine clean sand" to "clayey gravelly sand" and found the slopes of the compression wave velocity vs. confining pressure curves (plotted on the log-log scale) to be 1/6 or lower. Generally the clean materials followed the 1/6 slope and the materials having some clay content showed the flatter slope.

From the test results gathered together up to the present time, it appears that the elastic wave velocities (both compression and shear for clean granular materials) increase about in proportion to the 1/6 power of the confining pressure at relatively high pressures, and may drop off to about proportional to the 1/4 power at low or moderate pressures. This means that the elastic moduli vary with a power of the confining pressure between 0.33 and 0.50. Hardin (1961) showed the influence of change in void ratio for Ottawa standard sand, which brings out the possibility that some

of the steeper slopes may include the effects of void ratio changes.

For silts and clays the effect of confining pressure are not yet clearly defined. Some data on clays shown by Brandt (1955), and that given by Wilson and Dietrich (1961) illustrate extreme ranges of the effects of confining pressure on the compression wave velocity. A few pilot tests by Hardin (1961) help to point out some of the problems involved in testing fine-grained materials by the resonance method. Hardin used crushed quartz powder of which 100 per cent passed the No. 200 sieve and about 80 per cent passed the No. 400 sieve. The minimum and maximum void ratios obtained for this material were 0.76 and 3.05. As the pressure was increased to the next test pressure, consolidation of the material occurred and moved the dynamic response of the specimen into the regime of the new slightly lower void ratio. As a result of the consolidation which occurred the process of increasing the test pressures, the resultant test curve had a slope greater than 1/6. Upon reducing the pressure by increments, and measuring the dynamic properties at each of these steps, it was found that the effect of pressure was relatively insignificant because the shear wave velocity varied approximately as the 1/11 power of the pressure value.

The pulse method has been used for studying the effects of consolidation on elastic wave velocities and dynamic moduli. Laughton (1957) determined the variation of the compression wave with confining pressure, and Whitman, Roberts, and Mao (1960) have reviewed Laughton's work particularly with respect to the effects of degree of consolidation, as well as contributing new information obtained by the pulse method. The pulse method is particularly well suited for the problem of measuring the difference between the elastic wave velocities in the horizontal and vertical directions. Ward, Samuels, and Butler (1959) used the pulse technique on undisturbed blocks

of clay, apparently with no confining pressure, in order to determine the
elastic constants.

Thus, for fine-grained soils we have the problem of consolidation
during the increase of loading, and after unloading we have the effect of
prestress. Systematic and comprehensive investigations must be made to
evaluate the effects of soil composition and structure, water content, con-
fining pressure, prestress, and other variables on the dynamic properties
of silts and clay soils.

It should be noted that much of the significant work in the dynamic
properties of soils has been carried out within the past ten years, and
that an accelerated activity has occurred within the past three or four
years.

C. DAMPING OF ELASTIC WAVES IN SOILS

Many field investigations have been made of the effects of elastic
wave propagation and its effect on structures at some distance from the
source of vibrations. Crandell (1949) reduced the observations from
numerous tests of blasting and its effects on structures to equations and
design charts which may be used to prevent structural damage. Steffens
(1952) and the Building Research Station (1955) have determined the vibration
intensity which causes various degrees of structural damage, and Reiher
and Meister (1931) have determined the human sensitivity to vibrations.
These studies represent analyses of the effects of vibrations which may be
transmitted through soils. What is lacking is a good understanding of the
propagation and dissipation of this wave energy between the source and the
responding structure.

Elastic waves which are developed from a localized source decrease in amplitude with distance from the source. For the elastic, isotropic, homogeneous, semi-infinite body, Lamb (1904) found that both the horizontal and vertical components of the Rayleigh wave amplitude diminish according to the law of annular divergence (i.e. with $r^{-\frac{1}{2}}$). This reduction of wave amplitude is due to geometry alone, because the assumption of an ideal elastic body precludes energy losses because of internal damping within the medium.

In soils, it is desirable that the wave energy developed by blast loads, pile driving, reciprocating machinery, or construction operations be absorbed by the supporting soil and not transmitted to neighboring structures. Consequently, it is desirable to evaluate the factors that contribute to the damping capacity of different types of soils

Mintrop (1911) made the first comprehensive study of the energy transmitted through soils to nearby structures. He used a single impact developed by dropping a 4000 kg ball through a distance of 14 meters, and using a seismograph which had a magnification of 50,000 times, he obtained readings up to 2.5 km away. The soil was a stiff clay. He also used steady state vibrations which were generated by horizontal-cylinder type coal-gas engines which operated at 140-160 rpm and generated large unbalanced forces (up to 17,000 kg horizontally, 25,000 kg vertically). Readings were made 400 m away. Bornitz (1931) made similar observations in the neighborhood of a large bore, slow speed machine, and took measurements at different depths on the boundary of a convenient vertical mine shaft, down to a depth of 250 m. He described the amplitude of the propagated wave as

$$y_n = y_1 \sqrt{\frac{x_1}{x_n}} \; e^{-\alpha(x_n - x_1)}$$

where y_n is the amplitude at distance x_n, y_1 is the amplitude at a distance x_1, and α is defined as an absorbtion coefficient (in the more recent literature on acoustics, the quantity α corresponds to the coefficient of attenuation, which is a measure of the decay in intensity of an elastic wave with distance). In Eq. (1-2) it is seen that the wave amplitude varies both as a function of the annular divergence, as noted by Lamb (1904), and as a function of the absorbtion coefficient, α. Values of α were determined as 0.00001/m for the marshy soil of the Oder river flats, 0.001/m for a deposit of loamy, clayey soil, and 0.003/m for a layer of fine-grained, dense dry sand over a layer of heavy clay. These are only representative values, obtained for a particular amplitude of vibration at a particular frequency.

Experimental results of the damping in various solid and granular materials have shown that damping occurs even for very small strains. Often this damping effect, or the deviation from Hooke's law, is not of practical importance but it is of considerable interest to evaluate the quantities which influence its magnitude. The tests on steel spheres by Duffy and Mindlin (1957) found that the logarithmic decrement was independent of the amplitude of vibration within the range employed. The energy dissipated per cycle varied with the square of this amplitude instead of as the cube, as predicted by theory. Knopoff and MacDonald (1958) found that the specific dissipation function (which contains the coefficient of attenuation, α) was independent of the frequency over a range of 10^{-2} to 10^7 cps for solids other than ferromagnetic material. Data for Amherst sandstone shows that the logarithmic decrement was independent of frequency in the dry condition, but that it depended on frequency in the moist state.

Numerous other studies have been made of parts of the problem of elastic wave damping in solid materials, granular materials, or suspensions. Papers by Hamilton (1956), Nyborg, Rudnick, and Schilling (1950), Shumway (1960), to note a few, have each treated a part of the problem by studying selected materials.

II. REVIEW OF FUNDAMENTAL CONCEPTS

FOR DAMPING AND WAVE PROPAGATION

A. ONE-DEGREE-OF-FREEDOM VIBRATIONS WITH VISCOUS DAMPING

Because the terms and equations corresponding to this theory are applied so frequently for evaluation of damping, a brief review is justified.

The components of the vibrating systems, shown in Fig. 2-1, are a single weight W which slides on a frictionless base, an elastic spring with a spring constant k , a dashpot or viscous damper which develops a force directly proportional to the velocity, and a force Q(t) varying with time. By use of D'Alembert's principle, the equation of equilibrium at any instant is
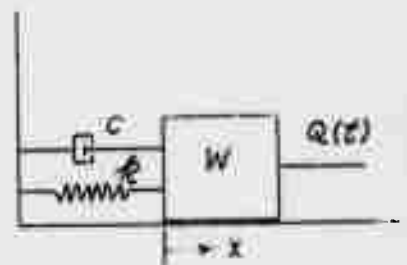
Fig. 2-1

$$\frac{W}{g} \frac{d^2x}{dt^2} + c \frac{dx}{dt} + kx = Q(t) \qquad (2-1)$$

Determination of logarithmic decrement from free vibrations with viscous damping

For the special case when Q(t) = 0, we have free vibrations with viscous damping and Eq. (2-1) may be rearranged to read,

$$\frac{d^2 x}{dt^2} + \frac{c}{m}\frac{dx}{dt} + \omega^2 x = 0 \qquad (2-2)$$

in which
$$m = \frac{W}{g}$$

and
$$\omega^2 = \frac{kg}{W}$$

The smallest amount of damping required to prevent periodic motion is called the "critical damping." Its value is expressed by

$$C_{CR} = 2m\omega = 2m\sqrt{\frac{k}{m}} = 2\sqrt{km} \qquad (2-3)$$

The case of most interest for the material damping problem is that for underdamping, in which periodic motion occurs with amplitudes decreasing with time. For this case the solution of Eq. (2-2) is

$$X = e^{-\frac{c}{2m}t}\left[X_0 \cos\sqrt{\omega^2 - \left(\frac{c}{2m}\right)^2}\; t + \frac{V_0 + \frac{c}{2m}X_0}{\sqrt{\omega^2 - \left(\frac{c}{2m}\right)^2}}\; \sin\sqrt{\omega^2 - \left(\frac{c}{2m}\right)^2}\; t\right]. \quad (2-4)$$

in which X_0 is an initial displacement at time $t = 0$

V_0 is an initial velocity at time $t = 0$

e is the base of natural logarithms.

On a plot of displacement vs. time (Fig. 2-2), Eq. (2-3) defines a sinusoidal type curve with decreasing amplitude.

Fig. 2-2
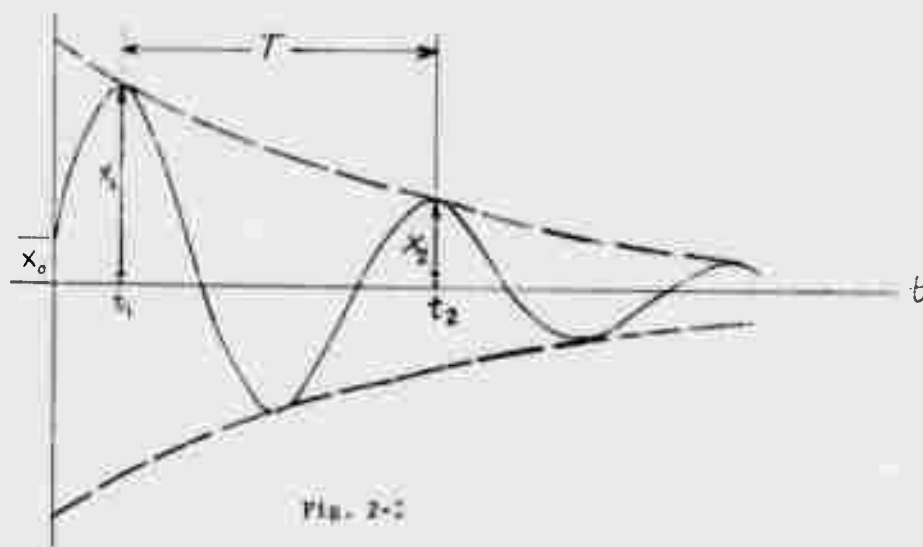
If we take advantage of the fact that the maximum point on the sin curve is very close to the point of tangency with the $e^{-\frac{c}{2m}t}$ curve, we can approximate the ratio of successive peaks, X_1 and X_2, at the times t_1 and t_2. The interval $t_2 - t_1$ represents the period, T. Thus,

$$\frac{X_2}{X_1} = \frac{e^{-\frac{c}{2m}t_2}}{e^{-\frac{c}{2m}t_1}} = e^{-\frac{c}{2m}(t_2-t_1)} = e^{-\frac{c}{2m}T} \qquad (2-5)$$

The period is equal to the reciprocal of the frequency of oscillation, or

$$T = \frac{1}{f} = \frac{2\pi}{\sqrt{\omega^2 - \left(\frac{c}{2m}\right)^2}} \qquad (2-6)$$

Then by substituting Eq. (2-6) into (2-5) and taking the logarithm of both sides,

$$\ln \frac{X_2}{X_1} = \frac{c}{2m} \frac{2\pi}{\sqrt{\omega^2 - \left(\frac{c}{2m}\right)^2}} = \frac{c}{2m\omega} \frac{2\pi}{\sqrt{1 - \left(\frac{c}{2m\omega}\right)^2}}$$

or $\quad \ln \frac{X_2}{X_1} = \dfrac{2\pi \frac{c}{c_{CR}}}{\sqrt{1 - \left(\frac{c}{c_{CR}}\right)^2}} = \delta = \quad$ LOGARITHMIC DECREMENT $\quad$ (2-7)

From Eq. (2-7) it is evident that for _small values_ of $\frac{c}{c_{CR}}$,

$$\delta \approx 2\pi \frac{c}{c_{CR}}$$

Forced vibrations with viscous damping

When the exciting force has the form

$$Q(t) = Q_1 \sin \omega_1 t$$

in which Q_1 is a constant, the solution of Eq. (2-1) determines the amplitude-frequency relation

$$X = \frac{Q_1/k}{\sqrt{\left[1 - \left(\frac{\omega_1}{\omega}\right)^2\right]^2 + \left[2 \frac{c}{c_{CR}} \frac{\omega_1}{\omega}\right]^2}} \qquad (2-8)$$

Since Q_1/k represents the static displacement, X_S , of the system under an imposed force of magnitude Q_1 , Eq. (2-8) is often rearranged as
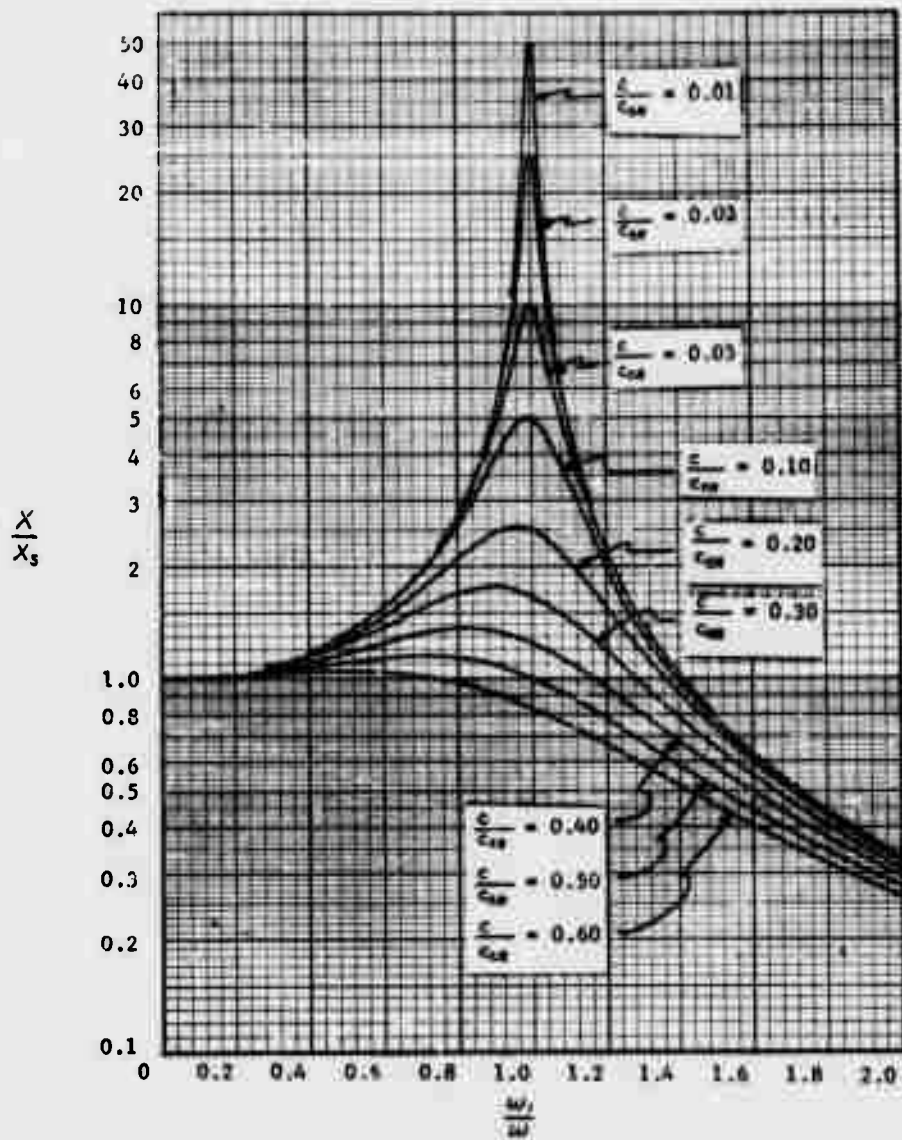
Fig. 2 - 3. Amplitude-Frequency Curves for One-Degree
of Freedom System with Viscous Damping Constant Force Excitation.

$$\frac{x}{x_s} = \frac{1}{\sqrt{\left[1 - \left(\frac{\omega_1}{\omega}\right)^2\right]^2 + \left[2\frac{c}{c_{CR}}\frac{\omega_1}{\omega}\right]^2}} \tag{2-9}$$

and is represented graphically in Fig. 2-3.

The exciting force may also be developed by an unbalanced mass at an eccentric radius e_1 rotating at the exciting frequency   . Then

$$Q(t) = m_1 e_1 \omega_1^2 \sin \omega_1 t \tag{2-10}$$

With the exciting force defined by Eq. (2-10) the solution of Eq. (2-4) is

$$x = \frac{\frac{m_1 e_1}{m}\left(\frac{\omega_1}{\omega}\right)^2}{\sqrt{\left[1 - \left(\frac{\omega_1}{\omega}\right)^2\right]^2 + \left[2\frac{c}{c_{CR}}\frac{\omega_1}{\omega}\right]^2}} \tag{2-11}$$

Fig. (2-6) illustrates the relation between $\frac{x}{\frac{m_1 e_1}{m}}$ and the frequency ratio ω_1/ω for different values of the damping ratio c/c_{CR}.

Damping determined from the amplitude-frequency curve

From computations based on Eq. (2-9) for the constant force type of excitation the logarithmic decrement can be defined in terms taken directly from an experimental amplitude-frequency curve. It depends primarily on the frequency range bounded by the curve at a specified amplitude. The

general expression is

$$\delta = \pi \frac{\Delta f}{f_0} \sqrt{\frac{A^2}{A_{max.}^2 - A^2} \left[\left(\frac{f_1 + f_2}{2 f_0} \right) \left(\frac{1}{1 - \left(\frac{c}{c_{cr}}\right)^2} \right) \right]} \qquad (2\text{-}12)$$

Usually the terms in the brackets are nearly equal to 1 0 For convenience, Eq (2-12) is often used in one of the following forms

$$\delta = 1.814 \frac{\Delta f_{AT\,0.5\,A_{MAX.}}}{f_0}$$

or

$$\delta = \pi \frac{\Delta f_{AT\,0.707\,A_{MAX.}}}{f_0}$$
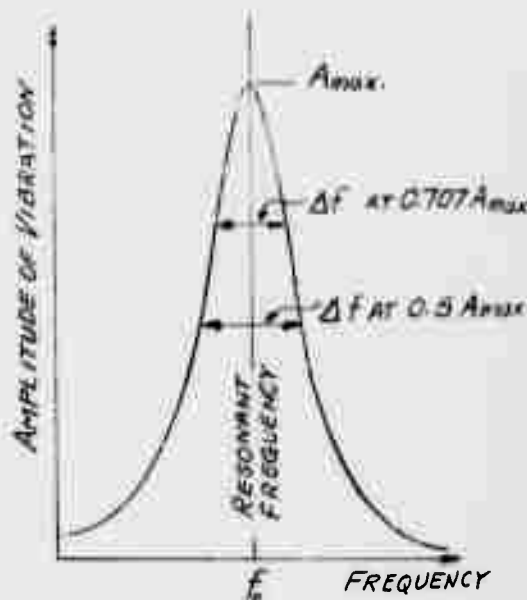
Fig. 2-5

B. ADDITIONAL METHODS FOR EVALUATING MATERIAL DAMPING

The literature covering internal damping in materials, particularly for metals, is voluminous. An indication of the type of work represented in these studies may be found in the references in the report of Jensen (1959) or in the bibliography prepared by Demer (1956). The terminology and definitions used in the following paragraphs will follow those given by Jensen.

One list of the quantitative expressions used to define the internal damping of materials includes: viscosity, damping capacity, constant of internal friction, hysteretic constant, specific damping capacity, log-arithmic decrement, elastic-phase constant, and coefficient of internal
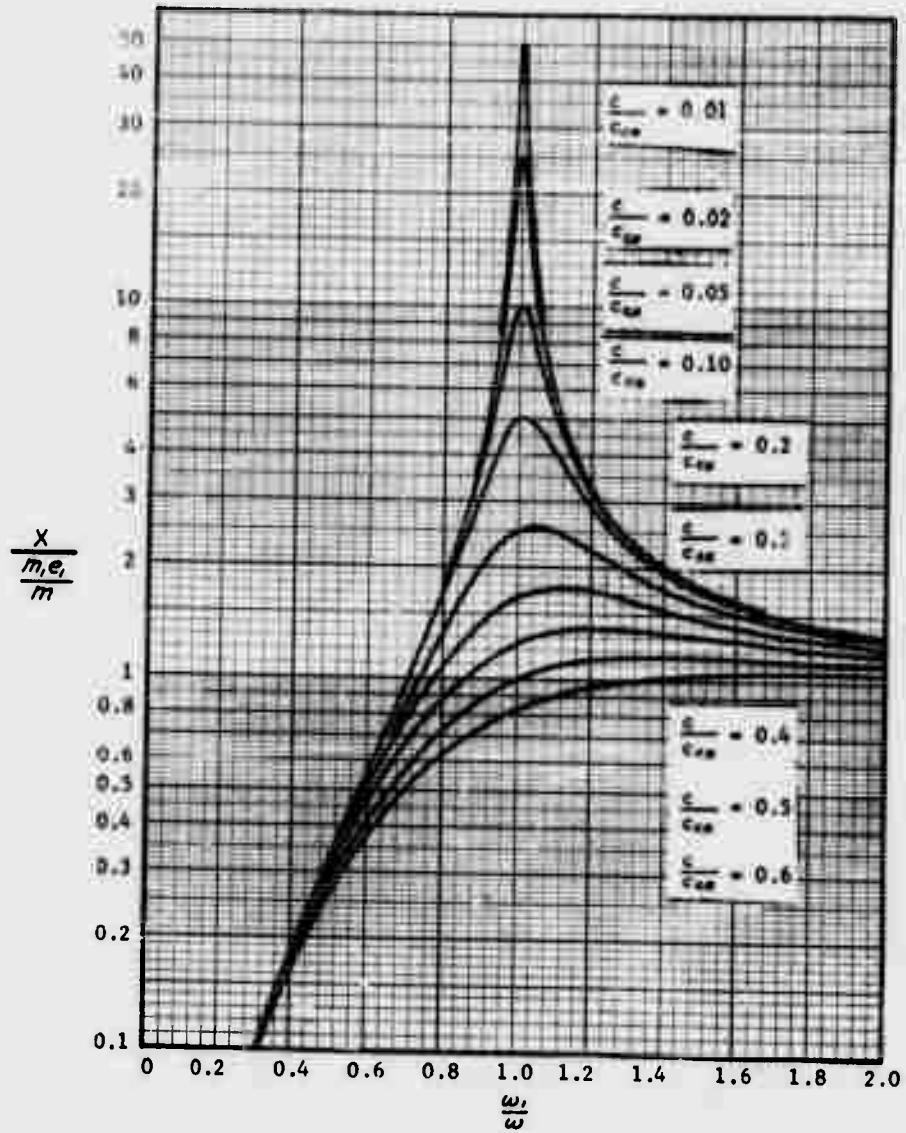
Fig. 2 - 6. Amplitude-Frequency Curves for One-Degree of
Freedom System with Viscous Damping Rotating Mass Oscillator.

friction. Other terms which may be added to this list are: damping modulus, resonance-amplification factor, damping factor, specific damping energy, stress-strain phase angle, specific dissipation function, and attenuation.

Of these terms, the logarithmic decrement was described by Eq. (2-7) and the resonance-amplification factor was described graphically by Fig. (2-3) and its relation to the logarithmic decrement was defined by Eq. (2-12). A measure of the force-displacement phase angle can also be obtained from the theory described in Section II-A.

Specific damping capacity

The term "specific damping capacity" has been used to indicate the ratio of the energy absorbed in one cycle of vibration to the potential energy at maximum displacement in that cycle. The "damping capacity" thus defined has a fairly wide acceptance and may be expressed in per cent or as a decimal. In terms of the stress-strain diagram the damping capacity represents the ratio of the area enclosed by the hysteresis loop to the total area under the input curve, or

$$p = \frac{\Delta W}{W} \tag{2.13}$$

The relationship between the specific damping capacity and the logarithmic decrement for a particular decay curve is

$$p = \left(1 - e^{-2\delta}\right) \tag{2.14}$$

By expanding $e^{-2\delta}$ into a series, Eq. (2-14) becomes

$$\mathcal{P} = \frac{2\delta}{1!} - \frac{(2\delta)^2}{2!} + \frac{(2\delta)^3}{3!} \cdots$$

and for small values of δ, $\mathcal{P} = 2\delta$.

Attenuation constant and specific dissipation function

Often it is desirable to evaluate the decrease in amplitude of vibration as a function of distance from a source. In addition to the reduction in amplitude caused by geometrical dispersion of the wave energy there is a reduction caused by energy losses within the soil. This is designated an "attenuation," a measure of energy loss as a function of distance and it is measured in terms of the coefficient of attenuation, α . The coefficient of attenuation is related to the logarithmic decrement by

$$\delta = \frac{2\pi C\alpha}{\omega} \tag{2-16}$$

in which C is the phase velocity and $\omega/2\pi$ is the frequency of the propagating wave.

A variation of this attenuation constant determines the specific dissipation function, $1/Q$. Thus the relation is
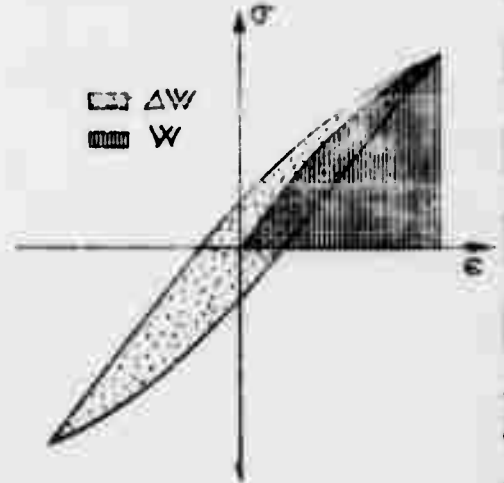
$$\frac{1}{Q} = \frac{2\alpha C}{\omega} \tag{2-17}$$

Summary of the quantities used to evaluate damping from linear one-degree-of-freedom system with viscous damping

A = amplitude of the vibrations at a given frequency f

A_{max} = maximum amplitude of vibration

C = phase velocity of wave propagation

$\frac{C}{C_{cR}}$ = damping ratio

$f = \omega/2\pi$ = frequency of vibration

f_o = resonant frequency

p = specific damping capacity

$1/Q$ = specific dissipation function

W = maximum energy available in one cycle

ΔW = energy dissipated in that cycle

α = coefficient of attenuation

δ = logarithmic decrement

ω = angular frequency of the vibration

$$\delta = \frac{2\pi \frac{C}{C_{cR}}}{\sqrt{1 - \left(\frac{C}{C_{cR}}\right)^2}} \approx 2\pi \frac{C}{C_{cR}} \tag{2-7}$$

$$\delta = \pi \frac{\Delta f}{f_o} \sqrt{\frac{A^2}{A_{max.}^2 - A^2}} \tag{2-12}$$

$$\rho = \frac{\Delta W}{W} = \left(1 - e^{-2\delta}\right) \simeq 2\delta \qquad (2.18)$$

$$\delta = \frac{2\pi C \alpha}{\omega} = \frac{\pi}{Q} \qquad (2.19)$$

C. SYSTEM WITH NON-LINEAR STRESS-STRAIN RELATION

Numerous solutions are available in the literature concerning the amplitude-frequency diagrams which result from a spring which exhibits non-linear characteristics. Solutions for some of these problems are given by Timoshenko (1955), for example. In this type of problem the loading and unloading curves are identical and no energy is lost within the spring.

A more realistic theory has been developed by Pisarenko (1962) which includes both the non-linear stress-strain relations for the material and the energy losses during a loading cycle.

Fig. 2-8

Among the problems treated by Pisarenko was that for the torsional oscillation of a circular shaft which has a non-linear stress-strain relationship as illustrated in Fig. 2-8. The details of this solution are reproduced
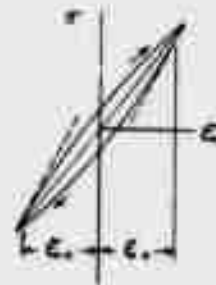
here in order that the quantities involved as well as the amplitude response curve may be compared with the experimental data given in Section III.

He assumed that the equation for increasing stress is

$$\frac{d \overrightarrow{\tau_{xv}}}{d \gamma_{xv}} = G \left[1 - \Gamma \left(\delta_{xY(max)} + \delta_{xY} \right)^{s} \right] \cdot \tag{2-20}$$

and the equation for decreasing stress is

$$\frac{d \overleftarrow{\tau_{xv}}}{d \gamma_{xY}} = G \left[1 + \Gamma' \left(\gamma_{xY(max)} - \gamma_{xY} \right)^{s} \right] \tag{2-21}$$

where $\gamma_{xY(max.)}$ is the amplitude of the shear vibration and Γ and S are hysteresis parameters to be determined experimentally. If we let $\Lambda = S + 1$ and integrate the above equations we have

$$\overrightarrow{\tau_{xY}} = G \left\{ \gamma_{xY} - \frac{\Gamma}{\Lambda} \left[\left(\gamma_{xY(max)} + \gamma_{xY} \right)^{\Lambda} - 2^{\Lambda-1} \gamma_{xY(max)}^{\Lambda} \right] \right\}$$

$$\overleftarrow{\tau_{xY}} = G \left\{ \gamma_{xY} + \frac{\Gamma}{\Lambda} \left[\left(\gamma_{xY(max)} - \gamma_{xY} \right)^{\Lambda} - 2^{\Lambda-1} \gamma_{x Y(max.)}^{\Lambda} \right] \right\} \tag{2-22}$$

Equations (2-22) are integrated over a circular shaft to determine the expressions for moment. These are substituted into the equilibrium equation which gives.

$$\frac{\partial^{2} \phi(x,t)}{\partial x^{2}} + \epsilon \frac{\partial}{\partial x} \overleftrightarrow{\Phi}(\phi',t) - \frac{\rho}{G} \frac{\partial^{2} \phi(x,t)}{\partial t^{2}} = \epsilon g \cos \omega t \tag{2-23}$$

where $\phi(x,t)$ represents the twist along the shaft, ε is a small parameter, g represents the driving force and $\vec{\Phi}(\phi',t)$ is given by

$$\vec{\Phi}(\phi',t) = -\frac{1}{\varepsilon}\left[\left(\frac{d\phi_m(x)}{dx} + \frac{\partial\phi(x,t)}{\partial x}\right)^{\lambda} - 2^{\lambda-1}\left(\frac{d\phi_m(x)}{dx}\right)^{\lambda}\right]\frac{4\Gamma s^{\lambda-1}}{\lambda(\lambda+3)}$$

A solution to Eq. (2-23) is sought in the form

$$\phi(x,t) = \psi(x)\,\phi_0\cos(\omega t+\alpha) + \varepsilon\phi_1(x,t) + \varepsilon^2\phi_2(x,t) + \cdots$$

$$\omega^2 = \omega_c^2 + \varepsilon\,\omega_1^2 + \varepsilon\,\omega_2^2 + \cdots$$

$$\bar{\alpha} = \bar{\alpha}_0 + \varepsilon\,\bar{\alpha}_1 + \varepsilon^2\,\bar{\alpha}_2 + \cdots$$

where ϕ_0 is the amplitude of vibrations, ω_c is the natural frequency of vibrations of the bar and $\bar{\alpha}$ is the phase angle between force and displacement. A solution which includes the first two terms of the series approximations given above is found for the boundary conditions of a bar fixed at both ends and is given by

$$\left(\frac{\omega}{\omega_c}\right)^2 = 1 + \frac{16\,\Gamma\,\pi^{\lambda-2}r^{\lambda-1}\phi_0^{\lambda-1}}{(\lambda+3)\,\ell^{\lambda}}\int_0^{\ell}\cos^{\lambda-1}\frac{\pi x}{\ell}\,\sin^2\frac{\pi x}{\ell}\,dx \qquad (2\text{-}24)$$

$$\times\int_0^{\pi}\left[(1-\cos\theta)^{\lambda}-2^{\lambda-1}\right]\cos\theta\,d\theta + \frac{48_0\,\ell^2}{\pi^3\,\phi_0}\cos\bar{\alpha}_0$$

$$\sin \bar{\alpha}_c = -\frac{4\,r^{\lambda-1}\,\pi^{\lambda+1}\,\Gamma\,\phi_0^{\lambda}}{g_c\,(\lambda+3)\,\ell^{\lambda+2}} \int_0^{\ell} \cos^{\lambda-1}\frac{\pi x}{\ell}\ \sin^2\frac{\pi x}{\ell}\ dx$$

$$\times \int_0^{\pi} \left[\left(1-\cos\theta\right)^{\lambda} - 2^{\lambda-1} \right]\sin\theta\ d\theta$$

(2-25)

The above equations were solved for the conditions representative for Ottawa sand. The values used were as follows.

$$\left(\phi_0\right)_{max.} = 0.005$$

$$G = 18,000\ \text{lb./in.}^2$$

$$r = 2\ \text{cm.}$$

$$\ell = 50\ \text{cm.}$$

$$\lambda = 3$$

$$\Gamma = 2 \times 10^7 \text{ (calculated to give a value of } \delta \approx 0.10)$$

The resulting resonance curve is shown in Fig. (2-9). The variation of the frequency of maximum amplitude with exciting force is a second degree parabola with its origin at $\omega/\omega_c = 1.0$ as shown by the dashed line. The stress-strain relationships used in the derivation are such that the logarithmic decrement will be independent of the magnitude of vibrations.

D. EXAMPLE OF DISPERSION DAMPING IN IDEAL ELASTIC SOLIDS

A dispersion type damping results from the loss of energy through radiation by elastic waves from a source. In the example to be considered, the source of input energy is an oscillator vibrating vertically on the
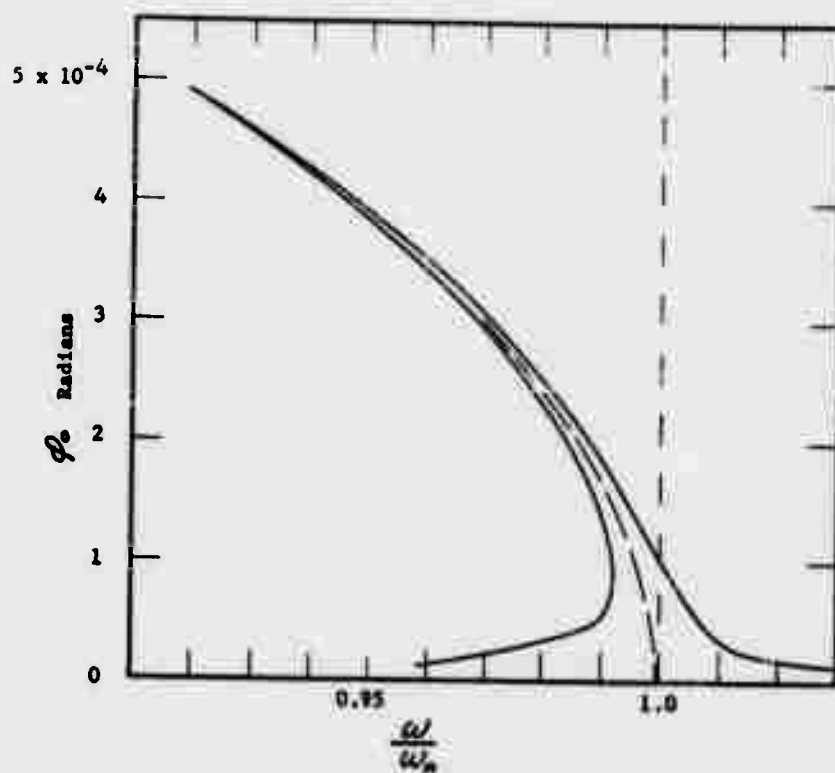
Fig. 2-9.- Theoretical variations of amplitude with frequency for torsional vibrations of a shaft as given by theory of Pisarenko.

surface of a semi-infinite ideal elastic solid which has weight. Reissner (1936) developed the theory and considered that the oscillator produced a uniformly distributed pressure over the circular contact area. Sung (1953) extended Reissner's theory to cover the cases for which the stress distribution was parabolic, uniform, or corresponded to that produced by a rigid base. The latter case appears to be the best approximation to actual conditions. Recently, Hsieh (1962) has reworked the fundamental equations in the Reissner-Sung theory in order to place them in a form comparable to that developed for the conventional one-degree-of-freedom system with viscous damping. The following equations are a condensation of Hsieh's study.

In order to evaluate the force transmitted to the elastic body we first consider a weightless rigid circular disk which rests on the surface of the body (Fig. 2-10). The elastic body is homogeneous and isotropic, has a shear modulus, G , and a mass density of $\rho \; (= \gamma/g)$. A vertical periodic force $P = Z e^{i\omega t}$ acts on the disk. The vertical displacement ω , given by the Reissner-Sung theory is
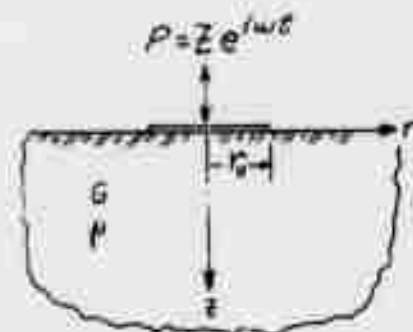
$P = Z e^{i\omega t}$

Fig. 2-10

$$\omega = \frac{Z}{G r_0} \left[f_1 + i f_2 \right] e^{i\omega t} \qquad (2\text{-}26)$$

in which f_1 and f_2 are functions of the frequency of oscillation, $(= \omega/2\pi)$ and $i = \sqrt{-1}$. The time variable is t and $e = 2.71828\cdots$.

In order to eliminate the imaginary term, Hsieh took the derivative of Eq. (2-26) with respect to time to obtain

$$\frac{d\omega}{dt} = \frac{Z\omega}{Gr_0}\left[if_1 - f_2\right]e^{i\omega t} \qquad (2-27)$$

and by combining Eqs. (2-26) and (2-27) he determined

$$f_1\omega\omega - f_2\frac{d\omega}{dt} = \frac{Z\omega}{Gr_0}\left[f_1^2 + f_2^2\right]e^{i\omega t} = \frac{P\omega}{Gr_0}\left[f_1^2 + f_2^2\right] \qquad (2-28)$$

or

$$P = \frac{-Gr_0}{\omega}\left(\frac{f_2}{f_1^2 + f_2^2}\right)\frac{d\omega}{dt} + Gr_0\left(\frac{f_1}{f_1^2 + f_2^2}\right)\omega$$

Eq. (2-28) indicates that the force transmitted to the elastic body is a function not only of the displacement of the disk, but also is a function of its velocity. For convenience in computations, the dimensionless frequency term, a_0 , from the Reissner-Sung theory,

$$a_0 = \omega r_0\sqrt{\frac{\rho}{G}} = \frac{\omega r_0}{v_s} = \frac{2\pi r_0}{L_s} \qquad (2-29)$$

may be substituted into Eq. (2-28). Then by using the notation,

$$F_1 = \frac{-f_1}{f_1^2 + f_2^2}$$

$$F_2 = \frac{f_2}{f_1^2 + f_2^2}$$

$(2-30)$

Eq. (2-28) becomes

$$P = -\frac{\sqrt{G\rho}}{a_o} \, r_o^2 F_2 \frac{dw}{dt} - G r_o F_1 w \qquad (2\text{-}32)$$

For vertical oscillation, the functions F_1 and F_2 can be expressed approximately by the following expressions:

for Poisson's ratio, $\mu = 0$ $\qquad F_1 = 4.0 - 1.2 \, a_o^2$

$\qquad\qquad\qquad\qquad\qquad\qquad F_2 = 3.40 \, a_o - 0.12 \, a_o^4$

$\qquad\qquad\qquad \mu = 1/4 \quad F_1 = 5.33 - 1.35 \, a_o^2 \qquad (2\text{-}33)$

$\qquad\qquad\qquad\qquad\qquad\qquad F_2 = 4.20 \, a_o - 0.12 \, a_o^4$

$\qquad\qquad\qquad \mu = 1/2 \quad F_1 = 8.0 - 2.40 \, a_o^2$

$\qquad\qquad\qquad\qquad\qquad\qquad F_2 = 6.45 \, a_o - 0.35 \, a_o^4$

Eq. (2-32) can be further simplified by substituting

$$R_v = \frac{\sqrt{G\rho}}{a_o} \, r_o^2 \, F_2 \qquad (2\text{-}34a)$$

and

$$K_v = G \, r_o \, F_1 \qquad (2\text{-}34b)$$

to give $\qquad P = -R_v \frac{dw}{dt} - K_v w \qquad (2\text{-}35)$
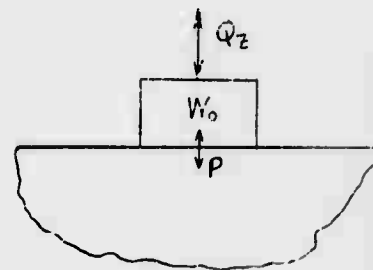
Now, if a cylindrical mass of radius r_o and weight w_o $(ie.\ m_o = w_o/g)$ is placed on the weightless rigid disk and subjected to a vertical exciting force Q_z , (Fig. 2-11) the equation of motion is

Fig 2-11

$$m_o \frac{d^2 \omega}{dt^2} = Q_{\bar{z}} + P \tag{2-36}$$

or by substituting Eq. (2-35) into Eq. (2-36),

$$m_o \frac{d^2 \omega}{dt^2} + R_v \frac{d\omega}{dt} + K_v \omega = Q_z \tag{2-37}$$

Equation (2-37) is similar to Eq. (2-1) for the one-degree-of-freedom system with viscous damping, with the important exception that both R_v and K_v depend upon the frequency factor a_o. From Eqs. (2-33) it is evident that R_v is almost linearly dependent upon frequency while for small values of a_o the frequency effect on K_v is small.

E. DUFFY AND MINDLIN'S THEORY FOR ELASTIC SPHERES

Duffy and Mindlin (1957) derived a differential stress-strain relation for a medium composed of a face centered cubic array of elastic spheres in contact. They retained the classical Hertz theory for normal forces and used the theories of Cattaneo (1938), Mindlin (1949) and Mindlin and Deresiewicz (1953) to include the tangential components of the forces at the contacts between the spheres. The theory predicts that when a tangential force is applied to two spheres in contact, slip occurs at the circumference of the contact surface. Because of this fact the stress-strain relation depends upon the entire stress history of the material. This phenomenon gives rise to a frictional dissipation

of energy which does not occur when only normal forces are considered.

Solutions are found for the case of a small increment of stress applied to a medium under an initial isotrpic plus uniaxial stress. The resulting medium is anisotropic and the stress-strain relation depends on the direction of orientation. Orientation which avoids coupling with flexural waves gives a solution in the x , or (1, 0, 0) direction and the (1, 1, 0) direction. The solutions are

$$E_{(1,0,0)} = \frac{2(8-7\bar{\mu})}{(8-5\bar{\mu})} \left[\frac{3\bar{G}^2 \sigma_o}{2(1-\bar{\mu})^2} \right]^{\frac{1}{3}}$$

(2-38)

$$E_{(1,1,0)} = \frac{2(4-3\bar{\mu})(8-7\bar{\mu})}{(4-3\bar{\mu})^2 + (8-7\bar{\mu})(2-\bar{\mu})} \left[\frac{3\bar{G}^2 \sigma_o}{2(1-\bar{\mu})^2} \right]^{\frac{1}{3}}$$

where $\bar{\mu}$ and $\bar{G}$ are Poisson's ratio and shear modulus of the individual spheres. The two values of E differ depending upon μ . At $\bar{\mu} = 0.25$ the difference is about 2 per cent.

The theoretical frictional energy loss per cycle was found by a summation of the energy dissipated at the individual contacts and by taking a sinusoidal displacement distribution along the length of the bar. The theory predicts an energy loss proportional to the cube of the amplitude. For small amplitudes the total energy stored is proportional to the square of the amplitude. This would indicate a variation of logarithmic decrement which is proportional to amplitude. The theory also predicts a minus one-third power variation of logarithmic decrement with pressure.

F. BIOT'S THEORY FOR WAVE VELOCITY IN A SATURATED POROUS ELASTIC SOLID

Biot (1956 a) presented a theory dealing with the propagation of elastic waves in a fluid-saturated porous solid assuming that the solid was elastic and that the fluid was compressible and viscous. He also assumed that the walls of the main pores (interconnected pores) were impervious and that the pore size was concentrated around some average value.

For the case in which the viscosity of the fluid is taken as zero the equations of equilibrium have the form

$$\frac{\partial \sigma_x}{\partial x} + \frac{\partial \tau_{xy}}{\partial y} + \frac{\partial \tau_{xz}}{\partial z} = \frac{\partial^2}{\partial t^2}\left[\bar{\rho} u_x + \rho_a(u_x - U_x)\right] \qquad (2\text{-}39)$$

$$-\frac{\partial \rho^*}{\partial x} = \frac{\partial^2}{\partial t^2}\left[\rho^* U_x + \rho_a(U_x - u_x)\right] \qquad (2\text{-}40)$$

in which
u_x = displacement of the frame

U_x = displacement of the fluid

$\bar{\rho}$ = mass density of the frame

ρ^* = mass density of the fluid

ρ = mass density of the aggregate

$$\rho = \bar{\rho} + \rho^*$$

ρ_a = additional apparent mass.

The equations of wave propagation are of the form

$$G \nabla^2 u_x + (D+G) \frac{\partial \bar{\varepsilon}}{\partial x} + Q \frac{\partial \tilde{\varepsilon}}{\partial x} = \frac{\partial^2}{\partial t^2} \left[\bar{\rho} u_x + \rho_a (u_x - U_x) \right] \qquad \text{(2-41)}$$

$$R \frac{\partial \tilde{\varepsilon}}{\partial x} + Q \frac{\partial \bar{\varepsilon}}{\partial x} = \frac{\partial^2}{\partial t^2} \left[\rho^* U_x + \rho_a (U_x - u_x) \right] \qquad \text{(2-42)}$$

where
$\tilde{\varepsilon}$ = dilatation of the fluid

$\bar{\varepsilon}$ = dilatation of the frame

G = shear modulus of the frame

$Q \text{ and } R$ are constants relating to the coupling

$$-p^* = Q \bar{\varepsilon} + R \tilde{\varepsilon} \qquad \text{(2-43)}$$

Bito and Willis (1957) give a discussion of the methods for measuring the quantities G, D, Q and R used in the equations for wave propagation.

Three waves result from this theory, dilatational waves in the frame and in the fluid which involve coupled motion and stiffness of the fluid and the frame, and a rotational wave. The rotational wave is uncoupled from the dilatational waves and involves only coupled motion of the frame and the fluid.

Biot modifies the equations of wave propagation by including the damping due to the viscosity of the pore fluid which is a function of the frequency of vibration. Solutions for the dilatational waves are found by applying the divergence operator to the equations of wave propagation and

the solution for the rotational wave is found using the curl operator.

When the viscosity of the fluid is equal to zero we have the un-damped case. This gives an expression for the rotational or shear wave which is

$$
\mathcal{V}_s = \left[\frac{G}{\overline{\rho} + \dfrac{\rho^* \rho_a}{\rho^* + \rho_a}} \right]
$$
(2-44)

The Biot theory was programmed for the IBM 709 digital computer using numerical values which correspond to Ottawa sand saturated with water. Below is a list of these values.

e = void ratio = 0.55

$\overline{B}$ = bulk modulus of the grains = 3.9×10^6 lb./in.^{2}

B^* = bulk modulus of the fluid = 3×10^5 lb./in.^{2}

G_s = specific gravity of the grains = 2.66

μ = Poisson's ratio of the frame = 0.45

G = shear modulus of the specimen = 1×10^4 lb./in.^{2} at a confining pressure of 1000 lb./ft.^{2}

γ_f = unit weight of the fluid = 62.4 lb./ft.^{3}

η = viscosity of the fluid = 2×10^{-5} lb. sec./ft.^{2}

$\mathcal{R}$ = permeability = 4.5×10^{-10} ft.^{2}

K = apparent mass coefficient = 0.33

$\mathcal{S}$ = structure factor = 2.5

f = frequency of vibrations = 1000 cycles/sec.

σ = confining pressure = variable

The values given above are experimental except for the values of K and S. The variables K and S are related to the coupling between the fluid and the solid. Kosten and Zwikker (1949) explain the significance of the variable K with respect to a system composed of randomly oriented tubes. If each tube is oriented at an angle θ with the macroscopic pressure gradient, the pressure gradient in the tube is $\cos\theta$ times the macroscopic pressure gradient. The component of acceleration in the tubes in the direction of the macroscopic pressure gradient is $\cos\theta$ times the acceleration in the direction of the tubes. For a random orientation of tubes $\cos^2\theta$ = 1/3. This would indicate a value of $K = (1 - \cos^2\theta)$ = 2/3. Experimental results by Hardin (1961) indicate that the apparent mass coefficient should be about 0.3 to 0.4. The value used for the program was such that $\rho_a = 0.33\rho$.

Biot gives a range of values for the structure constant S. For a value of the sinuosity factor between 1.0 and 1.5 a value of S was chosen which lies between that for slit-like pores and circular pores. Biot showed that S was not a very significant parameter.

A value for G was used which corresponded to that determined by the experimental results of Hardin (1961). His results indicated that the shear modulus varied with the 0.50 power of confining pressure. Thus, the program was set up to calculate shear modulus from the expression

$$G = G'\left(\frac{\sigma}{\sigma'}\right)^{0.5}$$

where G' is the shear modulus at the confining pressure σ'. The value of σ' was arbitrarily chosen to be 1000 lb./ft.^{2}

The coefficient of permeability, k , is that found from experimental results on Ottawa sand which are common to most textbooks on soil testing. It should be pointed out that the coefficient of permeability used here is not that conventionally used in soil mechanics. The coefficient commonly used in soil mechanics is found by multiplying k by the ratio of unit weight divided by viscosity. This changes the dimensions from ft.^{2} to ft./sec.

The computer results for velocity and damping are shown in Fig. 2-12. The variation of the shear wave velocity with pressure is determined entirely by the variation of the shear modulus with pressure. The variation chosen for shear modulus results in a variation of velocity with the 1/4 power of confining pressure. The damping of the shear wave is independent of confining pressure. The velocity of sound in a fluid is not significantly affected by the confining pressure but when the fluid and solid are coupled as is the disturbed fluid wave a slight variation of velocity with confining pressure is observed. As the confining pressure is increased the damping of the fluid wave is decreased. It can be seen that the variation of velocity with confining pressure for the dilatation wave of the frame is the same as for the shear wave. The logarithmic decrement is affected only slightly by confining pressure and for the values considered here the damping increases slightly at higher confining pressure.

G.   THEORIES USED IN CONNECTION WITH THE EXPERIMENTAL DETERMINATIONS OF WAVE VELOCITY AND DAMPING FROM LABORATORY SPECIMENS

The measurement of wave velocity through a column of soil was determined by measurement of the resonant frequency of the column for the type of wave in question. Resonance was found by varying the frequency of
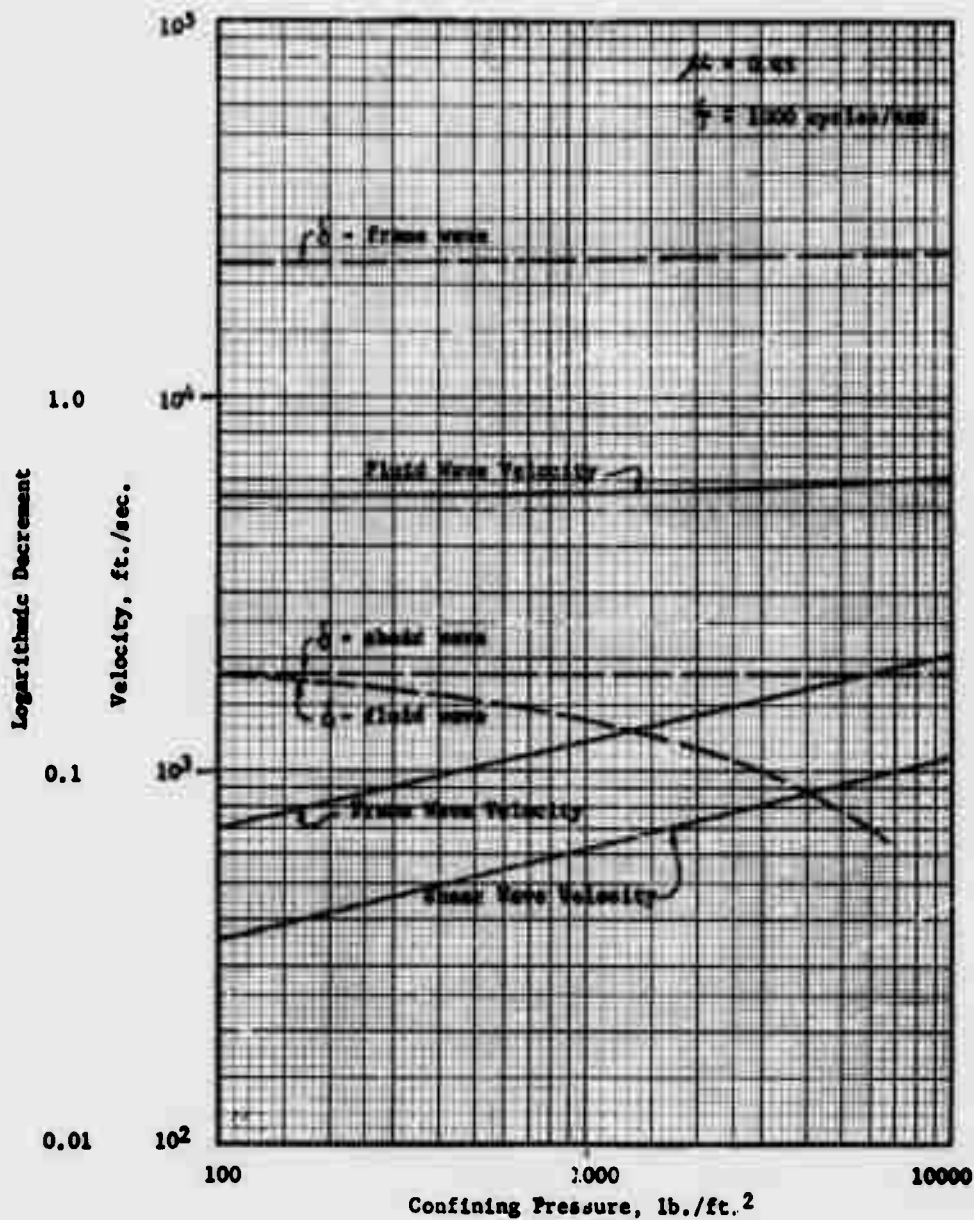
Fig. 2-12.- Variation of damping and velocity with confining pressure
for water-saturated Ottawa sand as given by the Biot theory.

vibration and determining the frequency for maximum amplitude. By knowing the mode of vibration the wave length may be determined using the length of the specimen. From these two measurements velocity may be calculated from the relationship

$$\nu = f L$$

where L represents the wave length of the stress wave.

If the shear wave velocity and the longitudinal wave velocity are known, the dynamic shear modulus and the dynamic modulus of elasticity may be computed. Love (1944) showed that in a cylindrical specimen the velocity of a longitudinal wave is given by

$$\nu_L = \left(1 - \frac{\pi^2 \mu^2 r^2}{L^2} \right) \left(\frac{E}{\rho} \right)^{1/2}$$

where r is the radius of the specimen. Equation (2-45) is valid for small values of r/L. The specimens used in this research had an $r/L = 0.02$ for the first mode of vibration. Using this value and a maximum value of Poisson's ratio of 0.5 the first term of Eq. (2-45) is 0.999 which is $\approx$ 1.00. Thus, for the specimens used in this research we can use the relationship

$$\nu_L = \left(\frac{E}{\rho} \right)^{1/2} \tag{2-46}$$

for calculating the dynamic modulus. The dynamic shear modulus may be

found by using the relationship

$$\nu_s = \left(\frac{G}{\rho} \right)^{1/2}$$

$$(2-47)$$

In order to vibrate a specimen some sort of a driving mechanism must be attached and another mechanism must be connected for measurement of the response. The addition of a mass to a material in which the resonant frequency is to be measured results in a slight change in the resonant frequency. The conditions of the specimen in the present investigation may be represented by Fig. 2-13. The solution governing the natural frequency of such a system under torsional vibrations is given by

$$\omega l \sqrt{\frac{\rho}{G}} \, \tan \omega l \sqrt{\frac{\rho}{G}} = \frac{I}{I_0}$$

$$(2-48)$$
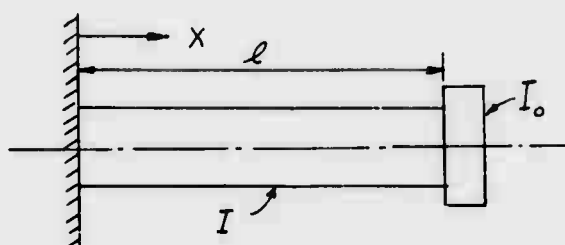
Fig. 2-13. - Model representing theoretical conditions in present research.

where I is the mass polar moment of inertia of the specimen and I_0 is the mass polar moment of inertia of the mass attached to the free end.

Equation (2-48) must either be solved graphically or by trial and error. It is convenient to put Eq. (2-48) into the form

$$\beta \tan\beta = \frac{I}{I_o} \tag{2-49}$$

Thus,

$$\gamma = \frac{2\pi f \ell}{\beta} \tag{2-50}$$

Figure 2-14 shows the graphical solution to Eq. (2-49) for the first mode of vibration.

In this investigation the values obtained for damping by measurement of the decay of vibrations were corrected to compensate for the added mass of the pickup and driver. The effect of the added mass is approximated by considering a single degree-of-freedom system as shown in Fig. 2-15.
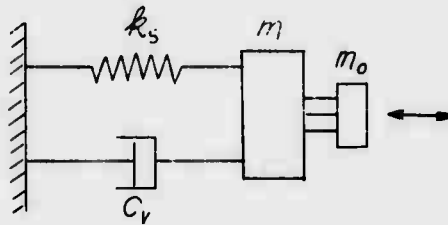
Fig. 2-15. - Single degree-of-freedom system.

The mass of the specimen is represented by m , the mass of the driver and pickup by m_o and the spring constant is k_s . First consider the case without m_o . We have the relationships
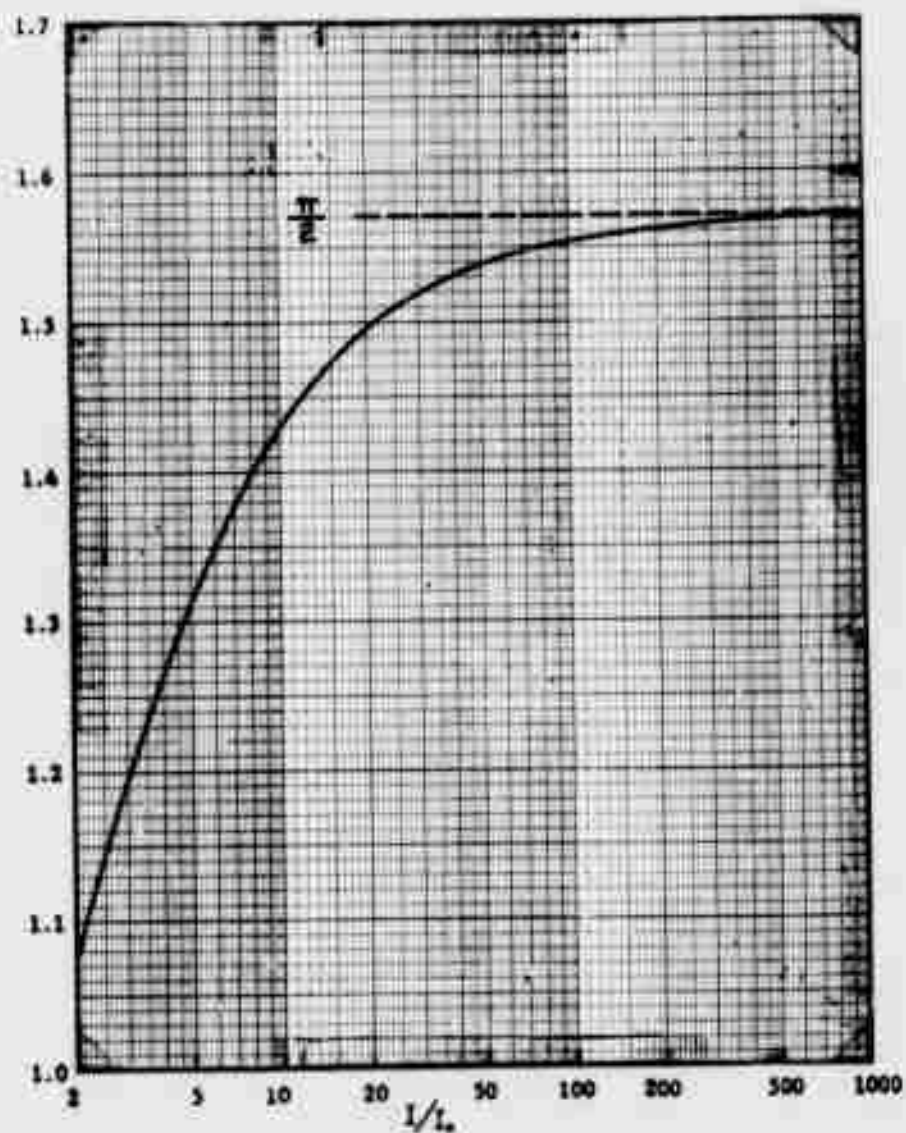
Fig. 2-14. - Graphical solution to Eq. (2-49) for the first mode of vibration.

$$\delta = \frac{\pi C_v}{\omega m}$$

$$\omega = \sqrt{\frac{k_s}{m}}$$

Thus,

$$\delta = \frac{\pi C_v}{\sqrt{k_s m}}$$

With the addition of m_o we have similarly

$$\delta' = \frac{\pi C_v}{k_s(m+m_o)}$$

Finally,

$$\frac{\delta}{\delta'} = \sqrt{\frac{m+m_o}{m}} \tag{2-51}$$

In order to use Eq. (2-51) it is necessary to convert the mass of the soil specimen into an equivalent concentrated mass. It can be shown that for the conditions in Fig. 2-16 the equivalent concentrated mass is $0.405\, m$.
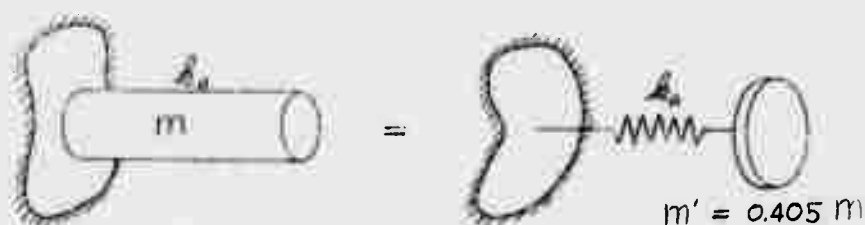
Fig. 2-16. - Conversion to a concentrated mass system.

This is based on the condition that both systems have the same undamped natural frequency. Using the above approximation the corrected value of logarithmic decrement is given by

$$\delta = \delta' \sqrt{1 + \frac{m_o}{0.405\,m}} \qquad (2\text{-}52)$$

The same correction may be used for torsion by substituting the analogous torsional inertias.

III. LABORATORY TESTS OF WAVE PROPAGATION

AND DAMPING IN GRANULAR MATERIALS

A. PURPOSE AND SCOPE

The purpose of the present research was to study the velocity
of shear and longitudinal waves and their damping in a column of granular
material. The effects of confining pressure, density, pore fluid (air,
water and dilute glycerin) amplitude of vibration and frequency were to
be considered. This is an extension of the work by Hardin (1961) to
include the effects of amplitude and the measurement of damping by use
of decay curves.

New apparatus was constructed for the measurement of the velocity
of shear and longitudinal stress waves at relatively large amplitudes
of vibrations which will not cause breakdown of the grain structure.
The largest amplitudes for a twelve-inch specimen fixed at one end were
5×10^{-4} in. longitudinally and 1.5×10^{-3} rad. torsionally. This is
on the order to ten times that attainable with the previous apparatus
and provides for a range of 250 times for controllable amplitudes. The
new equipment was also designed to permit evaluation of damping by
measuring the vibration decay from the steady state condition after
the driving mechanism was turned off. Hardin measured damping mainly
·by the shape of the amplitude vs. frequency curve. The pickups used
on the new apparatus were calibrated so that the amplitude of vibrations
could be measured at any time during a test.

Theoretical solutions of several persons have been presented for
the behavior of stress waves and damping in porous materials. The theory
by Biot (1956) may be used for theoretical evaluation of the stress wave
properties of velocity as well as the viscous damping associated with
saturated materials. The theory given by Duffy and Mindlin (1957) may
be used to calculate theoretical stress-strain relationships for granular
materials as a function of confining pressure and also the friction damp-
ing associated with contact stresses. The theory of Pisarenko predicts
the behavior of a material with non-linear stress-strain relationships in
torsion. The above theoretical solutions provide a basis for comparison
with experimental results.

B. MATERIALS, EQUIPMENT AND TEST PROCEDURES

Materials

There were four different materials used in this investigation.
Each is described below and the grain size curve for each is shown in
Fig. 3-1.

Ottawa sand. Standard Ottawa sand which had been sieved for the
fraction between the No. 20 and No. 30 sieves was used for most of the
investigation. This is the material prepared and used by Hardin (1961).
He reported that the minimum void ratio was 0.50 corresponding to a unit
weight of 110.5 lb./ft.^{3} and the maximum void ratio was 0.77 correspond-
ing to a unit weight of 93.6 lb./ft.^{3}

Glass beads No. 2847. Glass beads, all of which lie between the
No. 16 and No. 20 sieve, were obtained from the Prismo Safety Corporation,
Huntingdon, Pennsylvania. These beads are essentially perfect spheres
as viewed from a microcope. They have a specific gravity of 2.499.
The minimum void ratio was 0.57 and the maximum void ratio was 0.75.
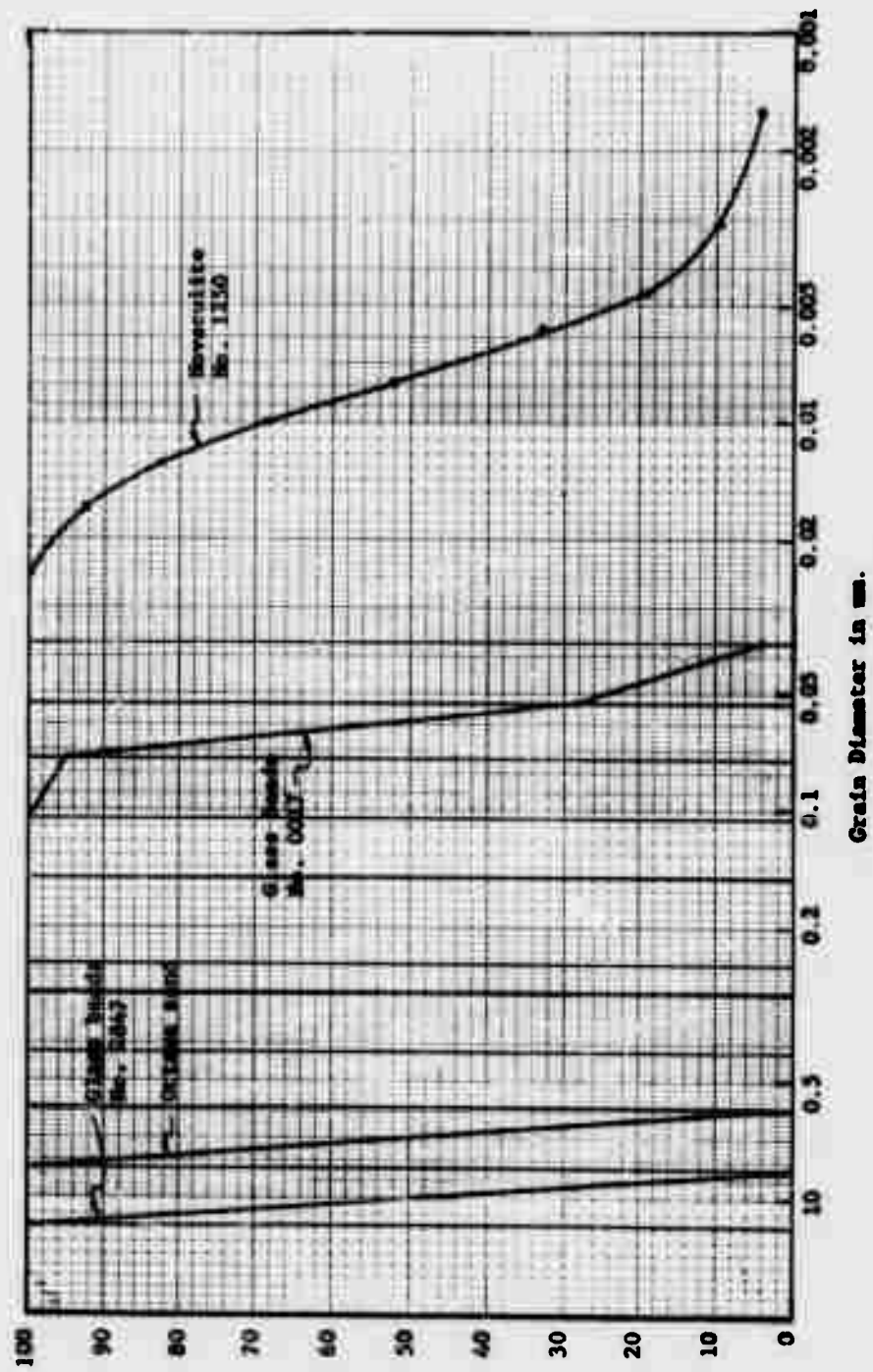
Fig. 3-1 - Grain size curves for the materials used in the present research.

Glass beads No. GO17. This material was also obtained from the Prismo Safety Corporation. These are very fine beads and near silt size. Ninety-five per cent pass the No. 200 sieve and 96 per cent are retained on the No. 400 sieve. They have a specific gravity of 4.31 which is very high. The reason for the high specific gravity is due to the fact that a high index of refraction is desired in their commercial use. The minimum void ratio for this material is 0.57 and the maximum void ratio is 0.76.

Novaculite No. 1250. This is a very fine quartz powder obtained from the American Graded Sand Co., 189-203 East Seventh Street, Paterson 4, New Jersey. This material was considered to be a silt as shown by the grain size curve in Fig. 3-1.

Tests

Three groups of tests were run and are summarized in Table 3-1 and as follows.

Group I. These tests were run with Ottawa sand to obtain data on the effects of amplitude, pore fluid (air, water and dilute glycerin), mode of vibration and density on velocity and damping for both torsion and compression.

Group II. After the tests of Group I were completed it was decided to run tests with the two sizes of glass beads described above in the dense condition both dry and saturated.

Group III. A torsional vibration test, as well as damping characteristics, was run on Novaculite No. 1250 in the dry condition.

Equipment of Previous Investigators

Several methods have been used to measure the stress wave velocities in a cylindrical specimen. The methods differ mainly in the

TABLE 3-1

Summary of Tests

Group	Test No.	Material	Void Ratio	Pore Fluid	Type
I	10	Ottawa sand	0.52	Air	Torsion
	11	Ottawa sand	0.67	Air	Torsion
	14	Ottawa sand	0.52	Water	Torsion
	21	Ottawa sand	0.64	Water	Torsion
	12	Ottawa sand	0.52	Air	Compression
	16	Ottawa sand	0.66	Air	Compression
	13	Ottawa sand	0.51	Water	Compression
	15	Ottawa sand	0.66	Water	Compression
	20	Ottawa sand	0.50	Dil. glycerin	Compression
	19	Ottawa sand	0.64	Dil. glycerin	Compression
II	25	Beads #2847	0.39	Air	Torsion
				Water	Torsion
	26	Beads #0017	0.58	Air	Torsion
				Water	Torsion
	23	Beads #2847	0.58	Air	Compression
				Water	Compression
	24	Beads #0017	0.58	Air	Compression
III	28	Novaculite	0.80 0.83	Air	Torsion

end conditions which are imposed or are assumed to exist.

Wilson and Dietrich (1960). The apparatus developed at the laboratory of Shannon and Wilson is shown in a schematic diagram in Fig. 3-2. An amplified audio-frequency signal is supplied to a driver unit adapted from a loudspeaker. For longitudinal vibrations the driver is directly connected by an aluminum rod to a clamped rim diaphragm of aluminum having a natural frequency several times greater than that of the soil specimen. For torsional vibrations the driver is directly connected to an aluminum clamp to provide a torsional twist to the specimen. The specimen rests on a brass plate and is enclosed with a lightweight cap and a rubber membrane. A standard phonograph crystal is suspended by rubber thread from a tie rod or stand and records the motion of the top cap on a cathode ray oscilloscope.

It is stated that the restraint of the specimen has been verified to correspond to the lower end clamp and the upper end free.

Hardin (1961). Hardin developed apparatus to measure shear wave velocities and compressive wave velocities for a soil specimen which was considered free at each end. Figure 3-3 shows a diagram of the driving equipment for each apparatus. A permanent magnet was attached to each end of the specimen by means of Plexiglas caps. For the compression wave the bottom magnet rested on rubber pads between electromagnets. The other end of the specimen was placed between two sets of coils which were identical to the driver, and these produced a signal which indicated the motion of the top of the specimen. The apparatus for torsional vibrations was identical except that the electromagnets were placed in a position that would produce torsional motion. In this case the specimen rested on a pivot.

Both types of equipment considered above have end conditions
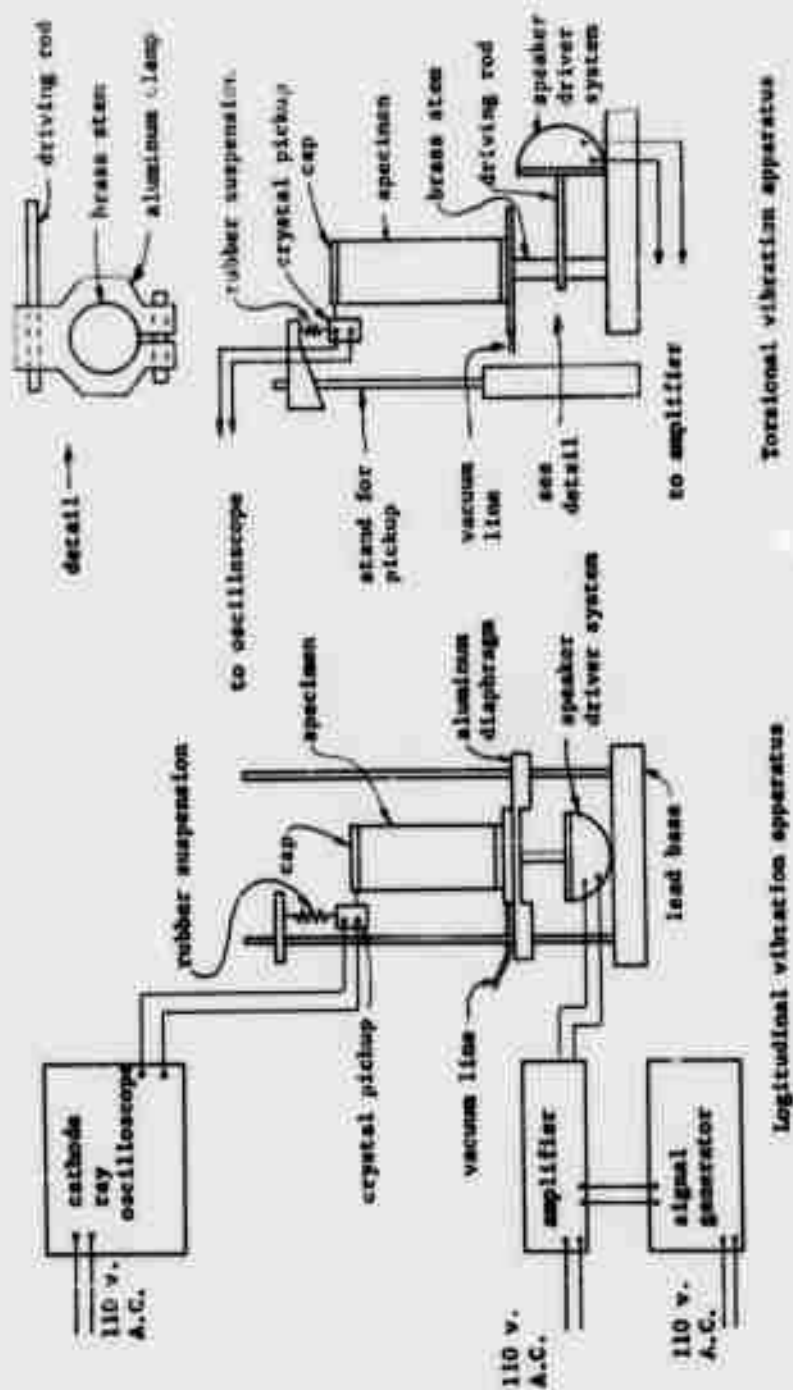
Fig. 3-2 - Schematic diagram of apparatus used by Wilson and Dietrich.
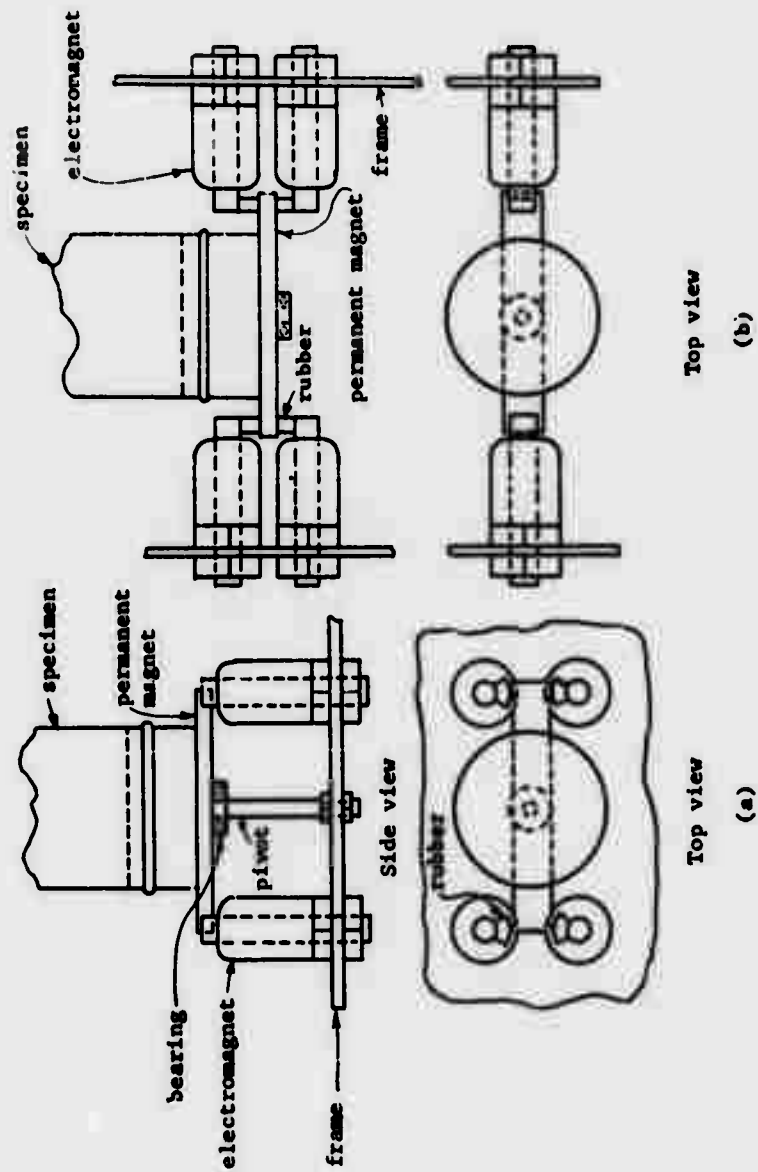
Fig. 3-3 - Drawing of vibration mechanisms used by Hardin (a) shear wave apparatus. (b) compression wave apparatus.

which are not completely specified. The equipment used by Wilson and
Dietrich is considered to be fixed at the driving end. If this were
true then there would be no vibrations in the specimen. The equipment
relies on the fact that at the natural frequency of the specimen very
little motion is needed at the base in order to maintain steady state
vibrations. The relative amount of motion between the top and bottom
of the specimen for small values of damping is such that the node is
very close to the base.
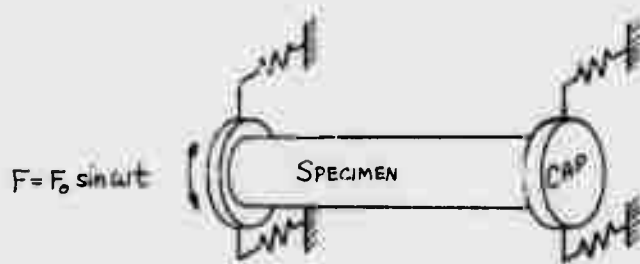
Fig. 3-4. - Model representing apparatus used by
Hardin.

A model of the conditions for the apparatus built by Hardin may
be considered as shown in Fig. 3-4. The torsional case is shown. The
rotational inertia of the end caps is represented by the discs at each
end of the specimen and the rubber pads are represented by springs.
The magnitude of the effect of the rubber pads is essentially indetermi-
nate. However, all of Hardin's tests were run at such small amplitudes
that this effect would be negligible.

Equipment for the Present Investigation

Several practical considerations must be made when deciding upon
the equipment for measuring the dynamic properties. The most important
thing to keep in mind is that the design must be as simple as possible,

otherwise, considerable time will be spent on refinement. In choosing between a free-free and a fixed-free type of test condition, the fixed-free condition has two main advantages. First of all, the end conditions are more easily determined, and second, the first mode of vibration will occur at one-half of the frequency for the free-free condition. Experience has shown that it is much easier electrically and mechanically to work with lower frequencies.

Two pieces of equipment were specially designed and built to vibrate the specimen at relatively large amplitudes with longitudinal and torsional vibrations. Each was based on the fixed-free condition. The equipment was different than that described above in that the base of the specimen was fixed to a large mass and the vibrations and displacements were applied and measured at the top of the specimen. (Fig. 3-5c)

Compression apparatus. The frame of the apparatus was built from a piece of 4" standard steel pipe. The base for bolting the aluminum bottom cap of the specimen was made out of a piece of steel 1/2" thick and 1-1/4" wide. The ends of the base were drilled and tapped with one hole on each end. Screws which fit through the sides of the pipe frame hold the base in place. The holes in the frame were drilled so that the base position may be adjusted in order to align the specimen vertically in the apparatus. In order to "fix" the base of the specimen the inside of the frame was lined with four sheets of lead 0.10" thick. This makes the mass of the specimen very small compared to the mass of the frame to which the specimen is bolted. The total weight of the above apparatus was 29 lb. as compared to 1.2 lb. for a specimen.

The driver and pickup used is shown in Fig. 3-5. The design of both the driver and pickup is similar to that of an ordinary loudspeaker. The coils were made by placing a piece of paper around a tube of the
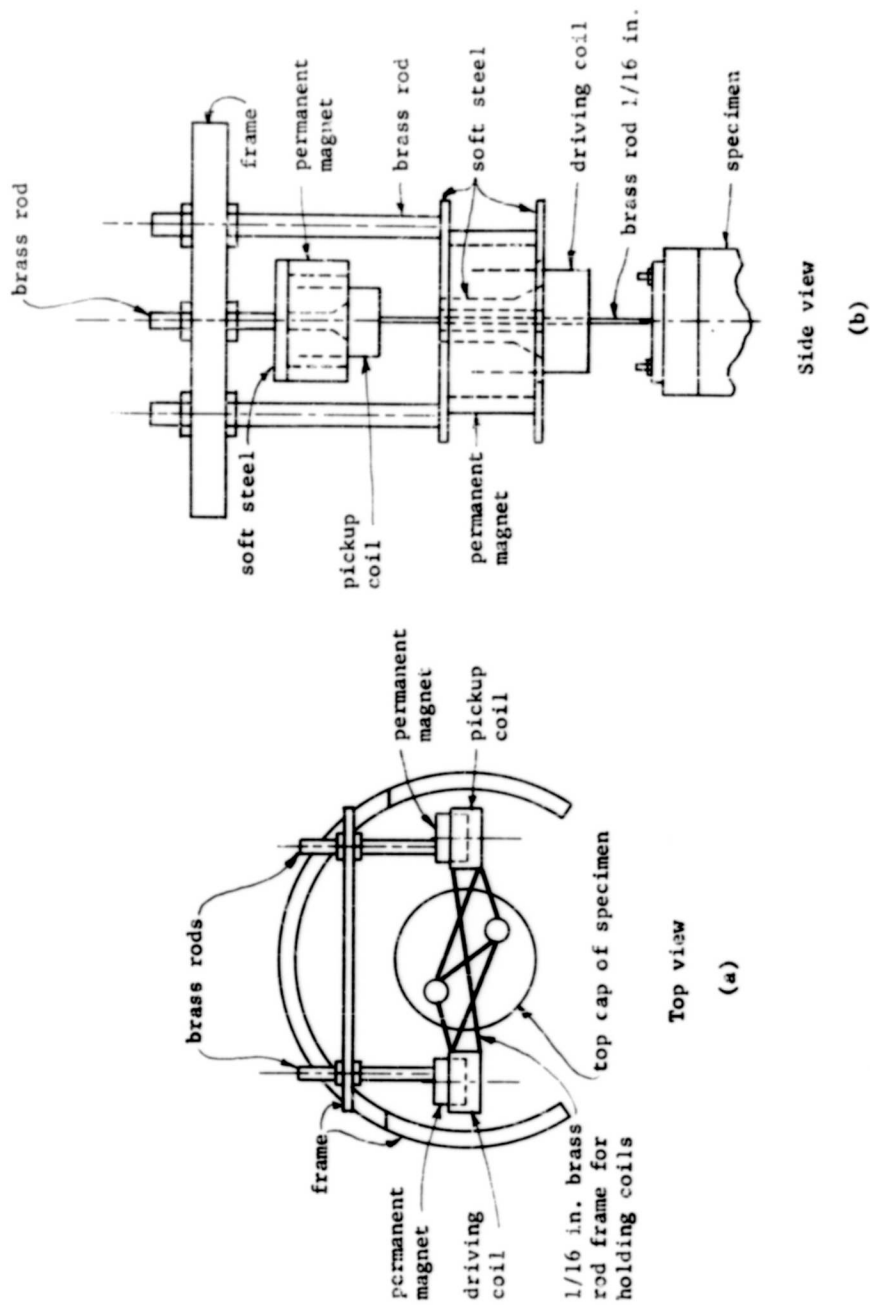
Fig. 3-5 - Vibration mechanisms used in present research (a) shear wave apparatus (b) compression wave apparatus.
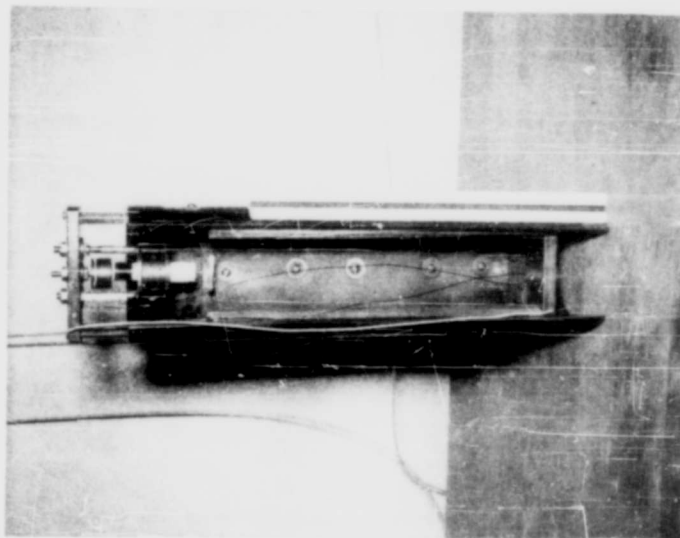
Torsion Apparatus
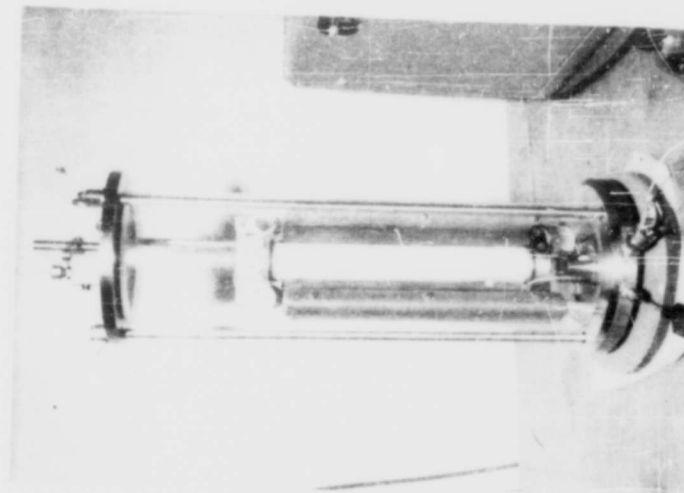
Compression Apparatus

Fig. 3-5c. - Fixed-free vibration equipment.

desired diameter. This paper is glued so that it will not unroll and
also be loose enough to be removed from the tube after the coil has been
wound upon it. After each layer of wire has been wound upon the paper
tube a layer of glue was applied to hold the coil together. If the coil
was to be used as a pickup a clear spray lacquer was used as a glue, but
for the driving coils it is necessary to use a glue that will withstand
high temperature. For this purpose "2-ton" brand epoxy glue was used.
It is absolutely necessary to insure that the loops of the coils are
rigidly held together, otherwise erratic wave forms will be recorded. It
is also essential to have a rigid connection of the coils to the top cap
of the specimen, i.e., the natural frequency of the connection must be
several times greater than the frequency range used in the experiments.
The driver and pickup must also be made as light as possible. The total
weight of the driver and pickup for the compression apparatus was 30.6 gm.

The permanent magnets were made from cylindrical Alnico V magnets.
Soft steel was machined and placed around the cylindrical permanent mag-
net so that the lines of flux would be concentrated in an annular opening
through which the coils would fit. The Alnico V is very hard and
brittle and cannot be machined easily. Therefore, it is necessary to
either glue or clamp the soft steel to the Alnico V. Non-magnetic ma-
terials should be used for clamping so that the magnetic flux is not
disturbed after the magnet has been constructed. The magnetism can be
increased several times by placing the finished magnet in a strong field.
If the soft steel is later removed it will be necessary to remagnetize
the magnet when it is put back together.

The magnets are fastened to the top of the frame by means of
threaded brass rods as shown in Fig. 3-5. These provide a means of ad-
justing the vertical position of the magnets. The holes through which

the threaded rods pass are much larger than the rods themselves. This allows a limited amount of movement so that the magnets may also be positioned with respect to the horizontal plane.

Torsion apparatus. The frame of the torsion apparatus is very similar to the frame of the compression apparatus except for the design of the driver and pickup, which is shown in Fig. 3-5. The coils were mounted in a frame constructed of brass rods 1/16" in diameter. The frame was made as rigid as possible while keeping the torsional inertia to a minimum. The permanent magnets were circular bar magnets which were mounted on the frame and projected into the center of the coil. Positioning of the magnet was accomplished by soldering a threaded brass rod in an off center position to the magnet. The threaded rod provided in and out movement and horizontal movement was obtained by rotating the eccentrically located rod. Vertical movement was accomplished by cutting a vertical hole in the frame of the apparatus.

The equipment described above could be used to measure the resonant frequencies for torsion and compression and also the decay curves after vibration in a steady state condition by cutting off the power to the driving coil. The decay curves were recorded photographically on an oscilloscope.

Commercial apparatus. An MB Electronics Type P 11, Model T 135234 power supply was used for driving the coils in the vibration apparatus and also for driving an MB Electronics Model C 31 pickup calibrator. The range of the Model C 31 calibrator is 5 to 1000 cycles per second with a maximum force vector of 25 lb. A probe type pickup, Model 115, also manufactured by MB Electronics was used for measurement of vibration amplitudes and for calibration. A Tektronix Model 502 dual beam oscilloscope was used for the measurement of output from the pickups and drivers.

Decay curves for damping measurements were recorded with a Dumont Type 450 oscilloscope camera.

The apparatus for measuring vibrations was placed in a triaxial cell for testing. The triaxial cell was manufactured by Geonor A/S, Oslo-Blindern, Norway. In order for the testing equipment to fit inside the cell a longer Plexiglas tube and fastening rods were made. Air was used for the confining pressure and pressures from 0 to 50 lb./in.^{2} were measured by a mercury manometer.

Electrical measurements

A schematic wiring diagram for the testing apparatus is shown in Fig. 3-6. Details of the high pass filter, attenuater and phase shifter, and time delay and triggering mechanism are shown in Figs. 3-7, 3-8 and 3-9.

Measurements were made on the oscilloscope which showed the input voltage to the driver and the output voltage of the pickup. However, due to the mutual inductance between the driving coil and the pickup coil, the output voltage of the pickup does not represent the motion of the pickup. It is necessary to compensate for this induction by applying a signal of equal magnitude and phase relationship to the differential input connection of the upper beam. The attenuater and the phase shifter is adjusted to give a correction of the correct amplitude and phase relationship. The frequency characteristics of the compression apparatus are such that the high pass filter is used with the phase shifter and attenuater. For the torsion apparatus it was not necessary to use the high pass filter. The adjustment of the induction correction was made by setting the frequency so that it was not near resonance and adjusting the attenuater and phase shifter so that there was no signal from the pickup. If the adjustment is correct then there should be practically no amplitude at each side of the resonant frequency. The adjustment is good for a limited frequency.
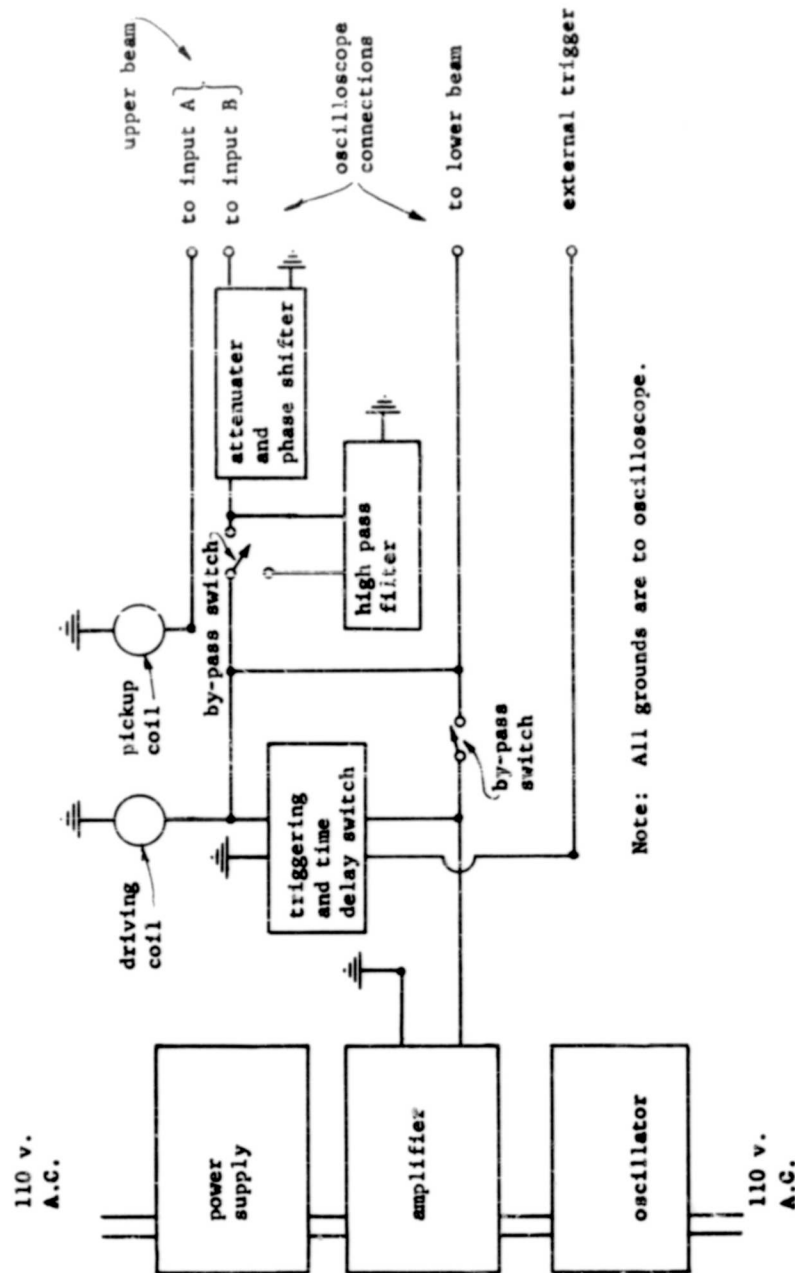
Fig. 3-6 - Schematic diagram of electrical equipment.
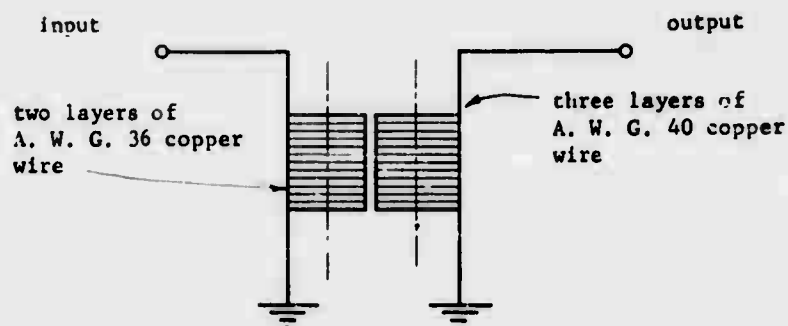
Fig. 3-7 - Detail of high pass filter.
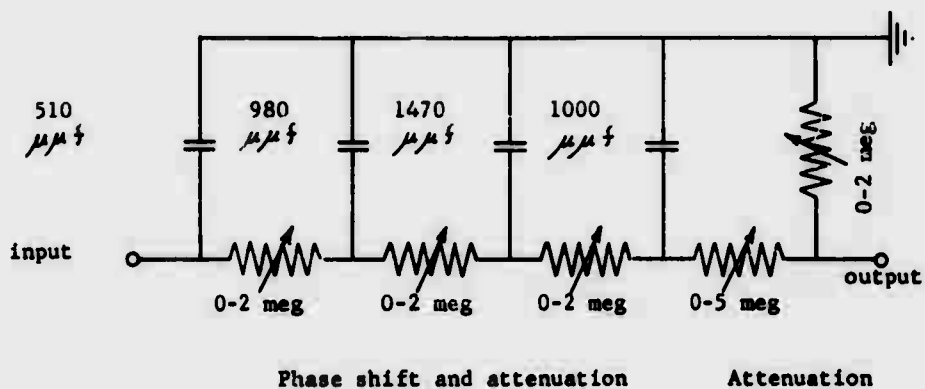
Fig. 3-8 - Detail of attenuater and phase shifter.

range and must be readjusted for each mode of vibration.

The time delay switch and triggering mechanism was used in the measurement of the decay curves. Its function was to trigger the sweep on the oscilloscope and then cut off the power to the driver after a small
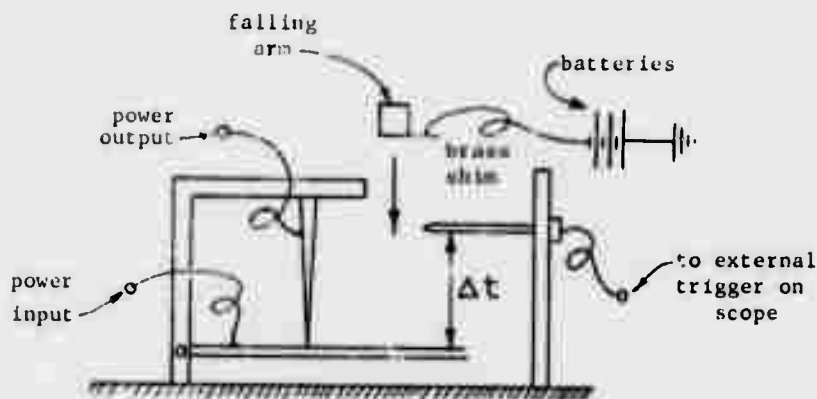
Fig. 3-9. - Detail of triggering and time delay switch.

time delay. The oscilloscope was triggered by an electric pulse from three small flashlight batteries connected in series. A hinged arm was dropped which would momentarily close a contact to trigger the oscilloscope and then fall a short distance and cut off the power to the driving coil. The distance that the arm fell after triggering the scope determined the time delay. This distance was adjustable. When only steady state vibrations were being made the triggering apparatus was disconnected.

TEST PROCEDURES

Preparation of membranes

The membranes for the test specimens were made at first with a liquid latex compound obtained from Testlab Corporation, Chicago, Illinois.

When this material was used up, the membranes were made from a liquid latex Type Vultex 1-V-10 from the General Latex and Chemical Corporation, 665 Main Street, Cambridge 39, Massachusetts. The latex used first had to be diluted to three parts latex and one part water, while the other was diluted to seven parts latex to one part water. Molds were made from 38 mm. glass tubing 14 in. long with rubber stoppers in each end. These were dipped into the liquid latex and allowed to dry a minimum of four hours between dips. Around eight to ten dips were used for each membrane. It was found that the latex was affected by absorption of water and to prevent this, the latex membranes were dipped in a liquid neoprene Type Vultex 3-N-10, which was also obtained from the General Latex and Chemical Corporation. The layer of neoprene was then placed on the inside next to the specimen.

The membrane was removed from the mold by first dusting the outside with talcum powder and then cutting off the ends with a razor blade. Next, the membrane was peeled from the mold and the inside was dusted with talcum powder.

Preparation of the specimen

The soil specimens were approximately 1.5 in. in diameter and 11 in. long. The top cap was made of Plexiglas and the bottom cap was made of aluminum as shown in Fig. 3-10. Rubber O-rings were used to hold the membrane against the cap. Dow Corning silicone stop-cock grease was used between the membrane and caps to provide a good seal.

When dealing with granular materials it is necessary to use a mold in forming the specimen. The mold was made from a piece of PVC tubing which was cut to form two halves. Tubes were placed on each half for vacuum line connections and filter paper strips were placed on the inside to allow a good distribution of the applied vacuum.
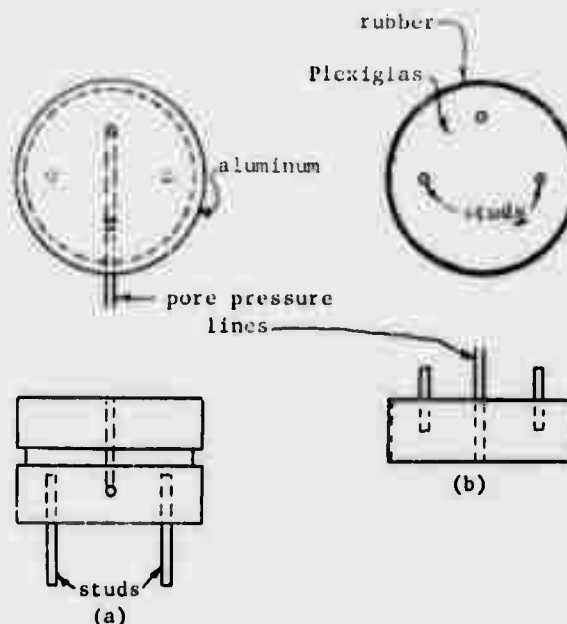
Fig. 3-10. - End pieces used with specimens (a) bottom cap (b) top cap.

The bottom cap was greased and the membrane was placed around it. The mold was then clamped around the cap and membrane with a hose clamp. The inside diameter of the mold was such that it fit snugly against the membrane, sealing off the end of the tube. The opposite end of the membrane was stretched over the end of the mold and a vacuum was applied which held the membrane securely against the inside of the mold.

Several methods were used for placing the soil into the mold, depending upon the soil type and density desired. For the Ottawa sand and the glass beads the dense condition was obtained by pouring in approximately 50 ml. layers and vibrating each layer with a 1/8 in. brass rod attached to a small vibrator. This resulted in a condition close to 100 per cent relative density. The loose condition for the Ottawa sand was obtained by pouring the sand through a funnel attached to a 3/16 in. internal diameter glass rod which extended to the bottom of the mold. The rod was kept full of sand and slowly retracted from the mold allowing the

3-21

sane to be deposited i. loose condition. The specimens prepared with
the Novaculite No. 1250 were compacted. Since the material is very fine
a special procedure had to be followed A vacuum was applied to the
bottom pore pressure line during the compaction to prevent the material
from blowing out of the mold and also as an aid to compaction. A teaspoon
of material was added and pressed five times with a No. 7 rubber stopper
attached to the end of a standard Proctor miniature compactor. Prior to
construction of the specimen the Novaculite was dried in the oven at
220° C. for a period of several days.

Recording of data

Sample data are shown in Tables 3-2, 3-3 and Fig. 3-11. Table 3-2
shows the data taken for computation of void ratio and the relation-
ships for velocity and modulus in terms of frequency. The volume of the
specimen was corrected for the membrane by weighing the membrane and
computing its volume on the basis of a unit weight of 0.92 gm. per cm.^{3}

The measurements recorded for the velocity and damping were
taken after the electrical equipment had warmed up a minimum of 30
minutes. There is considerable drift in calibration as the equipment
warms up and accurate measurements cannot be made during this period.

The variation of velocity with amplitude was recorded for the
first mode of vibration. Each amplitude was approximately half of
the preceding one which corresponds to the successive scales on the
oscilloscope. With a maximum of 6 volts peak to peak applied to the
torsional driver the double amplitude of vibrations was approximately
2×10^{-3} radians depending upon the shear modulus, damping and
density of the specimen. Since the torsion driver consists of a force
applied to a lever arm from the top of the specimen. both bending
and torsional modes of vibration will be measured. This is shown in

TABLE 3-2

Typical Data Sheet

Test No. 23
Material: glass beads #2347
Specific gravity: 2.499

Type of test: longitudinal wave
Driver and pickup dimensions:
A = 0.37"   B = 0.83"
Weight = 30.6 gm.

Beaker + specimen	= 854.22 gm.
Beaker - specimen	= 325.39 gm.
Dry weight of specimen	= 528.83 gm.

Weight of membrane = 12.65 gm.
Initial diameter in cm.

4.03	4.04	4.03	4.03	4.03
4.06	4.08	4.07	4.06	4.05
4.05	4.06	4.04	4.04	4.03
4.00	4.00	4.00	4.00	4.00

Relationships for velocity:

	Dry	Saturated
$\dfrac{\text{Wt. of specimen}}{\text{Wt. of driver}}$ =	17.3,	21.3
1st mode =	$3.791 \times f$,	$3.753 \times f$ ft./sec.
2nd mode =	$1.262 \times f$,	$1.250 \times f$ ft./sec.

Average diameter = 4.035 cm.
Initial height = 10.75", 10.76", 10.74"
Average height = 10.75 in., 27.30 cm., 0.896 ft.

Unit weights:

dry = 1.577 gm./cm.^{3}

sat = 1.946 gm./cm.^{3}

Total volume of specimen	= 349.90 cm.^{3}
Volume of membrane	= 13.75 cm.^{3}
Volume of specimen	= 335.34 cm.^{3}
Volume of beads	= 211.62 cm.^{3}
Volume of voids	= 123.72 cm.^{3}

Void ratio   = 0.585

TABLE 3-3

Typical Data for Velocity

Velocity Data

Frequency c.p.s. Press.	Output cm. = 5.0 psi	Frequency c.p.s. Press.	Output cm. = 10.2 psi	Frequency c.p.s. Press.	Output cm. 24.9 psi	Frequency c.p.s. Press.	Output cm. 50.6 psi
	5 mv/cm		5 mv/cm		5 mv/cm		5 mv/cm
138	3.28	150	5.50	186	5.18	218	6.70
		462	3.22	541	4.60		
	2 mv/cm		2 mv/cm		2 mv/cm		2 mv/cm
142	5.24	154	6.66	188	6.42	220	5.16
426	7.22	469	4.18	549	5.26	643	3.06
		156	4.16	189	3.96		
	1 mv/cm		1 mv/cm		1 mv/cm		1 mv/cm
144	7.20	159	5.30	190	5.10	222	5.44
436	7.08	472	4.78	550	5.98	643	6.10
145	4.72					642	3.89
	0.5 mv/cm		0.5 mv/cm		0.5 mv/cm		0.5 mv/cm
148	5.30	160	4.90	191	4.78	223	5.44
441	6.06	476	6.36	551	6.94	641	6.10
						642	3.89
							0.2 mv/cm
						224	3.6
						641	2.0

Fig. 3-11. - Typical decay curves.

Fig. 3-12 which shows the second mode for bending and the first mode for torsion. For small values of damping the amount of bending at the natural frequency for torsion will be insignificant. The bending and torsion may be distinguished by the phase relationship between the driver and the pickup. For bending the motion of the driver and pickup is in phase but for torsion they are in opposite phase. This is easily seen on the oscilloscope.
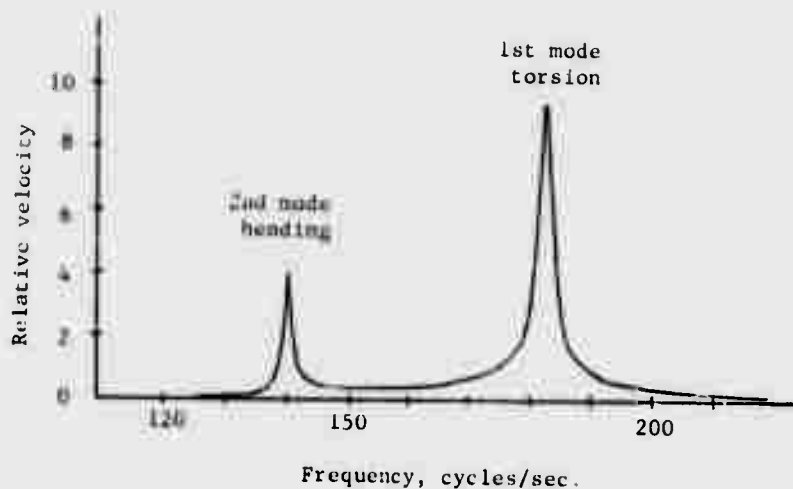
Fig. 3-12. - Resonance curves obtained with torsion apparatus.

With a maximum of 8 volts peak to peak applied to the compression driver a double amplitude of approximately 1×10^{-3} in. could be obtained. It was noted that at some pressures the bending mode of vibration and the compression mode were near the same frequency. This showed up as two resonances very close together. A change in position of the driving coil did not seem to correct this condition but it was found that a slight change in confining pressure would help remove the condition. The maximum effect of this condition seemed to occur near a confining pressure of 25 lb./in.^{2}

C. PRESENTATION OF RESULTS

Stress Wave Velocities

<u>Group I</u>

Figures 3-13 through 3-18 show the results for the velocity of torsional and longitudinal waves calculated from the tests of Group I on Ottawa sand. In these tests the variation of velocity with confining pressure, density, pore fluid (air, water and dilute glycerin) and amplitude of vibration was determined. The confining pressures chosen for each test were approximately 5, 10, 25 and 50 lb./in.^{2} and the results at each pressure are plotted in the same figure. Tests were run at both loose and dense conditions corresponding to a void ratio of approximately 0.65 and 0.51 respectively. The amplitude of vibrations was varied over the range of the smallest measurable vibration to the maximum attainable with the equipment which was approximately 5×10^{-4} in. for compression and 1.5×10^{-3} rad. for torsion. The ratio of magnitudes of any two successive amplitude measurements is approximately 2:1 as this corresponds to the ratio of two successive sensitivity settings of the oscilloscope.

Figures 3-13 through 3-16 show comparisons of velocity between dry and saturated specimens at the first mode of vibration. Figures 3-13 and 3-14 are torsion tests with loose and dense specimens respectively. Similar figures for the compression tests are shown by Figs. 3-15 and 3-16. In addition the tests in which the first and second mode velocities were measured are plotted individually. The second mode velocity could not be measured in the early compression tests since the apparatus was not fully developed until after test No. 15.
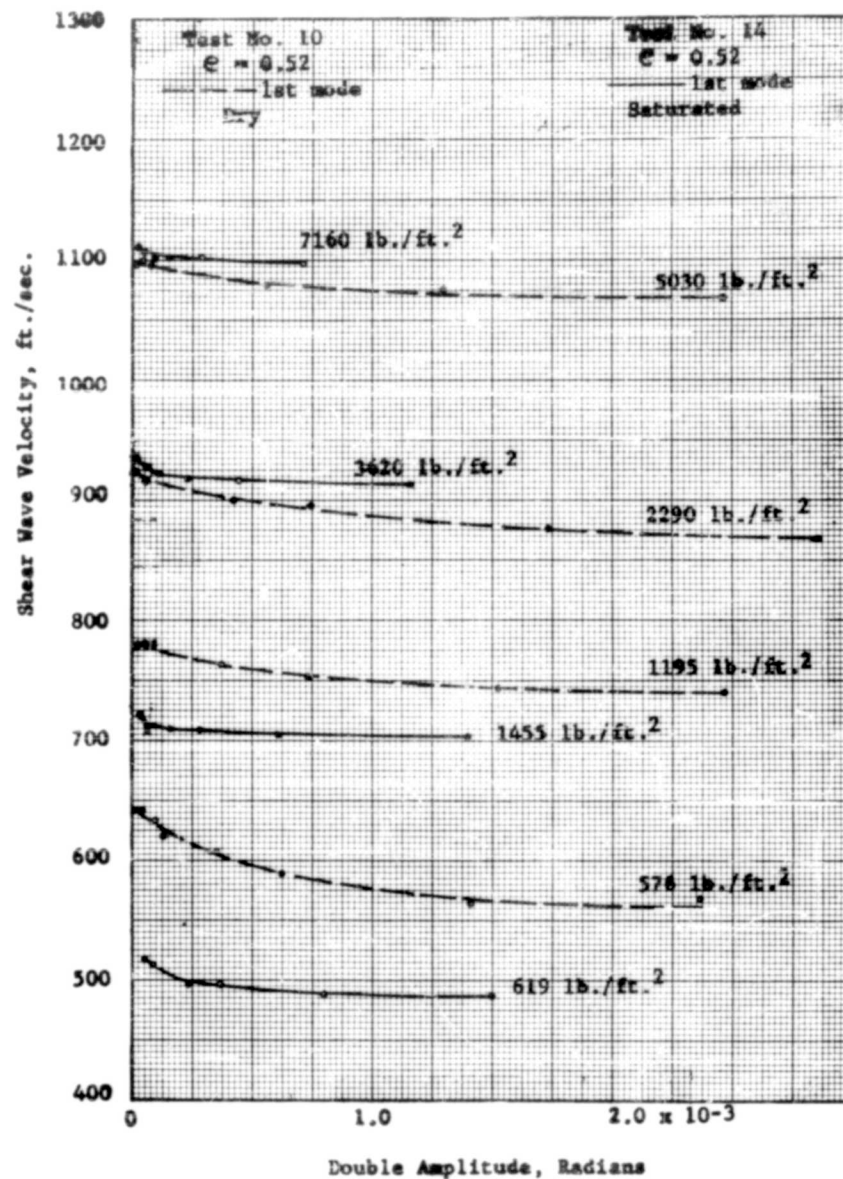
Fig. 3-13 Variation of velocity with amplitude for Ottawa sand dry and saturated with water.
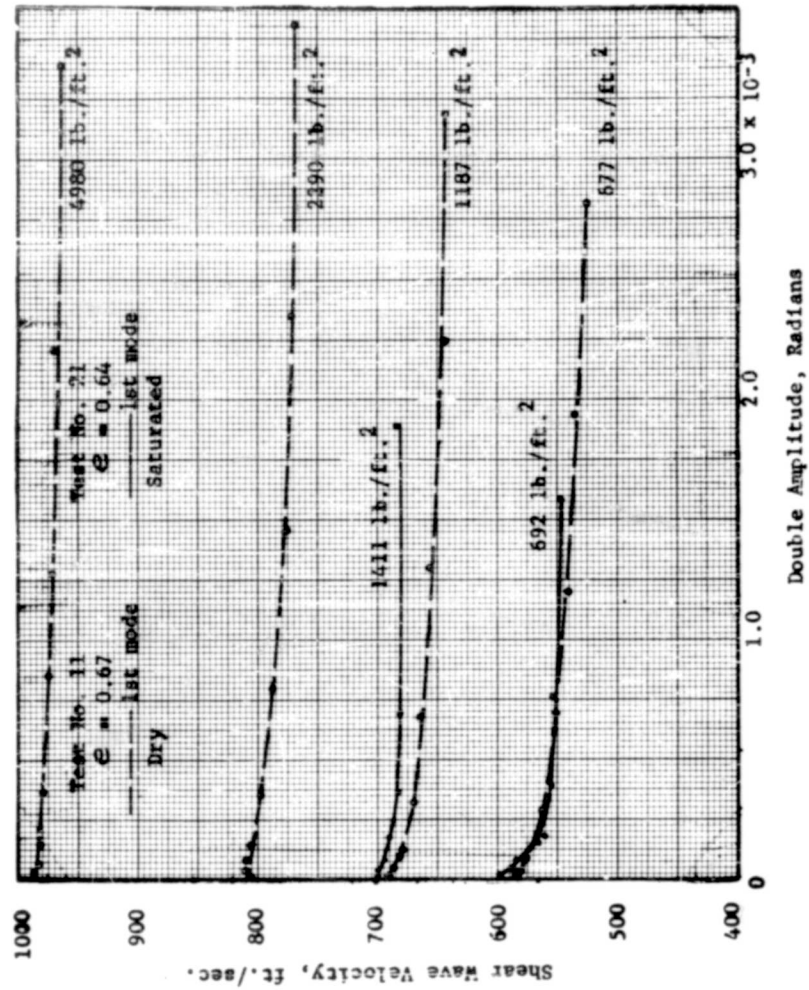
Fig. 3-14 Variation of velocity with amplitude for Ottawa sand dry and saturated with water.
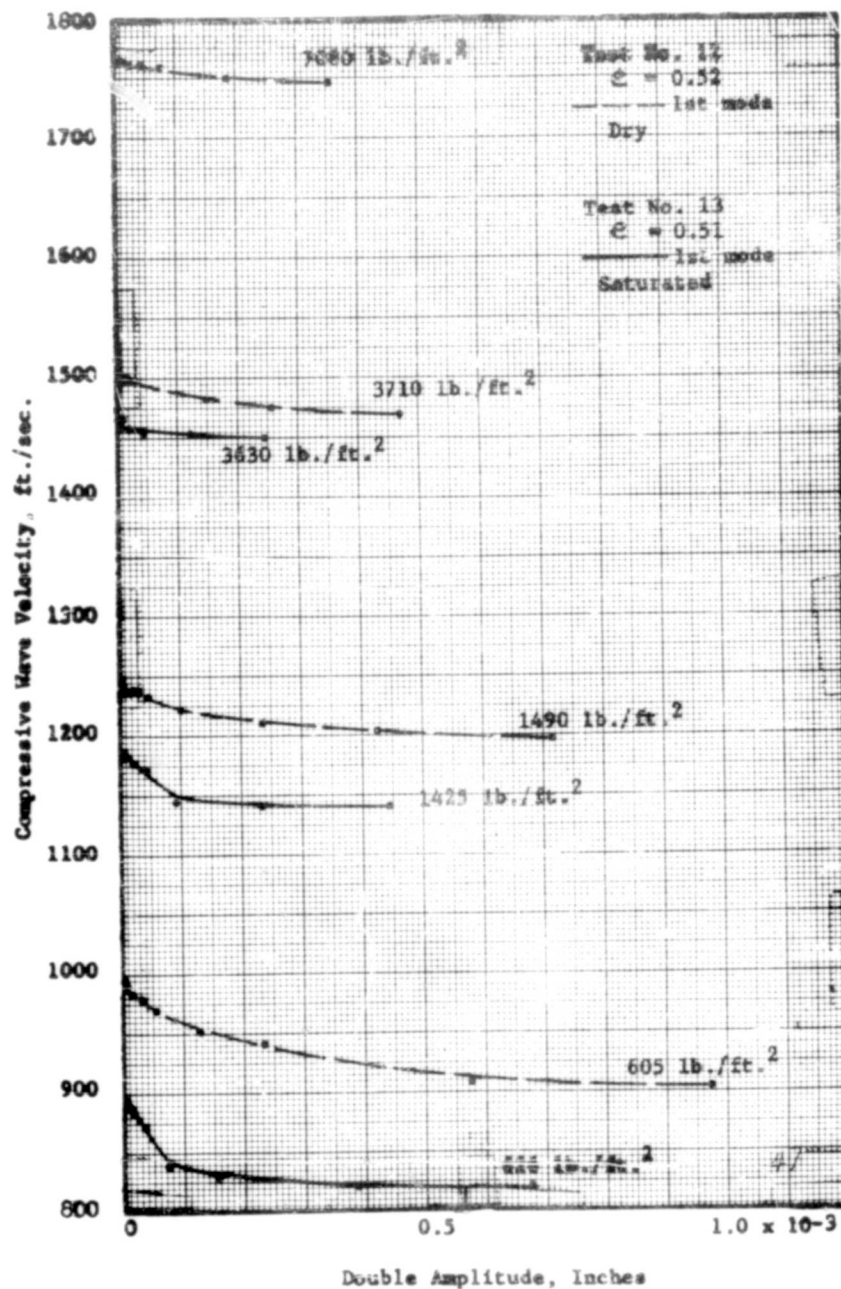
Fig. 3-15 Variation of velocity with amplitude for Ottawa sand dry and saturated with water.
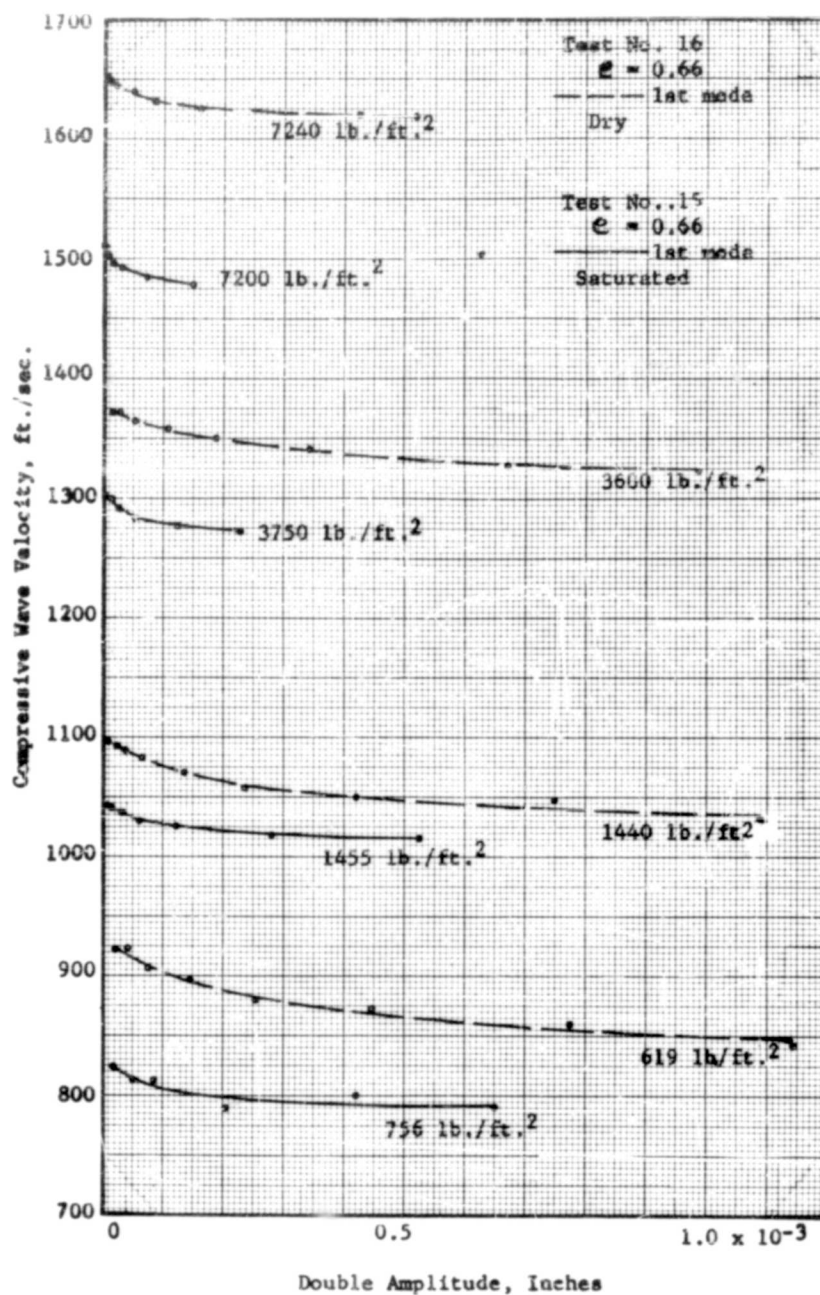
Fig. 3-16 Variation of velocity with amplitude for Ottawa sand dry and saturated with water.
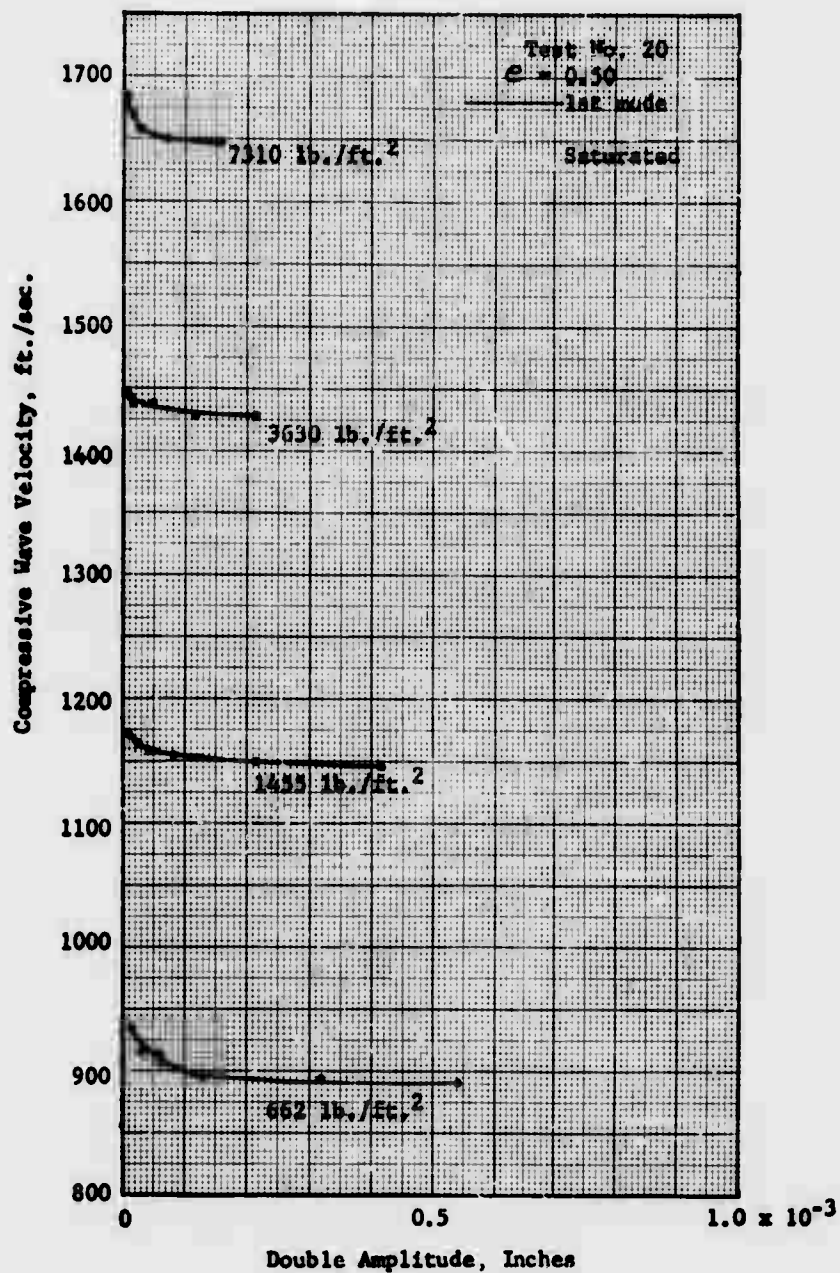
Fig. 3-17 - Variation of velocity with amplitude for Ottawa
sand saturated with dilute glycerin.
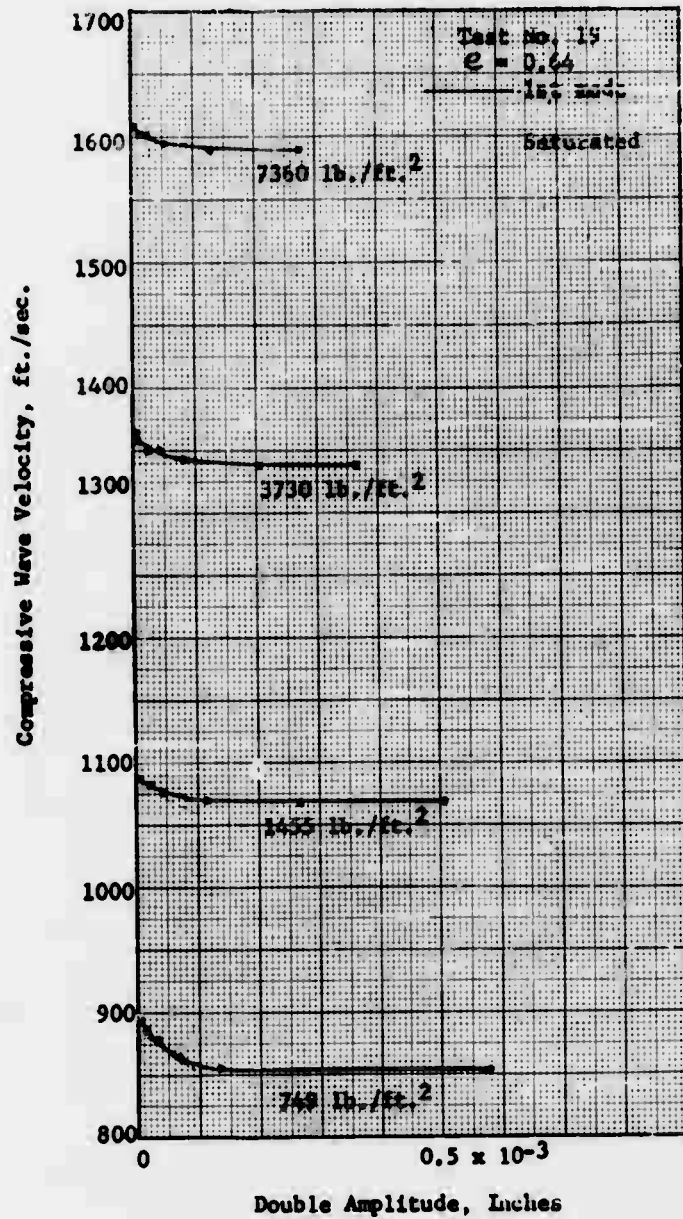
Fig. 3-18 Variation of velocity with amplitude for Ottawa
sand saturated with dilute glycerin.

Group II

The velocity test results for the glass beads are shown in Figs. 3-19 through 3-22. These tests included two sizes of beads one of which corresponds to a grain size near Ottawa sand and the other a silt grain size. The tests were performed the same as those in Group I except that only the dense condition was tested. This corresponded to a void ratio of around 0.58 for both sizes of beads. The large beads had a specific gravity of 2.499 which is slightly less than Ottawa sand but the silt size beads had a specific gravity of 4.31 which is much greater than most soils. Each specimen except that for test 24 was tested in the dry condition and then in the saturated condition. The results are plotted to show the comparison of dry and saturated conditions of each test.

Group III

Velocity tests were run on a compacted specimen of Novaculite No. 1250 with the torsion apparatus. This is a crushed quartz material with ten per cent of the particles less than 0.002 mm. The behavior of this material is quite different than for that of Ottawa sand and glass beads due to the very small grain size. The stress wave velocities depend upon time as well as stress history. During test 28, which started at a void ratio of 0.83 under a pressure of 14 psi, the specimen consolidated to a void ratio of 0.80 after having been subjected to a stress cycle with confining pressures as high as 50 lb./in.[2]

The computed velocities from the tests on Novaculite are shown in Figs. 3-23 and 3-24. A pressure was applied to the specimen and frequency readings were taken at different time intervals after the pressure increment was applied. These time intervals are noted in the figures and represent the total elapsed time after the pressure
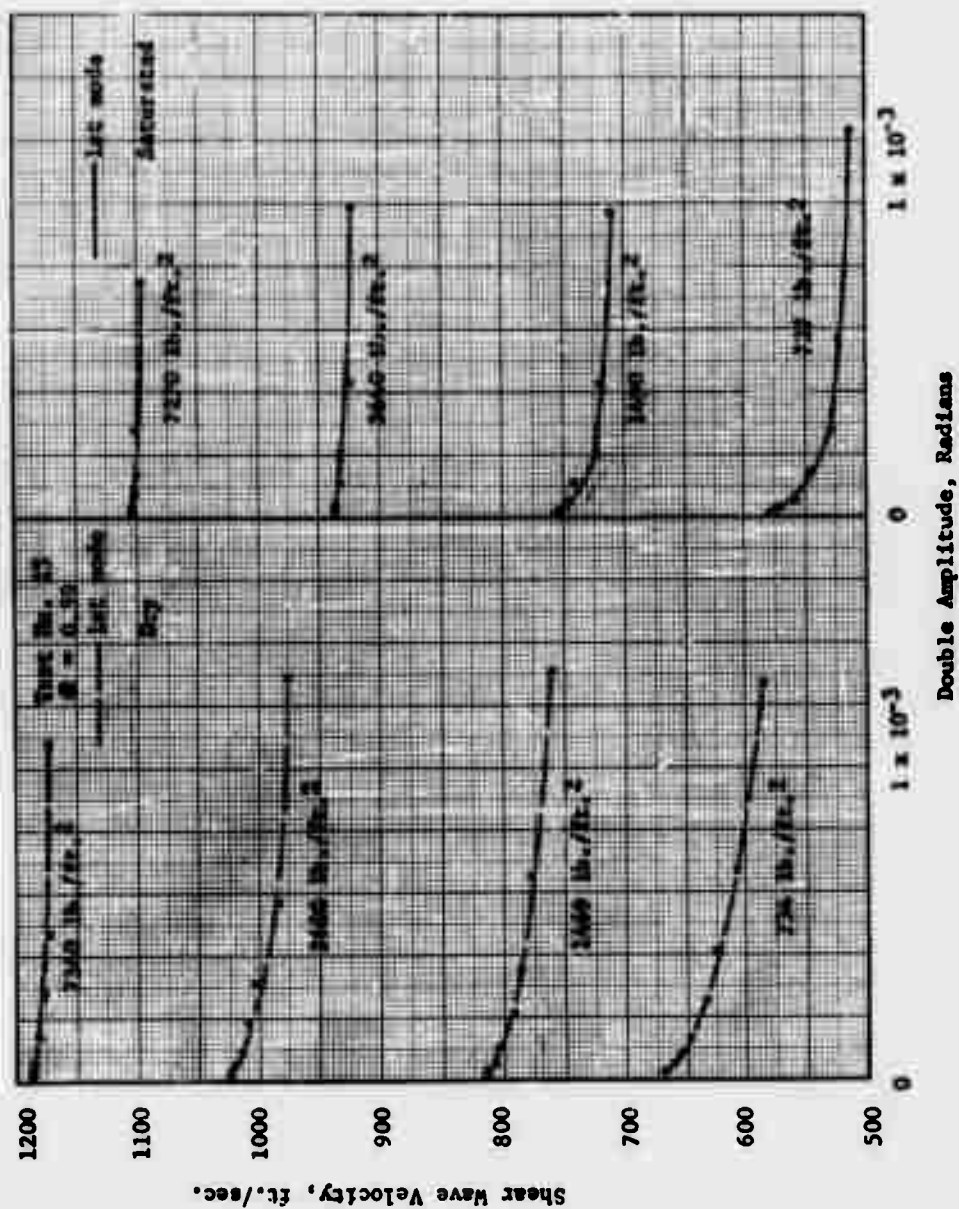
Fig.3-19 - Variation of velocity with amplitude for glass beads No. 2847 in the dry and water saturated condition.
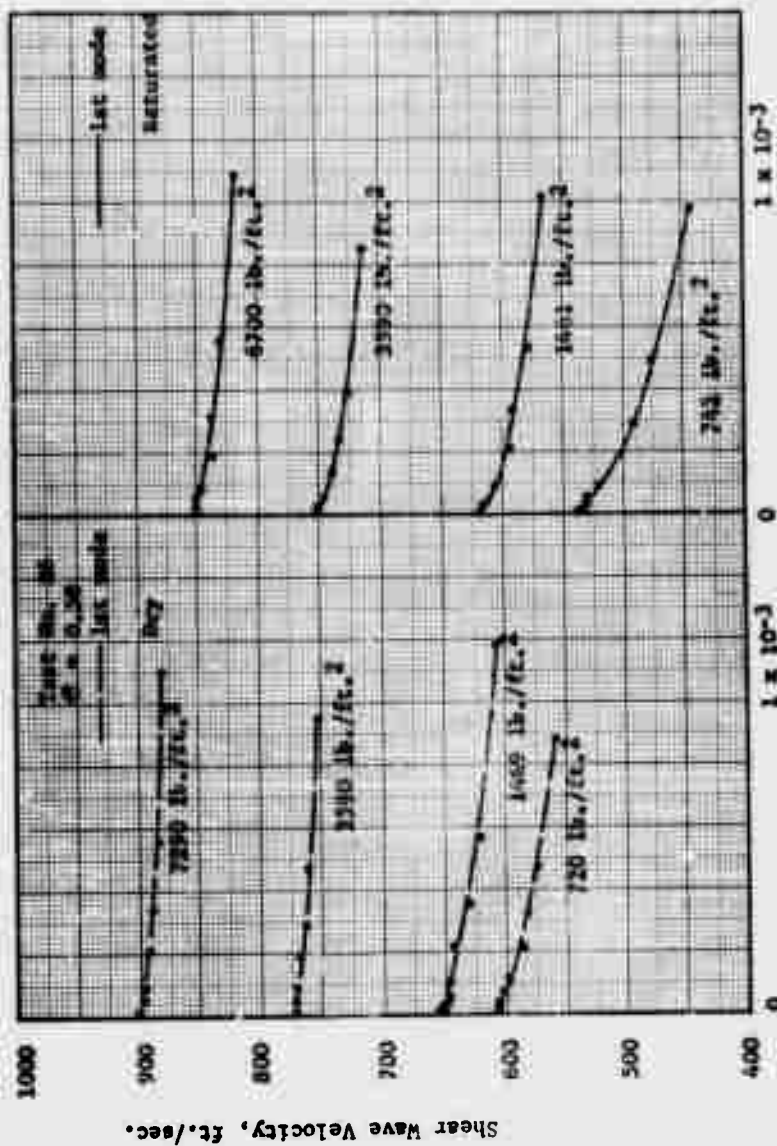
Double Amplitude, Radians

Fig.3-20 - Variation of velocity with amplitude for glass beads #0017 in the dry and water saturated condition.
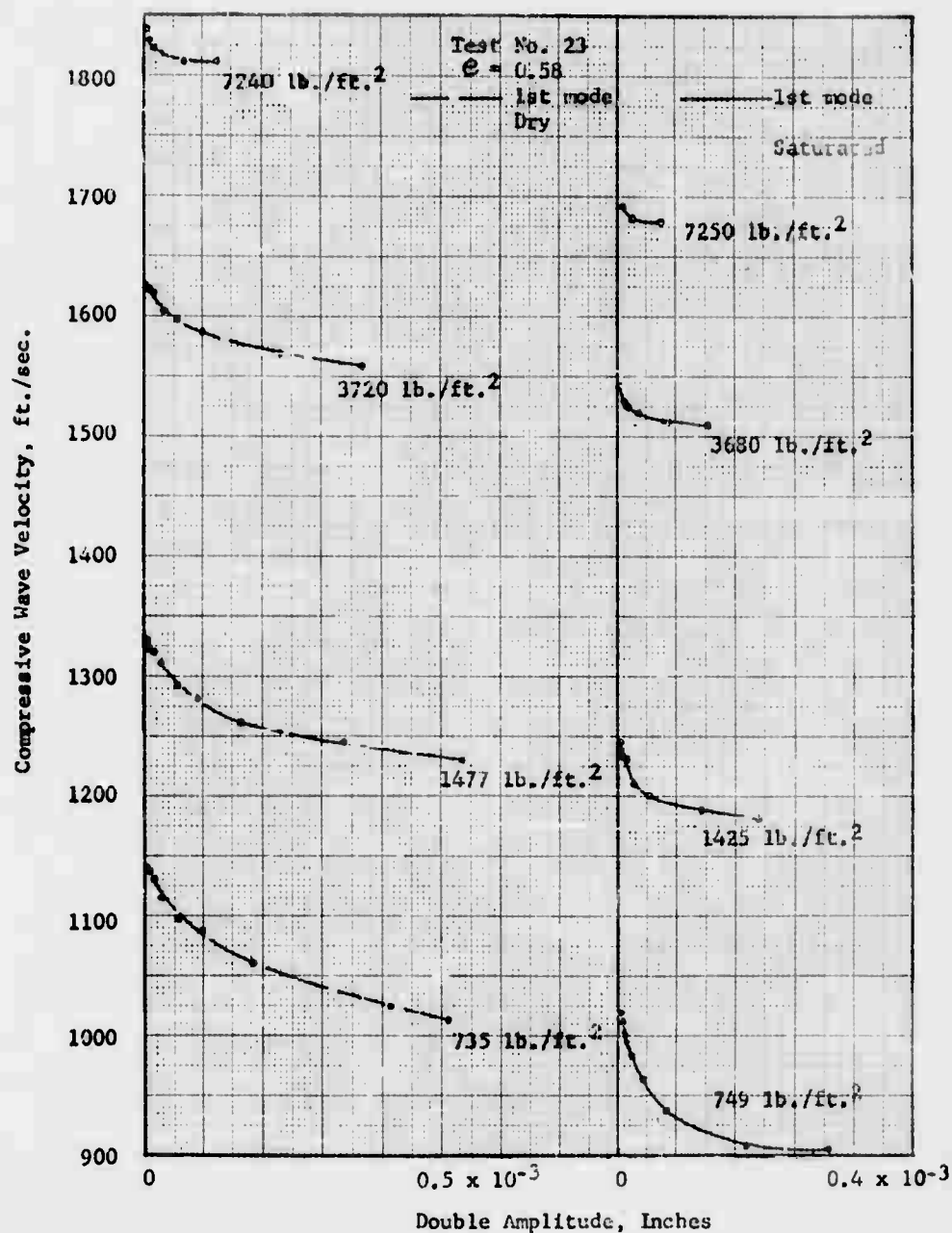
Fig. 3-21 - Variation of velocity with amplitude for glass beads
No. 2847 in the dry and water saturated condition.
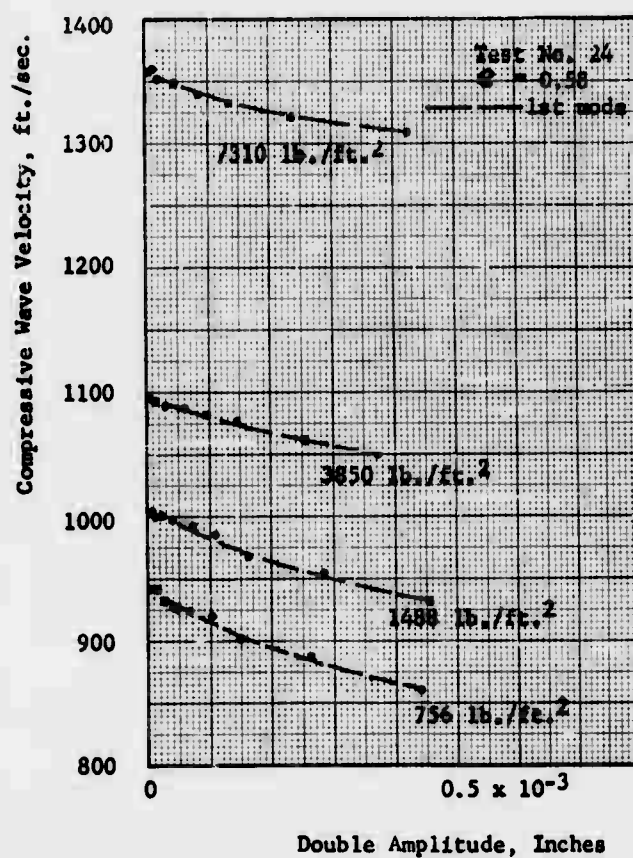
Fig. 3-22 - Variation of velocity with amplitude for glass beads
No. 0017 in the dry condition.
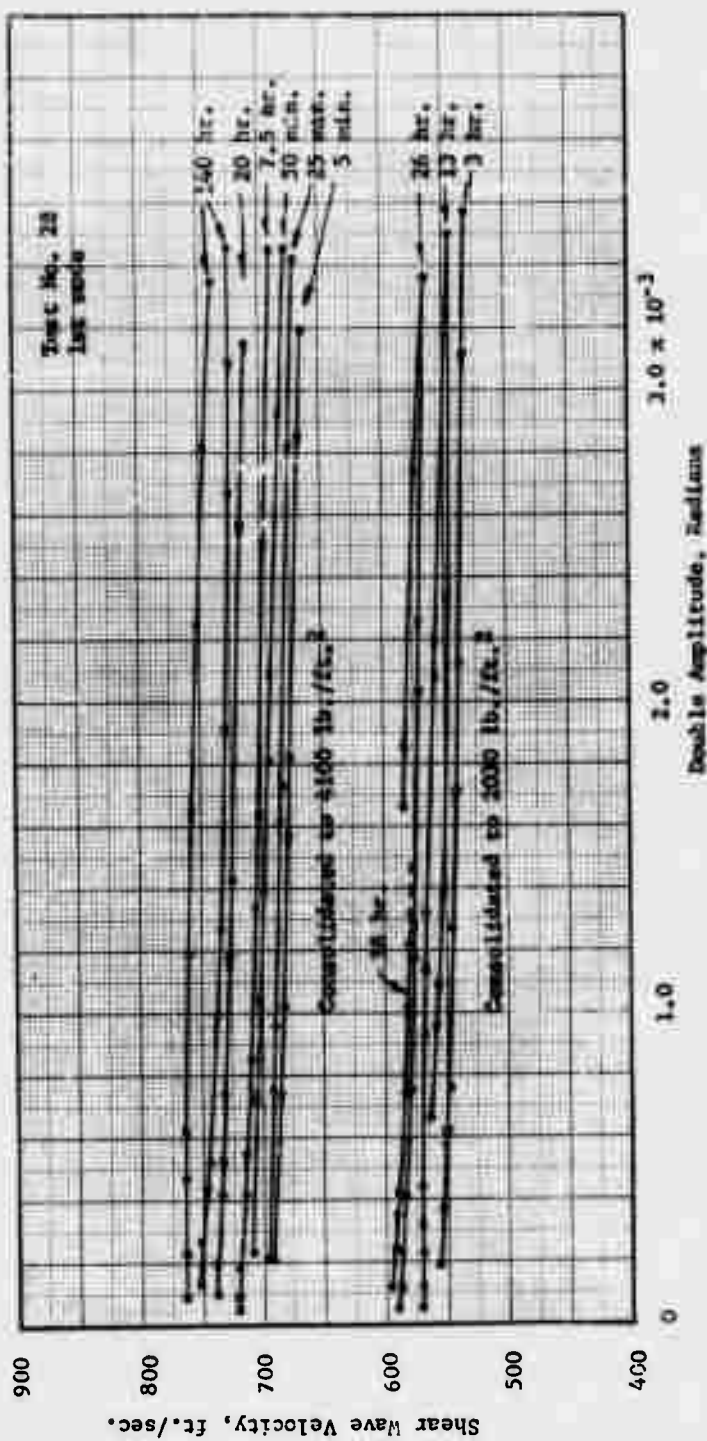
Fig. 3-23 Variation of velocity with amplitude for Novaculite No. 1250 consolidated to 2030 lb./ft.^{2} and 4100 lb./ft.^{2}
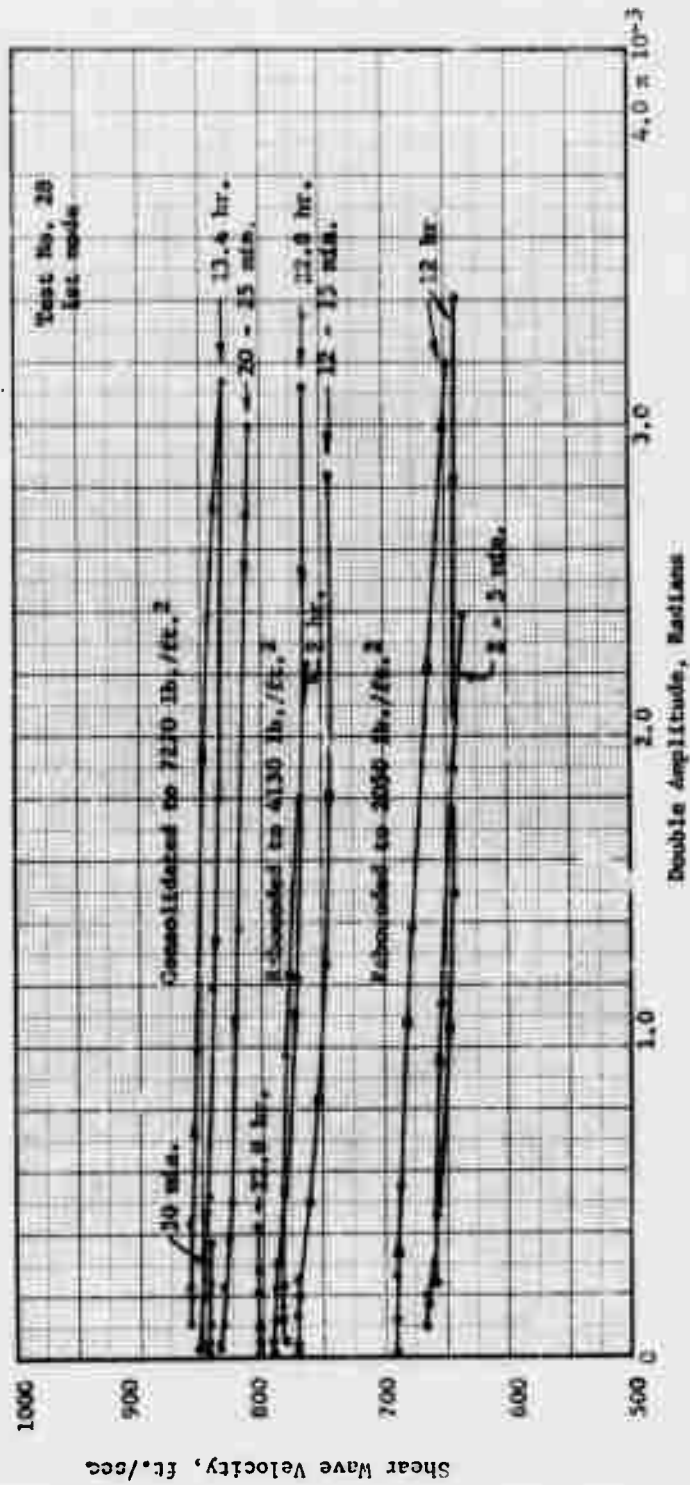
Fig. 3-24 Variation of velocity with amplitude for Novaculite No. 1250 consolidated to
7270 lb./ft.2 and rebounded to 4130 lb./ft.2 and 2050 lb./ft.2

was applied to the specimen. The stress history of test No. 28 was as follows.

1. The specimen was compacted and placed under a vacuum. Measurements were made for void ratio giving a value of $e = 0.83$.

2. The specimen was placed in the triaxial cell and a pressure of 2030 lb./ft.^{2} was applied. Velocity and damping measurements were made intermittently over a period of 38 hr.

3. The pressure raised to 4100 lb./ft.^{2} Velocity and damping measurements were made intermittently over a period of 140 hr.

4. The pressure was rebounded to 2050 lb./ft.^{2} and measurements of velocity and damping were made intermittently over a period of 12 hr.

5. The specimen was placed under a vacuum and measurements were made for void ratio which gave a value of $e = 0.81$.

6. The specimen was replaced and the triaxial cell and the pressure was raised to 7270 lb./ft.^{2} Measurements of velocity and damping were made intermittently over a period of 13 hr.

7. The pressure was reduced to 4130 lb./ft.^{2} and measurements of velocity and damping were made intermittently over a period of 30 hr.

8. Final measurements under a vacuum gave a value of $e = 0.80$.

The Novaculite properties were not only sensitive to time and stress history but also to vibrations. During the time intervals between measurements the specimen was not vibrated. The first measurements after each time interval were made at low amplitudes of vibration. The

following measurements were made at increasing amplitudes until the maximum amplitude obtainable with the apparatus was reached. Since the high amplitude vibrations affect the low amplitude measurements a second set of measurements were usually taken after the specimen had been vibrating at high amplitude for a period of approximately five minutes. These two methods of measurement are indicated in the figures by arrows on each curve.

Damping

Group I

Figures 3-25 through 3-29 show the results of logarithmic decrement for Ottawa sand obtained from decay curves of Group I. In general the decay curves were such that the logarithm of amplitude plotted against wave number on semi-log paper was a straight line. The slope of this line represents the value of logarithmic decrement which is computed from the relationship given by Eq. (112). This value of logarithmic decrement was taken to be the value corresponding to an amplitude equal to the steady state amplitude at which the specimen was vibrating before the power was turned off. In cases of high amplitude and large values of δ the plot of logarithm of amplitude vs. wave number was not a straight line but a curve of decreasing slope. In this case the value for logarithmic decrement was taken as the average slope of the first several cycles of the decay curve.

Tests in Group I were to determine the variation of damping with confining pressure, amplitude of vibration, pore fluid (air, water or dilute glycerin) and density for both torsion and compression.

Figure 3-25 shows the comparison of logarithmic decrement in the first mode for the dry and saturated condition of loose Ottawa sand in

Double Amplitude, Radians

Fig. 3-25 Comparison of the variation of logarithmic decrement with amplitude
for dry and saturated Ottawa sand.

1 9 SEP 196_

REFER TO   WESAR

SUBJECT: Transmittal of Publication

TO: Director of Defense Research and
                  Engineering
               Washington 25, D. C.
               ATTN: Technical Library   .

"Study of the Propagation and Dissipation of 'Elastic' Wave

Energy in Granular Soils," published by the Department of Civil

Engineering, Engineering and Industrial Experiment Station, University

of Florida, for the U. S. Army Engineer Waterways Experiment Station

under Contract DA-22-079-eng-314, Weapons Effects Board Subtask

No. 13.009, is forwarded herewith for your retention.

FOR THE DIRECTOR:

1 Incl   K. H. JONES
   Report   Chief, Reports Section
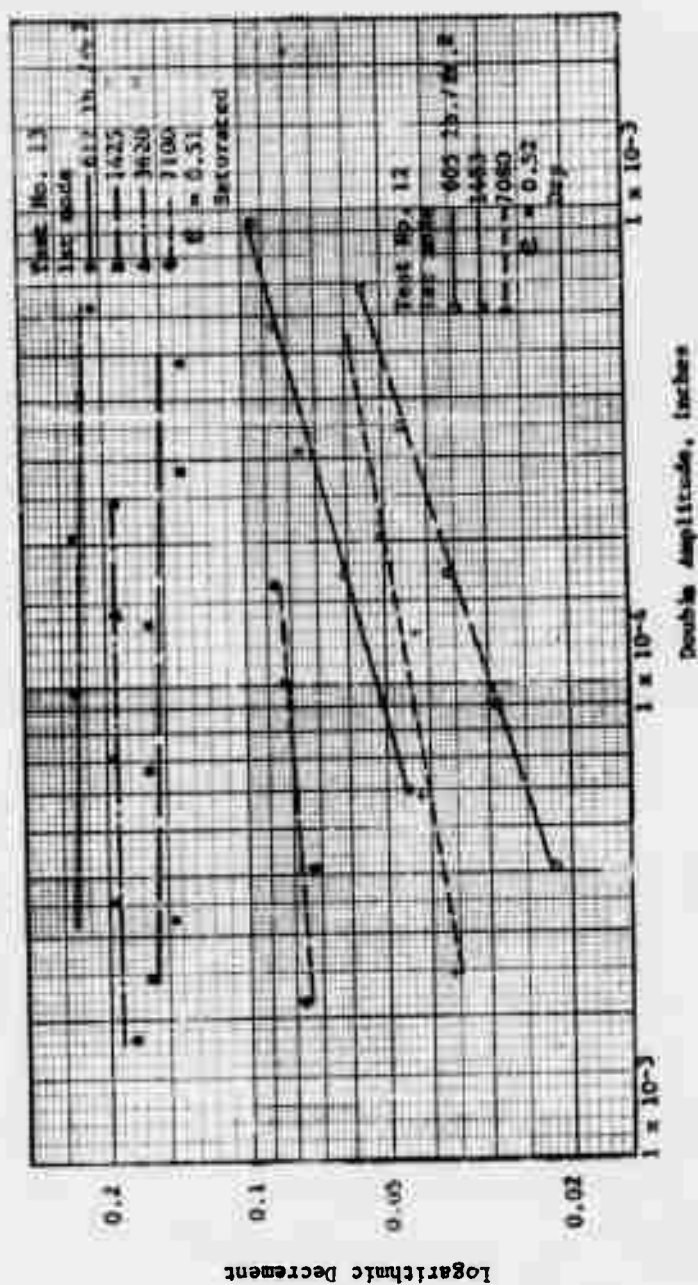
Fig. 3-26 Comparison of the variation of logarithmic decrement with amplitude for dry and saturated Ottawa sand.

Fig. 3-27 Comparison of the variation of logarithmic decrement with amplitude for dry and saturated Ottawa sand.
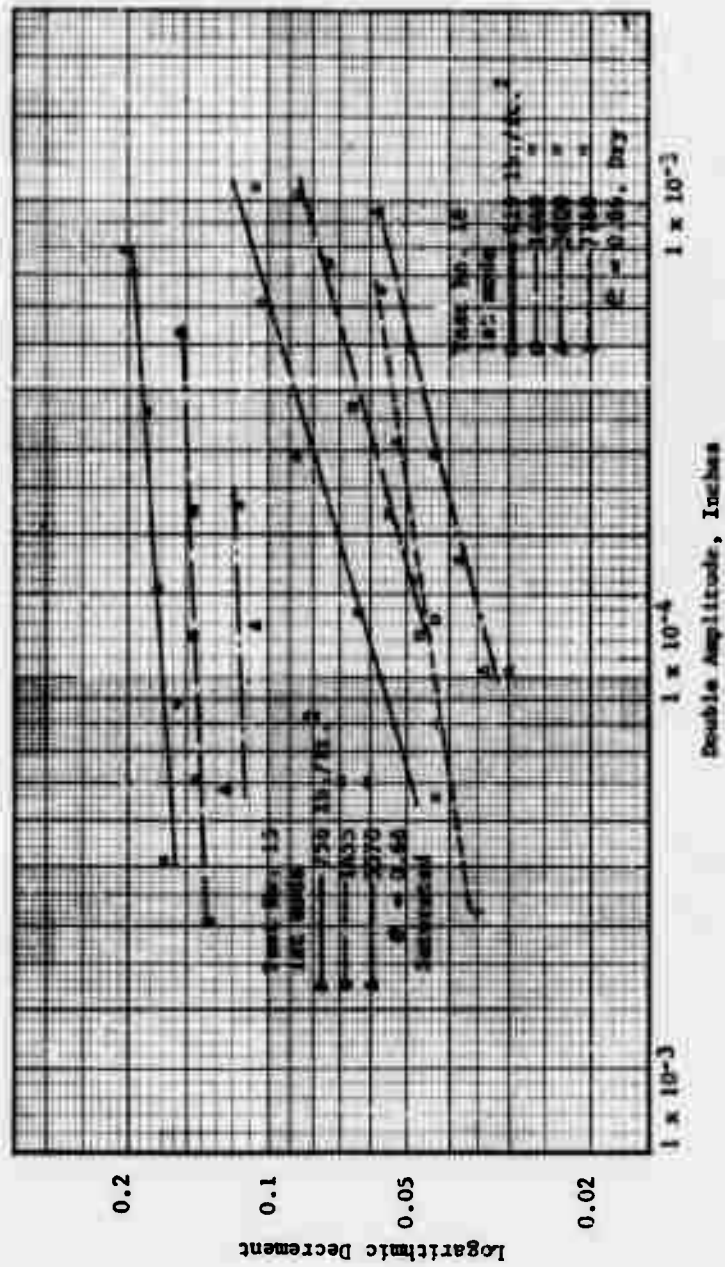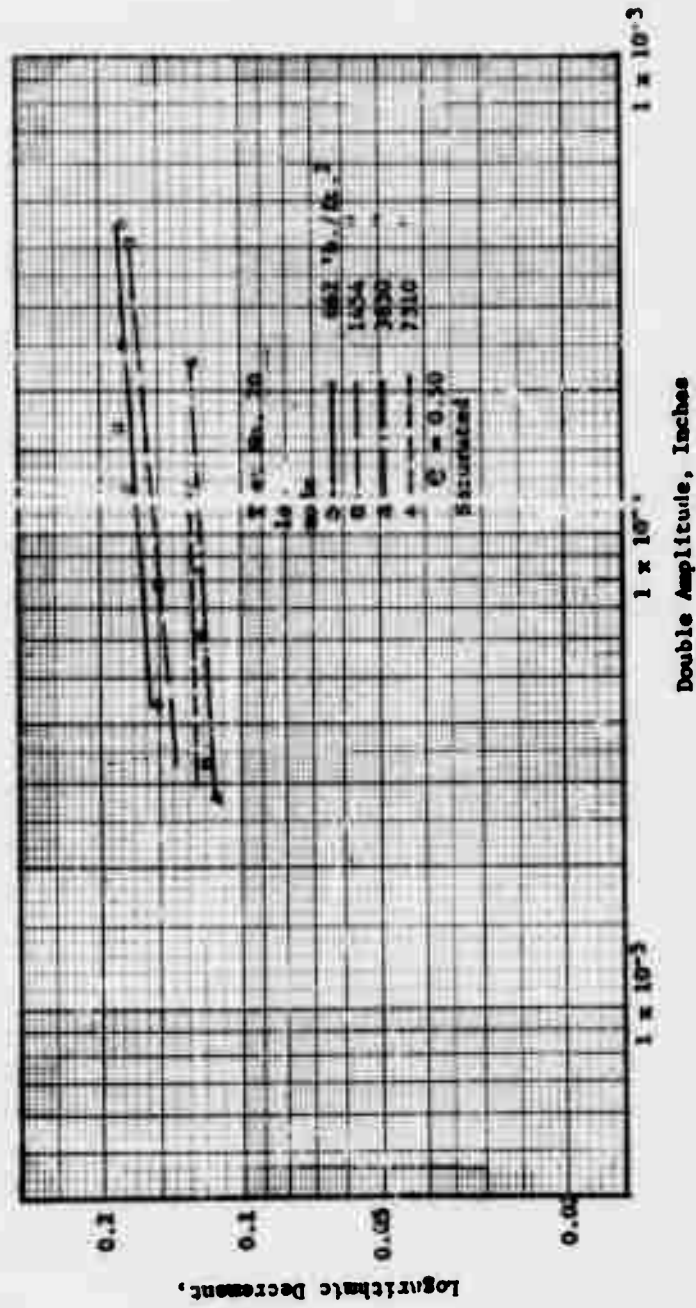
Fig. 3-28 Variation of logarithmic decrement with amplitude for Ottawa sand saturated
with dilute glycerin.
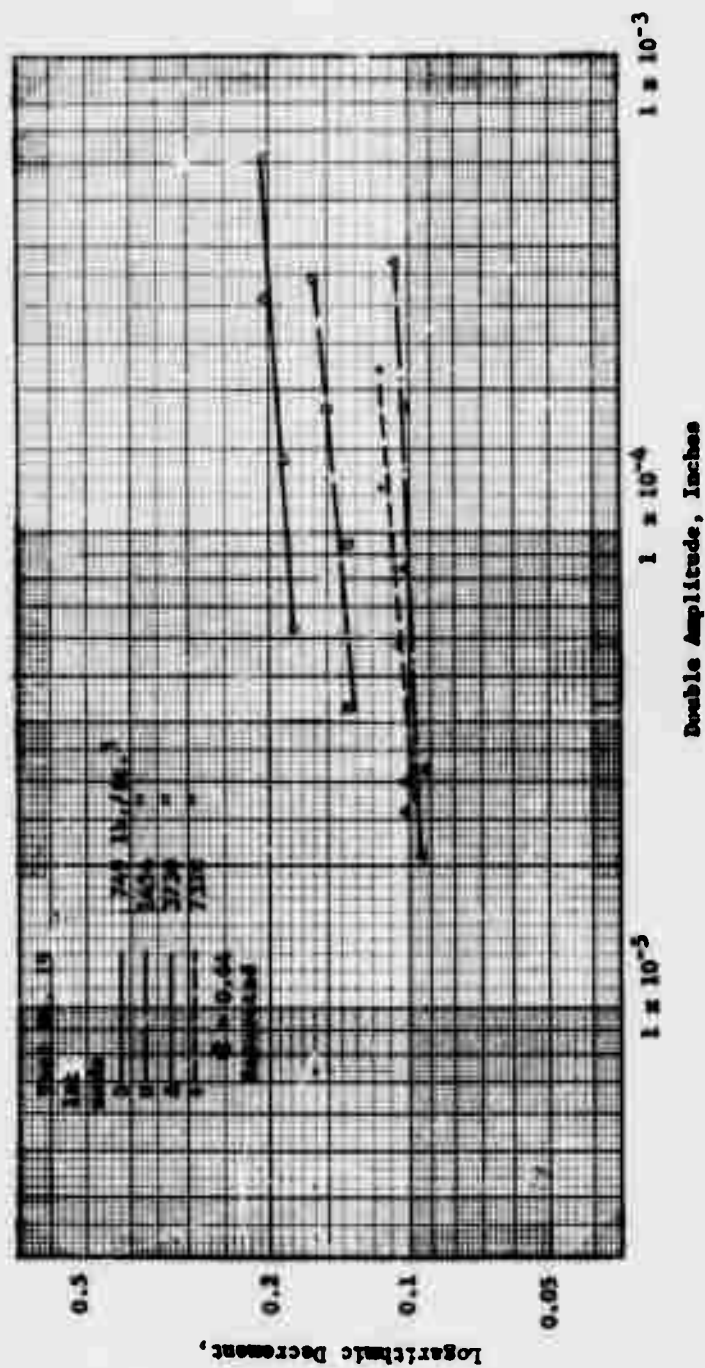
Fig. 3-29 - Variation of logarithmic decrement with amplitude for Ottawa sand saturated with dilute glycerin.

torsion. The same comparison is made for the longitudinal wave in the dense and loose conditions as shown in Figs. 3-26 and 3-27 respectively. Figures 3-28 and 3-29 show the results for Ottawa sand saturated with glycerin.

Group II

Figures 3-30 through 3-32 show the results for damping calculated from the test results for glass beads. These were tested in the dense condition for the dry and saturated case under torsion and compression. The results are plotted showing the variation with pressure and amplitude for the first mode of vibration.

Group III

Figures 3-33 through 3-36 show the damping results in torsion for Novaculite. The same procedure for taking measurements as described in the results for velocity was followed. The stress history is also as described in the velocity results. The group of measurements made at each pressure are plotted separately. The damping results obtained when the specimen was rebounded to a confining pressure of 2050 lb./ft.^{2} were affected by the pickup touching the permanent magnet and are not shown.

D. DISCUSSION OF RESULTS

Results for Velocity

Groups I and II

The materials used in Groups I and II are quite distinct in their behavior compared to the Novaculite No. 1250 used in Group III and will therefore be discussed separately. The effect of amplitude of vibration, confining pressure, density, pore fluid and type of material will be discussed separately.

Double Amplitude, Radians
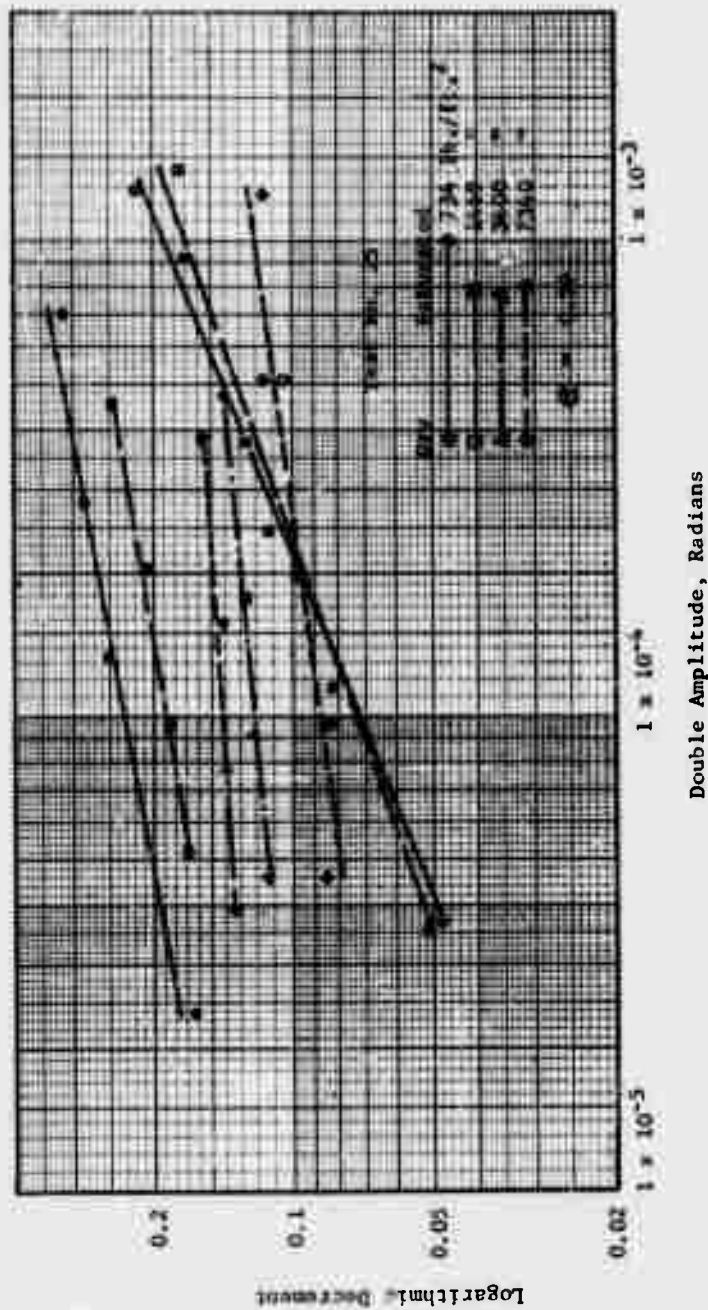
Fig. 3-30. - Variation of logarithmic decrement with amplitude for glass beads No. 2847 in the dry and saturated condition.

Double Amplitude, Radians
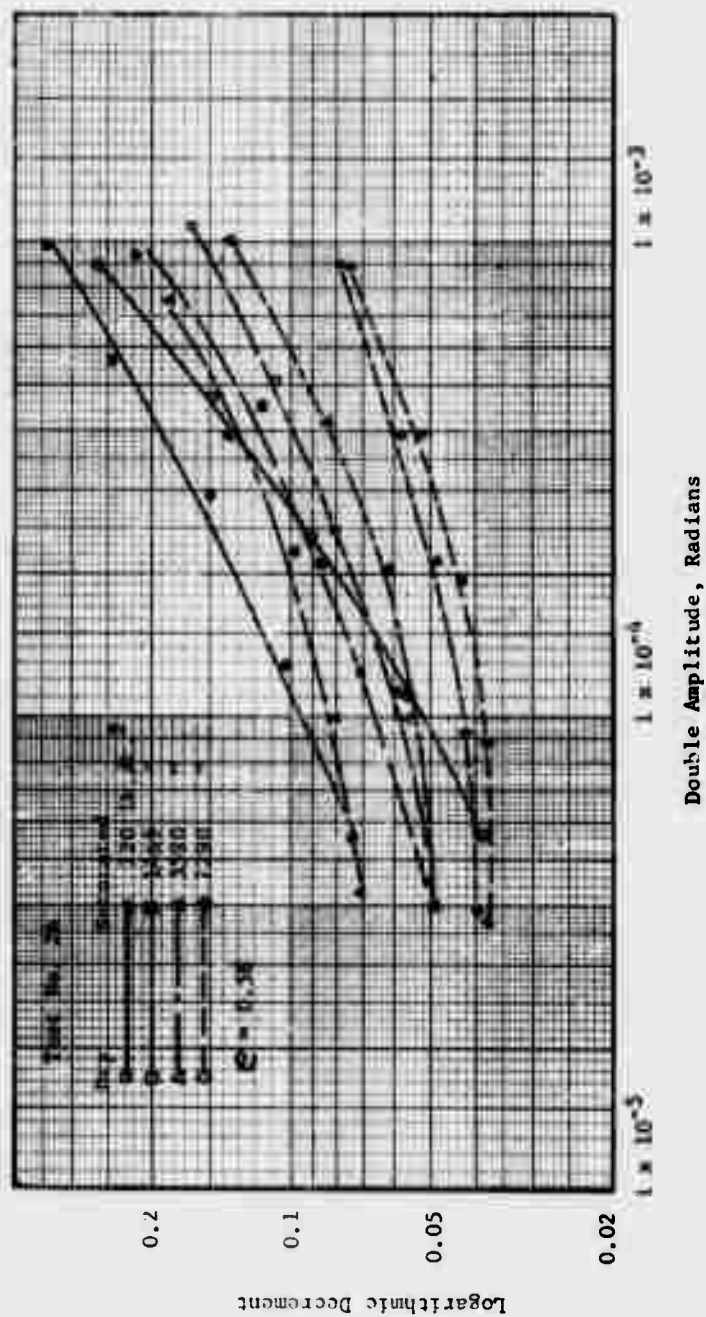
Fig. 3-31. - Variation of logarithmic decrement with amplitude for glass beads No. 0017 in the dry and saturated condition.

Double Amplitude, Inches
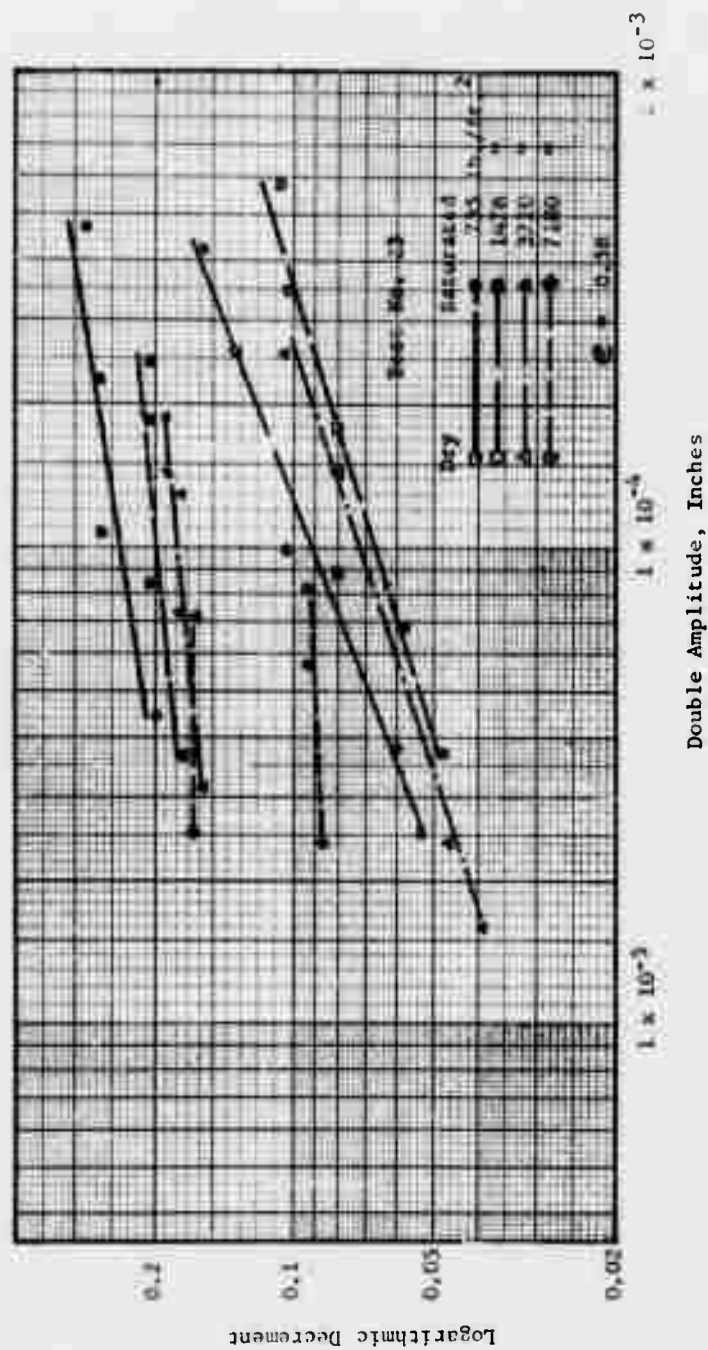
Fig. 3-32. - Variation of logarithmic decrement with amplitude for glass beads No. 2847 in the dry and saturated condition.
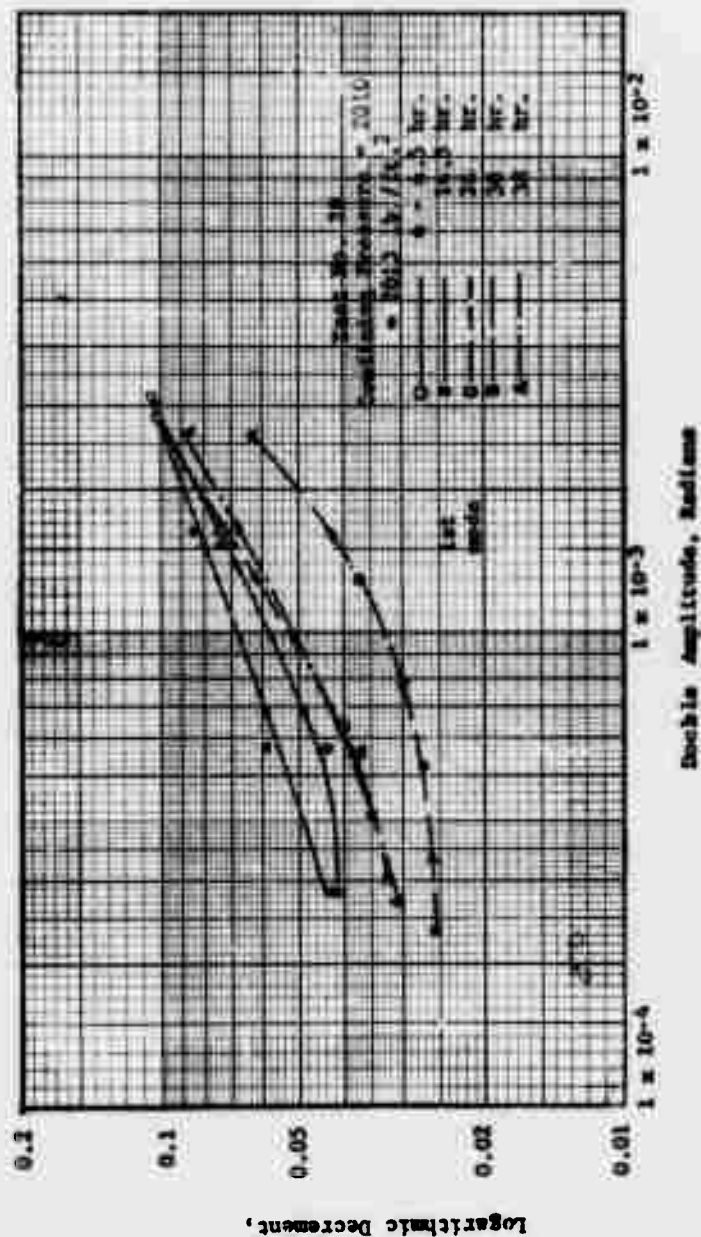
Fig. 3-33 Variation of logarithmic decrement with amplitude for Novaculite No. 1250
consolidated to 2010 lb./ft.^{2}
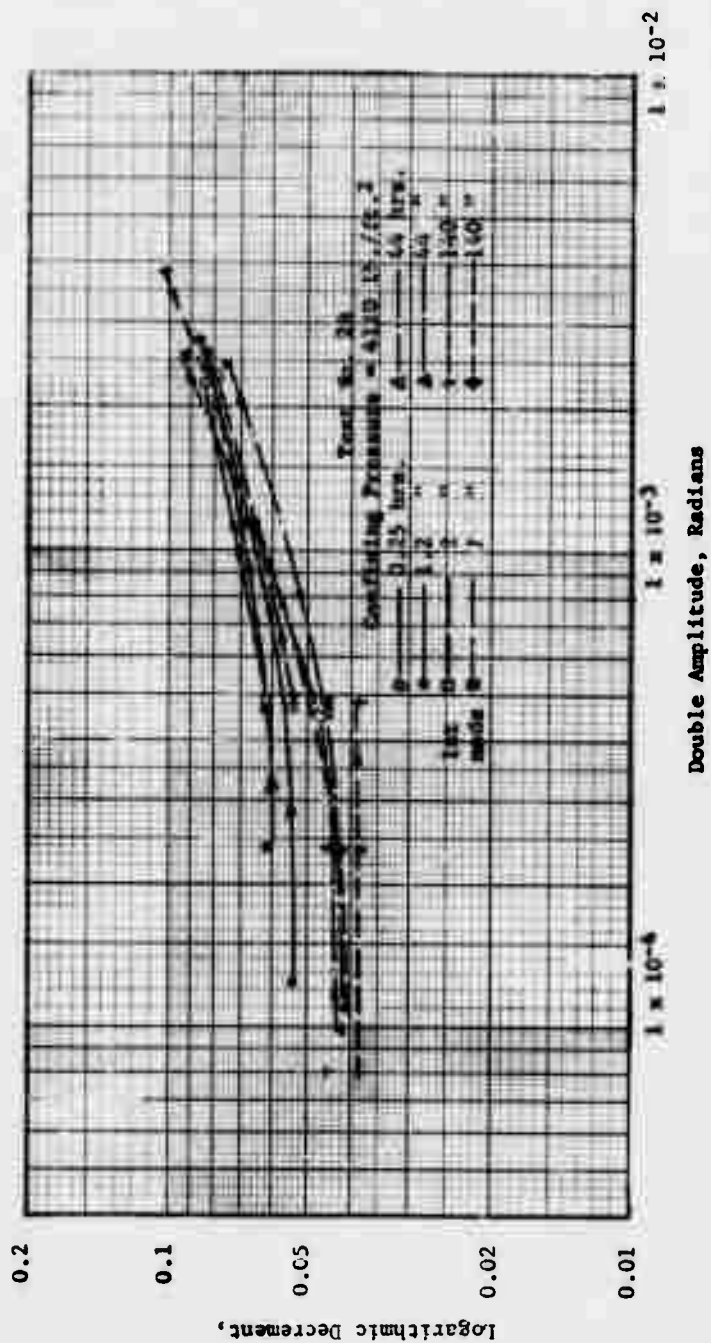
Fig. 3-34 Variation of logarithmic decrement with amplitude for Novaculite No. 1250 consolidated to 4100 lb./ft.²
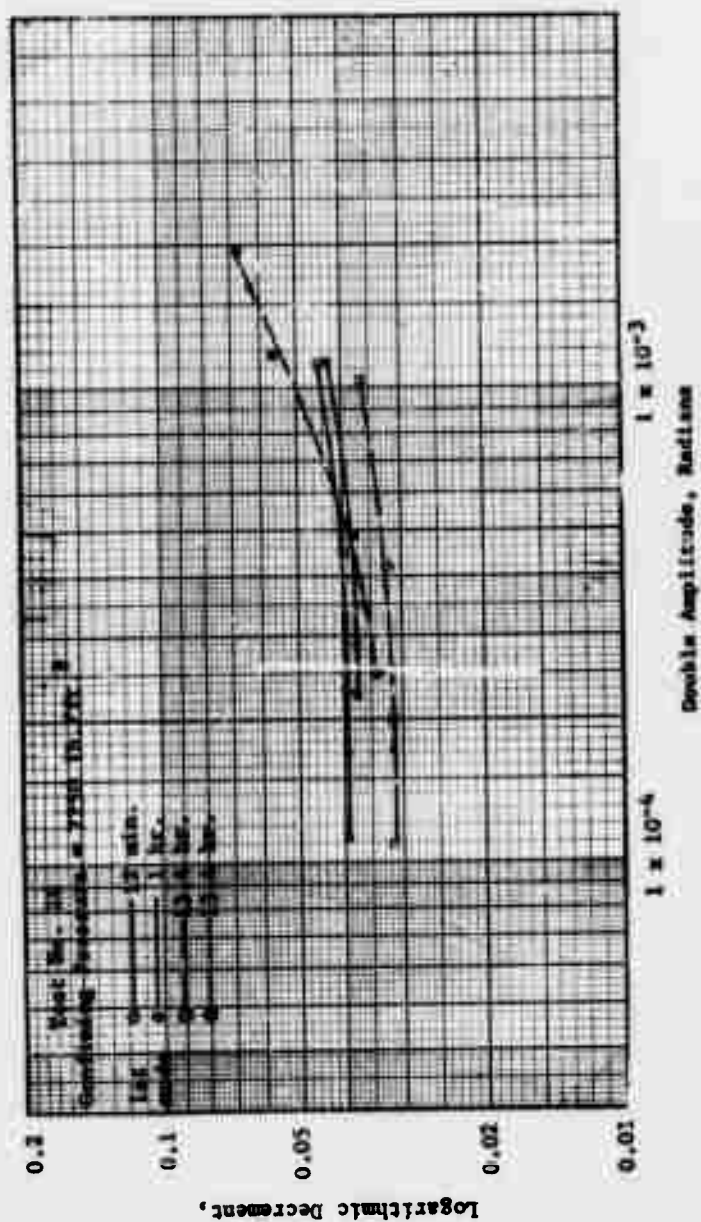
Fig. 3-35 Variation of logarithmic decrement with amplitude for Novaculite No. 1250 consolidated to 7250 lb./ft.^{2}
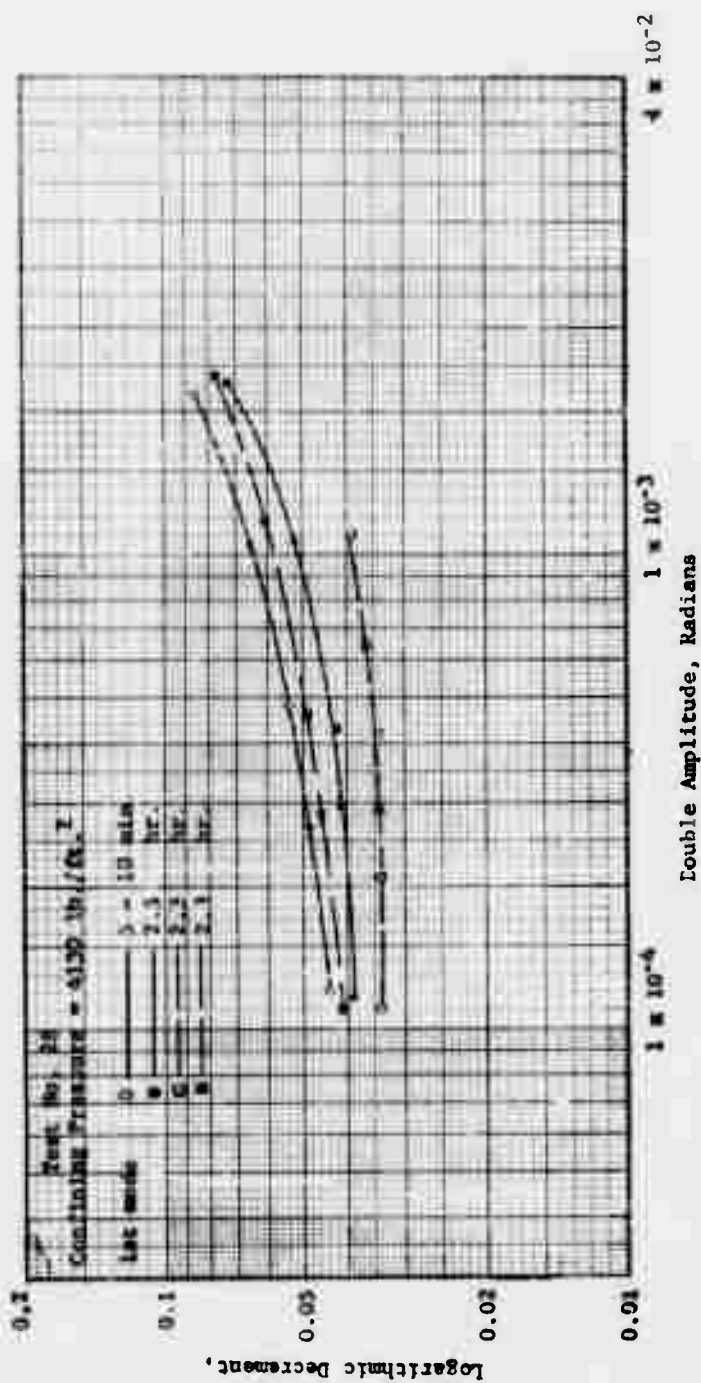
Fig. 3-36 Variation of logarithmic decrement with amplitude for Novaculite No. 1250 after rebounding from 7270 lb./ft.² to 4130 lb./ft.².

Effect of amplitude. When discussing the effect of amplitude on
wave velocity other variables must enter the discussion since the ampli-
tude effect on velocity differs under various conditions. First consider
the results for Ottawa sand in the dry and loose condition under torsional
vibrations as shown in Fig. 3-14. It can be observed that at any given
confining pressure the shear wave velocity decreases as tne amplitude of
vibration increases. The variation of velocity with amplitude in the
range of the highest measurable amplitudes is less than it is in the
range of the lowest measurable amplitudes. The velocity variation is
also smaller at high pressures than at low pressures. Figure 3-16 shows
the results for Ottawa sand in the dry and loose condition for compressive
waves. It can be seen that the velocity of the compressive wave also
decreases with increasing amplitude of vibration. The per cent variation
between the lowest and highest measured velocity is approximately the
same for torsion and compression at equal confining pressures. This
corresponds to approximately 10 per cent variation at the low con-
fining pressure and 2 per cent variation at the high confining pressure.
Comparison of the variation of velocity with amplitude for the loose
and dense conditions shows that the difference in the amount of variation
with amplitude between the two conditions is very small. Figure 3-13
compares the shear wave velocity vs. amplitude measurements for dry and
saturated Ottawa sand in the dense condition. Saturation causes the
curves to be almost flat except for double amplitudes below approximately
0.3×10^{-3} rad. The same thing happens in the loose condition as shown
in Fig. 3-14. Figure 3-15 shows comparison of the compressive wave velocity
vs. amplitude for dry and saturated Ottawa sand in the dense condition.
It can be seen that the curves for velocity vs. amplitude are affected in

much the same way as they are for the shear wave. At double amplitudes above approximately 0.2×10^{-3} in the curves are almost flat. The same behavior is also noted in Fig. 3-16 which shows the comparison between the dry and saturated variation of velocity with amplitude for loose Ottawa sand. Tests were run to determine the variation of the compressive wave velocity with amplitude for Ottawa sand saturated with dilute glycerin. These tests are shown in Figs. 3-17 and 3-18. The results for these tests are nearly the same as those saturated with water. There is a slight trend, however, for the curves to be flatter at double amplitudes above 0.2×10^{-3} in.

The glass beads which were tested in Group II behave somewhat differently than the Ottawa sand. Figure 3-19 shows the result for shear wave velocity with the beads No. 2847 which are approximately the same size as Ottawa sand. The effect of amplitude on shear wave velocity is about the same as that for Ottawa sand in both the dry and saturated condition. The results of the same beads for the compressive wave are somewhat different than that for Ottawa sand. There is a more pronounced variation of velocity with amplitude as shown in Fig. 3-21. Although the maximum amplitudes of vibration in the saturated condition are not as high as those in the dry condition, it appears that most of the velocity variation takes place at low amplitudes and the curves will flatten out at double amplitudes above 0.3×10^{-3} in. The shear wave velocity variation with amplitude for the glass beads No. 0017 is shown in Fig. 3-20 for both the dry and water saturated condition. In this case saturation of the material does not cause the change as it did for the other two materials. There are two factors which might account for this condition. One is the fact that the grain size is much smaller and the other is the fact that the specific gravity of the solids is

about 1.7 times that for the other materials. It seems reasonable to suspect that the difference is caused mostly by the change in specific gravity. The variation of velocity with amplitude for the compressive wave was only obtained for the dry condition with the glass beads No. 0017. This is shown in Fig. 3-22. Again there is a greater velocity variation with amplitude than for the other materials.

If a material has a non-linear stress-strain curve then the shape of the resonance curve will be distorted as compared to the case of a material with a linear stress-strain curve. If the elastic modulus of a material decreases with increasing strain, then the peak of the resonance curve will shift towards lower frequencies for increasing amplitudes of vibration. For the case when the modulus increases with strain, then the peak of the resonance curve will shift towards higher frequencies for increasing amplitudes. Figure 3-37 shows the variation of amplitude with frequency for longitudinal vibrations of dry Ottawa sand in the loose condition under a confining pressure of 619 lb./ft.[2] For different values of exciting force, the frequency for maximum amplitude will lie on the dashed line. The skewed shape of the resonance curve indicates that the elastic modulus of the Ottawa sand decreases with increasing strain.

Effect of confining pressure. Figures 3-38 and 3-39 show shear and compressive wave velocities plotted as a function of confining pressure for Ottawa sand. The shear wave velocities were chosen at a double amplitude of 0.5×10^{-3} in. The slope of the curves is generally greater at low confining pressures than at high confining pressures. At pressures above 2000 lb./ft.[2] the velocity varies with the 0.25 power of confining pressure. Density and saturation both affect the velocity. The dense
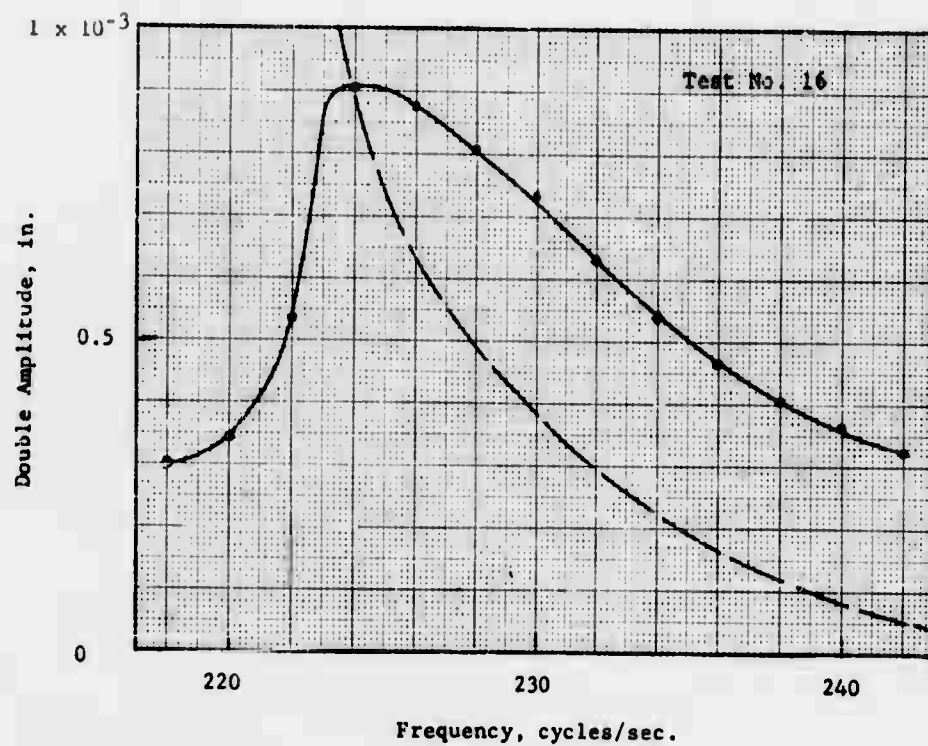
Fig. 3-37 Variation of amplitude with frequency for longitudinal vibrations of Ottawa sand in the dry condition under a confining pressure of 619 lb./ft.^{2}
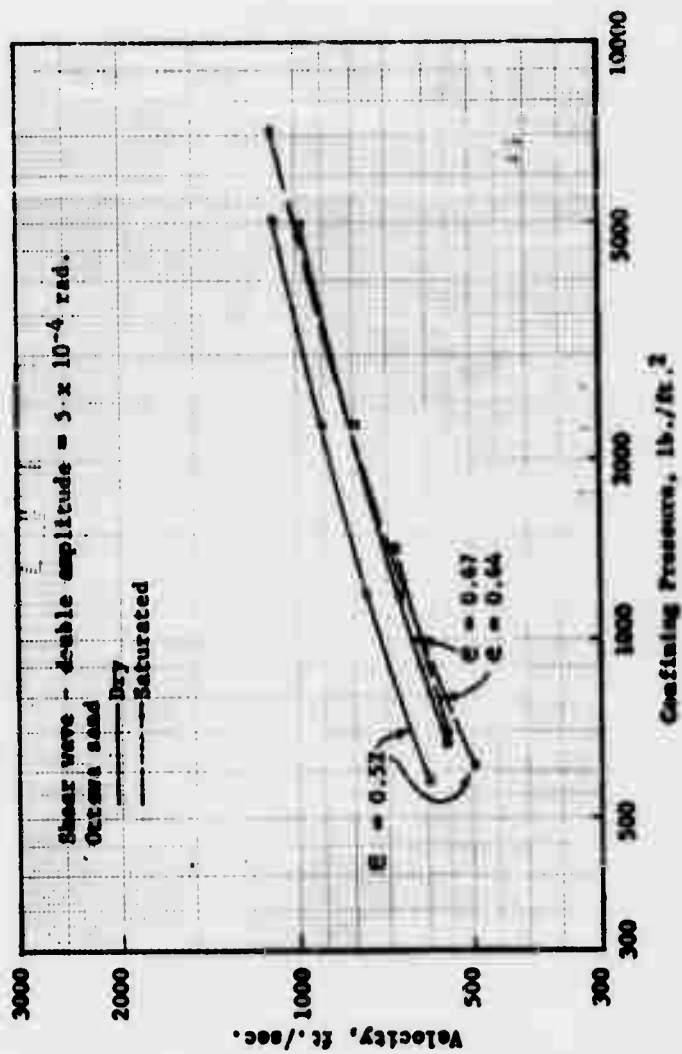
Fig. 3-38 Variation of shear wave velocity with confining pressure for Ottawa sand.
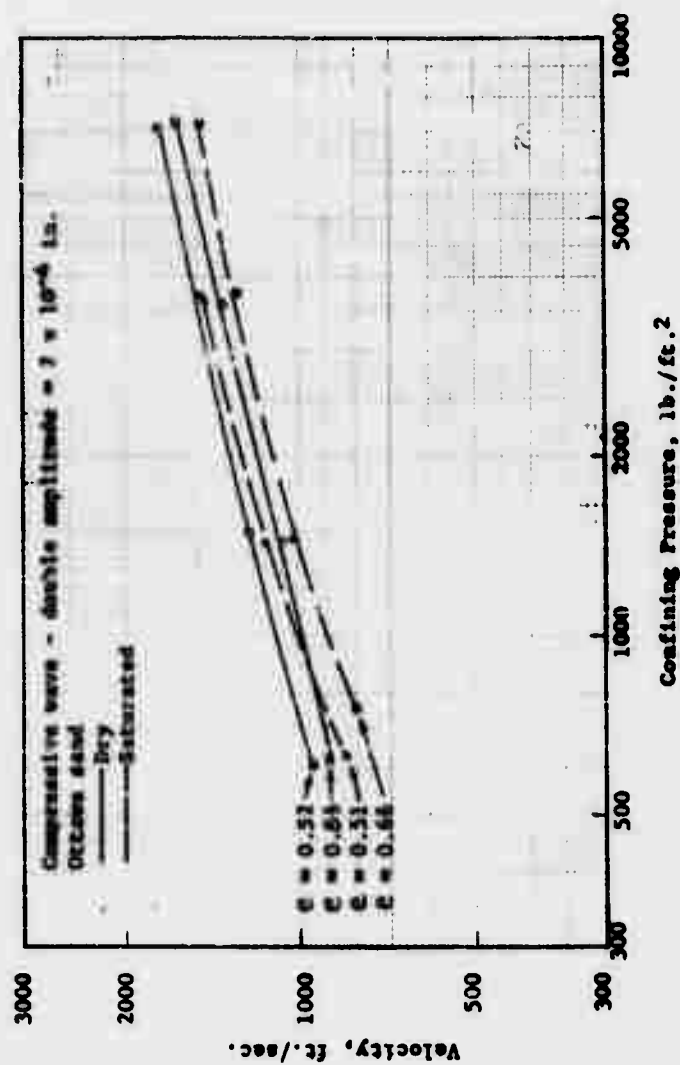
Fig. 3-39 Variation of compressive wave velocity with confining pressure for Ottawa sand.

condition gives a higher velocity as would be expected since a dense
material will have a higher modulus than a loose material. An addition
of water to the specimen increases its mass without adding any stiffness.
This results in a decrease in velocity as would be predicted by the rela-
tionship given by

$$\nu = \sqrt{\frac{E}{\rho}} \ .$$

In the case of a saturated material all of the water does not move with
the solid particles and so the velocity will not decrease by the amount
indicated by an addition of mass equal to the total mass of water in the
pores. By assuming the same value for shear modulus in the dry and sat-
urated conditions the amount of water which contributes an additional mass
to the material for Ottawa sand is about 35 to 40 per cent of the total
amount of water in the pores.

The variation of velocity with confining pressure for the glass
beads is shown in Figs. 3-40 and 3-41. The velocities were taken at the same
amplitudes as mentioned for Ottawa sand. At the higher confining pressures
the velocity for the glass beads No. 2847 varies with about the 0.25 power
of confining pressure while the glass beads No. 0017 vary with about 0.21
power of confining pressure. More tests would have to be run to establish
definitely these values. The slope for the fine glass beads is low com-
pared to the other granular materials. For the torsion test of the dry
glass beads No. 0017 shown in Fig. 3-41 two points are designated at the low
pressure as A and B. This test was set up and allowed to stand for a
period of two days at the confining pressure indicated at point A. Velocity
measurements were made for point A and then the pressure was increased in
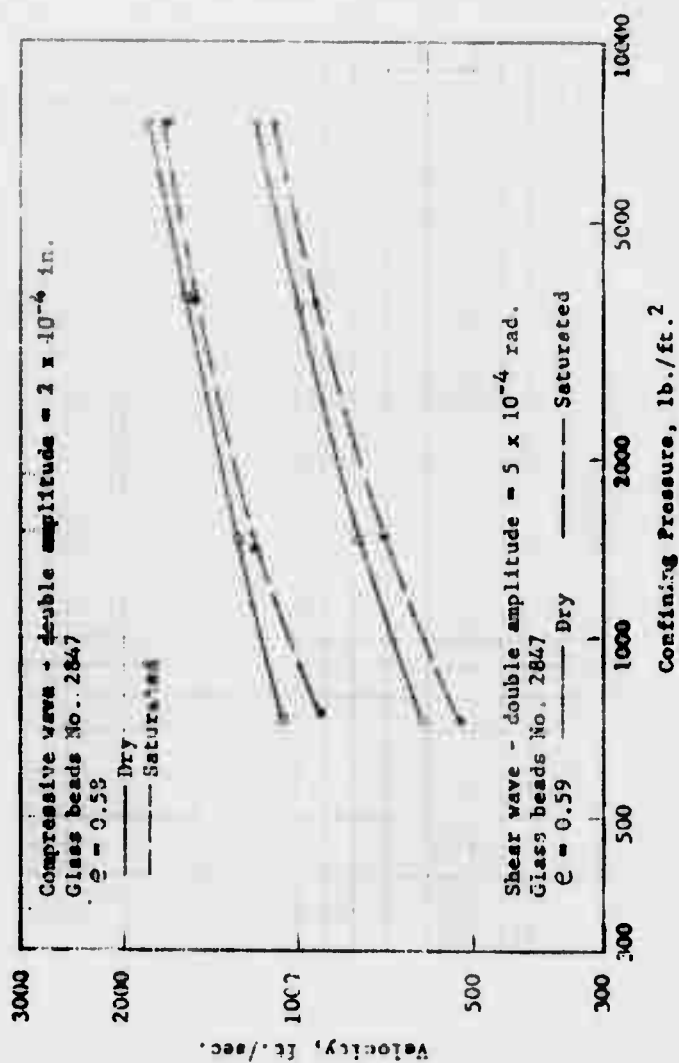
Fig. 3-40 Variation of compressive and shear wave velocity with confining pressure for glass beads No. 2847.

3-63
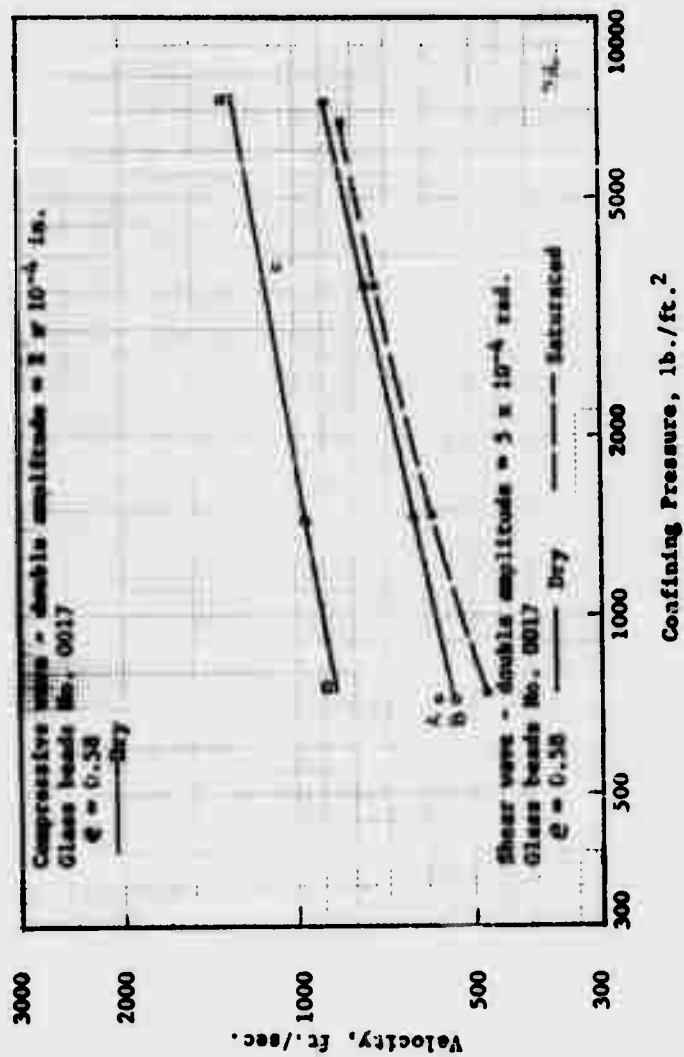
Fig. 3-41 Variation of compressive and shear wave velocity with confining pressure for glass beads No. 0017.

increments to determine the values of velocity for the higher pressures of the curve. After the specimen had been tested at its maximum confining pressure the pressure was reduced to the value corresponding to point B. The velocity at this point was less than the initial value that was measured. This decrease in velocity cannot be due to consolidation since this would cause an increase in velocity. During the test the pore pressure line was placed in water in order to detect any consolidation when the confining pressure was increased. No consolidation was detected in this way, but a slight time effect was noted after a change of confining pressure. Over a period of about 15 minutes there was an increase in velocity of about 1.5 per cent at 3580 lb./ft.^{2} One per cent of this occurred in the first 5 minutes.

Group III

There was only one test in this group for measuring velocity and it was performed on Novaculite No. 1250 in torsion.

Effect of amplitude. The measurements of the variation of shear wave velocity with amplitude of vibration are shown in Figs. 3-23 and 3-24. For this material there was also a variation of velocity with amplitude at any given time for a particular confining pressure. The times indicate the period over which the indicated pressure has been applied to the specimen. It can be seen that as the specimen is allowed to stand at a given pressure the velocity increases. The variation of velocity with amplitude of vibration depends upon how the measurements are taken. If the specimen sits for a long period of time and velocity measurements are made starting at small amplitudes, the velocity remains independent of amplitude up to a certain point after which the velocity decreases with amplitude. When continued up to the highest amplitude obtainable

a curve is defined which is concave downward. If the velocities are again measured starting at a high amplitude of vibration the curve of velocity vs. amplitude is concave upward and the velocities are smaller than those made before. This decrease in velocity is regained over a period of time as shown in Figs 3-23 and 3-24. The increase of velocity with time must be due to an intergranular action which can be destroyed by vibration but is built up again if the specimen is allowed to sit over a long enough period. A change of confining pressure also causes a temporary reduction in wave velocity. This was observed by the change of phase relationship between the driving force and the output of the velocity pickup. If the driving frequency is below the natural frequency of the specimen there will be a change of phase which will be opposite to that for the case when the driving frequency is above the natural frequency of the specimen. The driving frequency was adjusted to the natural frequency of the specimen and then the confining pressure was increased. As the pressure increased the change of phase relationships indicated that at first the velocity decreased and then increased above the value which was measured before the pressure change.

When the confining pressure was reduced from a higher value to a lower value the velocity decreased and then if allowed to sit, the value would increase, this is shown in the sets of curves which are designated as rebounded to the pressure indicated. The order of magnitudes of increase in velocity are still quite significant when the specimen is rebounded.

Since the velocity at any given confining pressure is time dependent the variation of velocity with pressure cannot be specifically defined.

Damping

Group 1

The results for the variation of damping with amplitude for the
Ottawa sand will be discussed first and then compared with the other
materials. The effect of amplitude, confining pressure and pore fluid
will be discussed.

Effect of amplitude. In general, the logarithmic decrement for
dry Ottawa sand decreases with a decrease of amplitude of vibration.
For the shear wave in the dry condition, as shown in Fig. 3-25, the
average variation in the first mode is with the 0.23 power ot amplitude.
The value of 0.23 is an average for all pressures, and the individual
values range from 0.16 to 0.29. Results for the compressive wave in
the dry condition are shown in Figs. 3-26 and 3-27. For the first
mode of vibration the average variation of logarithmic decrement is
with the 0.25 power of amplitude in both cases. Individual values vary
from 0.16 to 0.34. When the Ottawa sand is saturated with water the var-
iation of logarithmic decrement with amplitude is decreased. For the
shear wave the logarithmic decrement varies anywhere from the 0.0 to 0.13
power of amplitude. The compressive wave shows practically no variation
of logarithmic decrement with amplitude in the saturated condition.
Figures 3-28 and 3-29 show the results when dilute glycerin was used as
the pore fluid. The results are very much the same as those for the water
saturated condition in that there is practically no variation of logarithmic
decrement with amplitude of vibration.

Effect of confining pressure. The curves generally show that the
logarithmic decrement decreases as the confining pressure is increased.
However, in some cases the damping increases when the confining pressure

is increased. Also, since the curves of logarithmic decrement vs. amplitude are not parallel for different confining pressures this indicates that the pressure variation depends upon the amplitude of vibration. The inconsistency of the results is such that the only definite observation is that the damping tends to decrease with an increase of confining pressure

Effect of density. The effect of the specimen being loose or dense is rather small. Figures 3-26 and 3-27 show the results for the compressive wave in the loose and dense conditions. Any differences between the loose and dense conditions for the dry tests are too small to be detected. The effect of amplitude is much more significant than any effects due to differences in density. Figures 3-26 and 3-27 show results for Ottawa sand saturated with water and Figs. 3-28 and 3-29 show results for the same material saturated with dilute glycerin. Differences between the loose and dense conditions are also insignificant in these cases.

Effect of pore fluid. Figures 3-25, 3-26, and 3-27 compare the difference between dry and water saturated Ottawa sand. The effect of the water apparently depends upon the amplitude of vibration since the slopes for the dry condition are greater than the slopes for the saturated condition. Over the range of amplitudes measured the water increases the logarithmic decrement by a factor of 1.5 to 4 times that for the dry condition. Comparison of Figs. 3-26 and 3-28 as well as Figs. 3-27 and 3-29 show that there is practically no difference between the tests in which the specimen is saturated with water and with dilute glycerin.

Group II

Effect of amplitude. The results of damping for the glass beads are shown in Figs. 3-30 through 3-32. For the glass beads No. 2847 the average variation of logarithmic decrement in the dry condition is with about the 0.38

power of amplitude. In the saturated condition the damping varies with about the 0.15 power of amplitude. The glass beads No. 0017 behave somewhat different than the other beads or Ottawa sand. In Fig. 3-31 it can be seen that as the amplitude of vibrations is decreased the damping becomes less dependent upon amplitude. At higher amplitudes logarithmic decrement varies with about the 0.54 power of amplitude in the dry condition and with approximately the 0.47 power of amplitude in the saturated condition. It seems that the variation of damping with amplitude for the dry material is affected by the type of grain surface. The glass beads have a very smooth surface compared to the surface of Ottawa sand. It would be difficult to determine from the data whether the difference between the large and small glass beads is due to the size effect or the difference in density. An increase in density should tend to cause a decrease in the logarithmic decrement because of the increased mass. Comparison with the two types of beads shows that a smaller amount of damping is associated with the higher density beads.

Effect of confining pressure. As with the Ottawa sand the variations of damping with confining pressure are such that the only observation that can be made is that there is generally a decrease in damping with confining pressure.

Effect of pore fluid. The saturation of the glass beads No. 2847 has the same effect as it did in the Ottawa sand. The values for damping were increased and the variation of damping with amplitude was reduced, indicating that the amount of damping contributed by the water increases at smaller amplitudes. Figure 3-31 shows that for the glass beads No. 0017 the amount of damping contributed by the water is also greater at smaller amplitudes but to a much smaller extent. This difference is most likely due to the higher specific gravity of the beads in comparison to that of the water.

Group III

Effect of amplitude. The variation of logarithmic decrement with amplitude for this material does not plot as a straight line on a full logarithmic scale. At double amplitudes below about 3×10^{-4} rad. the logarithmic decrement does not vary much with amplitude. This corresponds to approximately the same order of magnitude in which there was very little variation of velocity with amplitude. At higher amplitudes there is a significant variation of damping with amplitude. As the specimen was allowed to stand under a given confining pressure the damping decreased. If values of damping were then measured starting with low amplitudes and increasing the amplitudes until measurements were finally made at the highest attainable with the equipment, a curve corresponding to the lowest curve in Fig. 3-33 was obtained. If the specimen was then allowed to vibrate at high amplitudes over a period of approximately 5 min., then the curve corresponding to the triangular points was obtained. Thus, the time effect which resulted in a decrease in damping could be destroyed by vibrations of high amplitude.

Effect of confining pressure. When the confining pressure was increased after having been maintained at a steady value over a long period of time, the damping increased. After a new pressure was reached the damping started to decrease with time. If high amplitude vibrations were applied to the specimen, the decrease of damping that occurred over a period of time could be destroyed. If the values of damping are compared at low amplitudes for the different confining pressures, it can be seen that time is more significant than confining pressure. The values of damping for low amplitudes at each confining pressure are all within the same order of magnitude.

Comparison of Results with Those of Previous Investigators

Effect of confining pressure. The most extensive study of the effect of confining pressure on the velocity of stress waves in Ottawa sand has been given by Hardin (1961). His results showed fair agreement with those of other investigators. He found that the velocity of both shear and compressive waves in Ottawa sand varied with the 0.25 power at confining pressures above 2000 lb./ft.^{2} At lower pressures he found that the power was between the 1/3 and the 1/2 powers. The results in this investigation also showed that the variation of velocity with confining pressure was with the 0.25 power at pressures above 2000 lb./ft.^{2} Thus, the results are in very good agreement with those obtained by Hardin. Figures 3-42 and 3-43 show the results of tests by Hardin for Ottawa sand. His measurements did not include an evaluation of the amplitude of vibrations, but they are estimated to be in the order of 5×10^{-4} rad. for torsion and 2×10^{-4} in. for compression.

Effect of amplitude. Hardin found that there was a decrease in the shear wave velocity of about 5 per cent when the amplitude was increased by a factor of 3.0. Duffy and Mindlin in their experiments on 1/8 in. diameter steel balls found that a reduction in amplitude from 12×10^{-7} in. to 2×10^{-7} in. resulted in a 1 per cent increase of velocity. Variations as great as 10 to 15 per cent in velocity were found in the present work, but these were measured over a much greater range of amplitudes than those above.

Comparison with Theoretical Results

Effect of confining pressure. The theory of Duffy and Mindlin predicts that the stress wave velocities for granular materials will
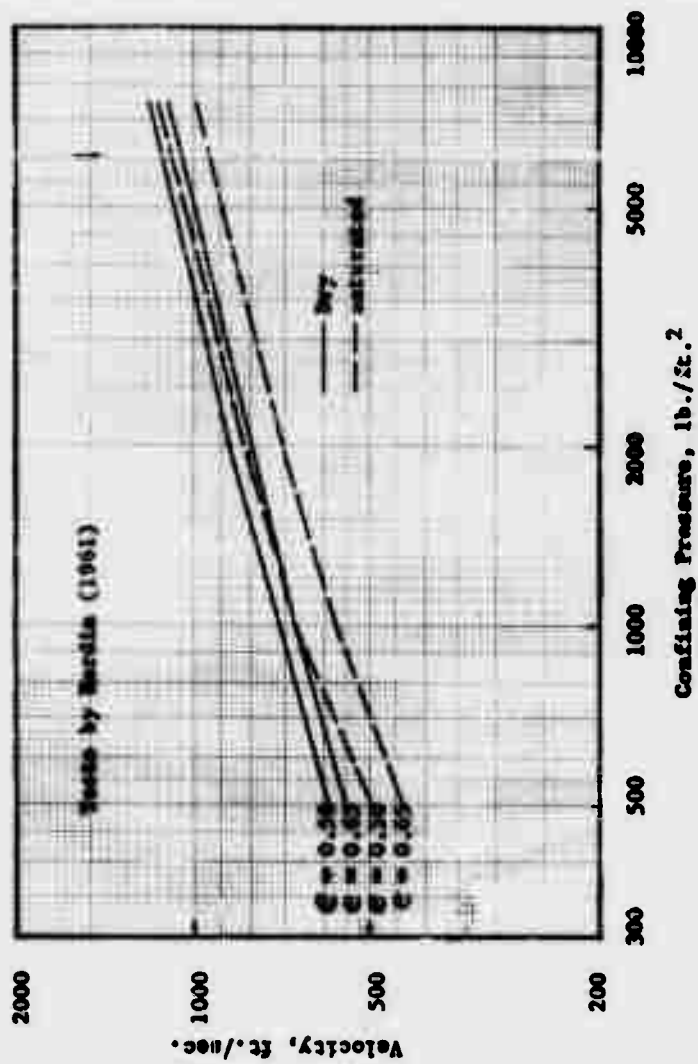
Fig. 3-42 Variation of shear wave velocity with confining pressure and void ratio for dry and saturated Ottawa sand.
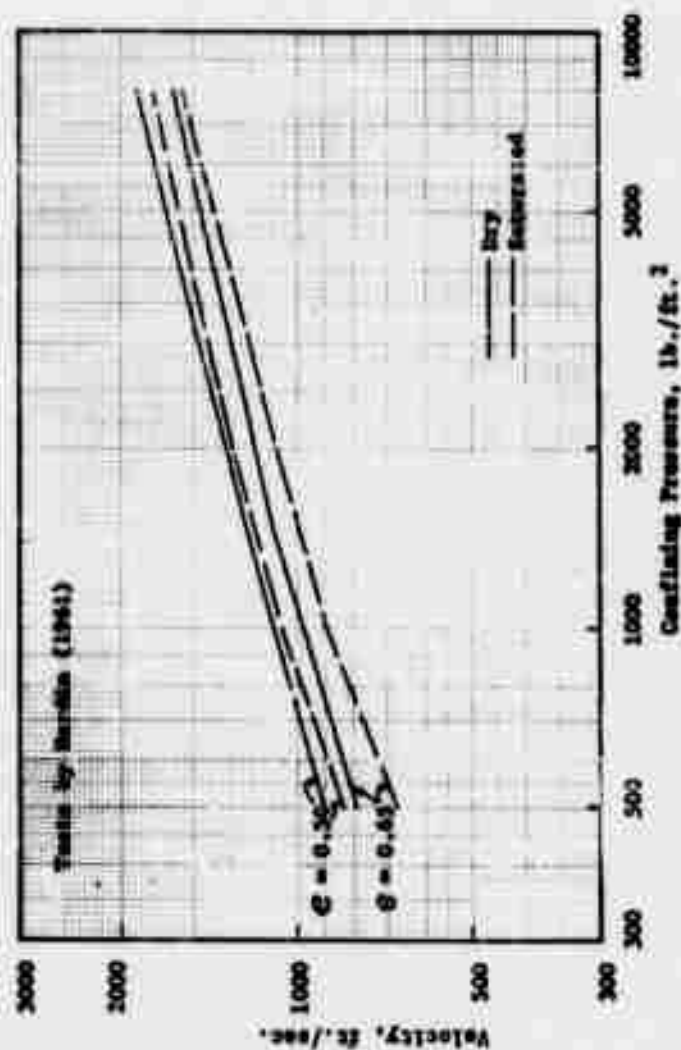
Fig. 3-43   Variation of compressive wave velocity with confining pressure and void ratio for dry and saturated Ottawa sand.

vary with the 1/6 power of confining pressure. This is based upon perfect spheres packed in a face centered cubic array. A square packing of spheres also predicts a variation of velocity with the 1/6 power of confining pressure. The experimental results of Duffy and Mindlin showed that the variation at low confining pressures was with about the 1/4 power of confining pressure. As the confining pressure was increased the variation more closely approached the 1/6 power. Thus, granular materials which are quite different than steel spheres would be likely to vary with a power greater than the 1/6 power. The experimental results which indicate a variation with the 1/4 power at higher confining pressures agree quite well when the difference between the actual and theoretical material is considered.

The theory of Duffy and Mindlin also predicts that the variation of logarithmic decrement will be with the -1/3 power of confining pressure. Results in this investigation indicated a trend towards a decrease of logarithmic decrement with confining pressure, but the results were not consistent enough to determine exactly what the variation was.

Effect of amplitude. The theory of Pisarenko predicts that for a material with a non-linear stress-strain relationship the frequency will decrease with an increase of amplitude of vibration. The maximum amplitude for various values of exciting force will lie on a line which forms a second degree parabola with an origin and vertical tangent at ω/ω_n = 1.0 Experimental results for Ottawa sand and glass beads show that the maximum amplitude for various exciting forces lies on a curve indicated in Fig. 3-37 which is concave upward instead of concave downward as predicted by Pisarenko's theory. The theory might possibly indicate a different relationship

If it is derived using a different assumption for the non-linear stress-strain relationship.

The theory of Duffy and Mindlin predicts that the logarithmic decrement for a dry granular material is proportional to the amplitude of vibration. The experimental results as measured tend to agree in that there is an increase of damping with amplitude. However, for any one decay curve the logarithmic decrement was generally independent of amplitude as described under presentation of results. The glass beads showed a greater variation of logarithmic decrement with amplitude than the Ottawa sand. This seems reasonable as the glass beads are closer to a perfect material than the Ottawa sand.

IV. STATIC TESTS FOR DETERMINATION OF
SPECIFIC DAMPING CAPACITY

As stated in Section II it is possible to calculate the specific
damping capacity from the hysteresis loop. In order to investigate this
possibility an apparatus was designed and built which makes it possible
to determine the shape of the hysteresis loop for the special case of a
cylindrical sand specimen subjected to torsional forces. A total of 36
tests on dry, dense Ottawa sand was conducted using different stress
levels and confining pressures.

Apparatus

Figure 4-1 shows the apparatus used for the torsion tests. The
specimen is confined by a rubber membrane and two plastic caps. It is
approximately 10" long and has a diameter of 1.5". This specimen is
fixed in a horizontal position on a steel frame in such a way that one
cap is in rigid contact with the frame while the other is able to turn
around an adjustable pivot. A possible slip between sample and caps
is prevented by a thin layer of sand which has been glued to the
surface of the caps.

The confining pressure on the sample can be controlled through a
vacuum line connected to the fixed end cap.

Torsional moments can be applied to the sample through a balanced
beam which is fixed to the free end cap. This beam is rigged up as a
balance with two pans, which can be loaded with weights to give the desired
twisting moment in either direction.
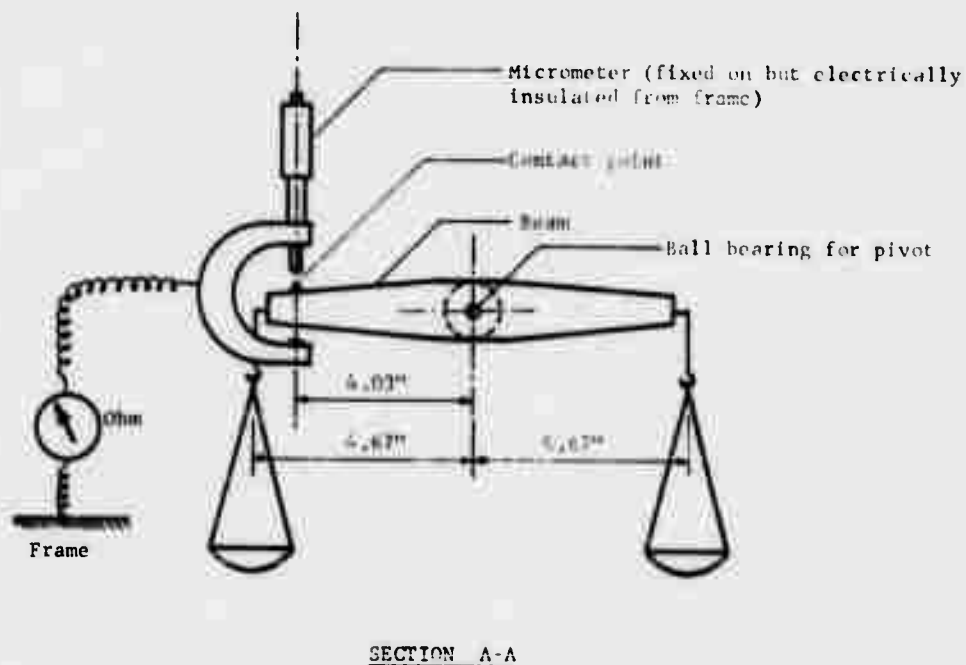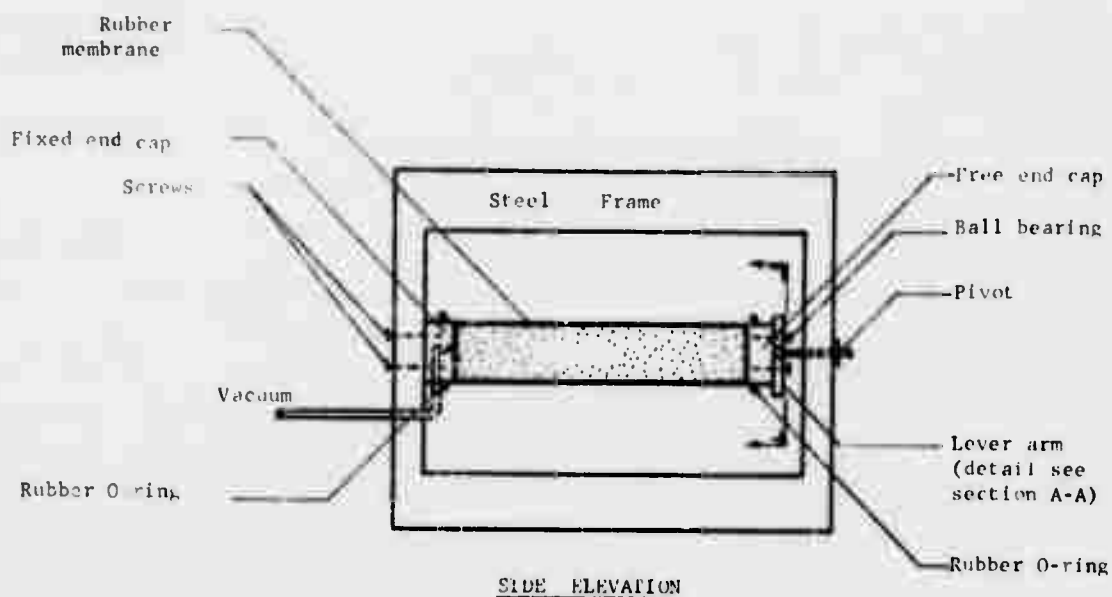
Fig. 4-1. - Apparatus for Torsion Test on Sand

Angular deflections of the specimen are measured by the vertical movement of an electrical contact point on the beam. The actual measuring device is a micrometer (accuracy 10^{-4} inch) which is fixed on, but electrically insulated from, the frame. Through an electrical circuit (Micrometer-Ohmmeter-frame-pivot-beam-contact point) it is possible to observe the exact moment of contact between the micrometer and the contact point. Thus, the vertical position of the contact point can be determined without loading the beam with a force from the micrometer.

The specimens

All specimens were prepared from oven-dried Ottawa sand, which was found to have the grain size distribution

Sieve No.	% Passing
20	99.0
30	55.7
40	6.2
60	1.2
80	0.4
140	0.1

and the specific gravity $G_s = 2.66$.

The specimens were compacted by vibration to maximum density corresponding to an approximate void ratio of $e = 0.49$.

The torsional strength of the above type of specimen was determined at two different values of confining pressure. The failure moment being defined as the moment which gave an angular deformation of 5×10^{-3} radians per inch. The results of these tests are given on Fig. 4-2.

Repeated loading tests

In this type of tests the specimen is subjected to a moment which is varied in steps between two levels. For each step the corresponding deformation is observed and the test result is a curve showing the relationship between moment and angular deformation of the sample. A typical test result is shown on Fig. 4-3, which also defines the terms
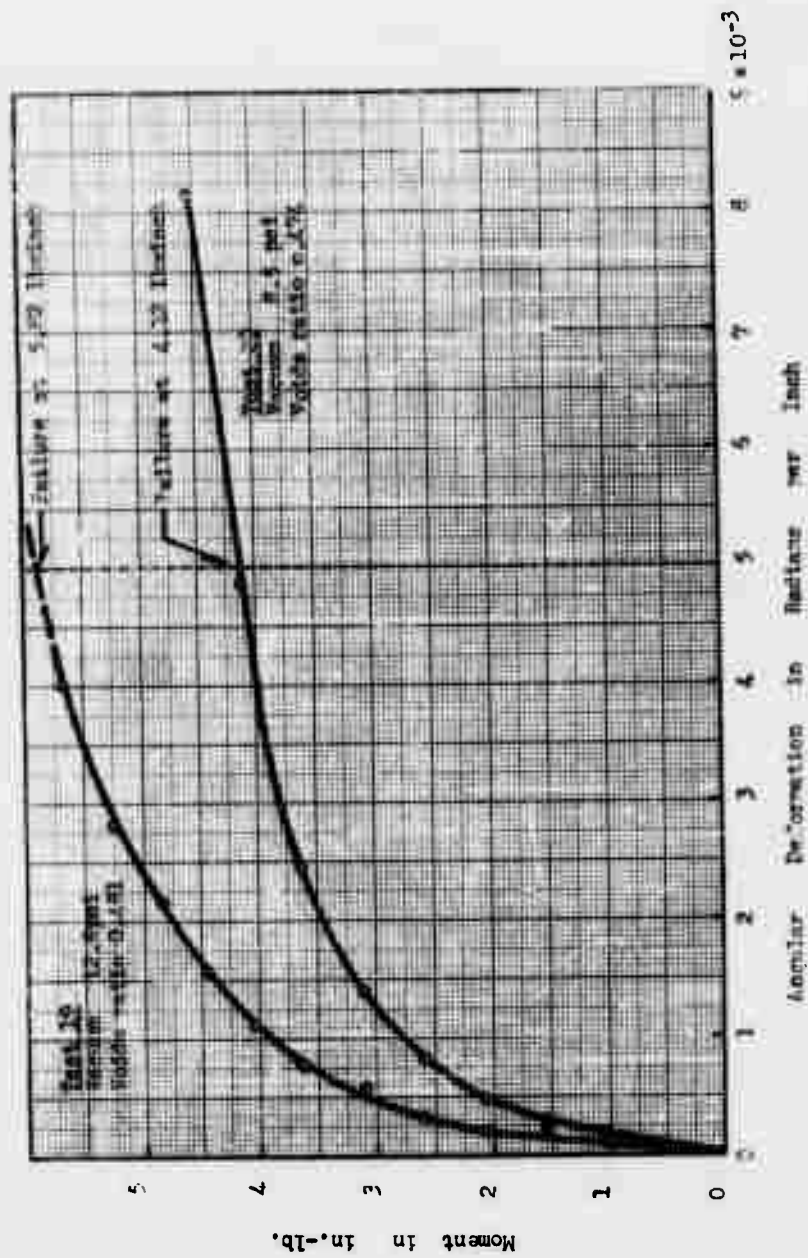
Fig. 4-2 Results of Torsional Strength Test
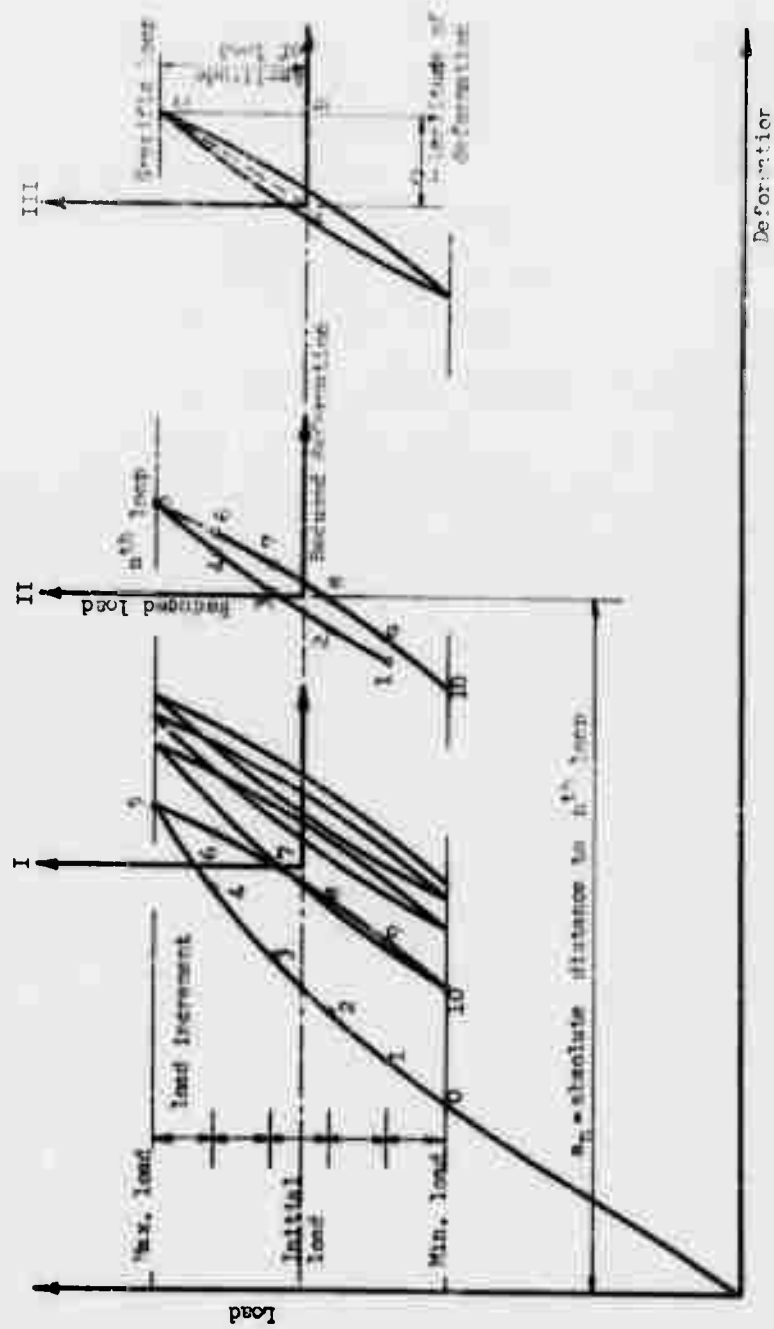
Fig. 4-3. - Typical load-deformation relationship for repeated loading tests.

Initial load, amplitude of load, minimum and maximum load and load increment.

It can be seen that the most important variables of the tests are

1. Confining pressure (vacuum)

2. Amplitude of load (moment)

3. Initial load (moment)

Tests were carried out at two levels of confining pressure, namely

Test series I (Test 1-18) at 12.8 psi (0.9 kg/cm^2)

Test series II (Tests 22-39) at 8.5 (0.6 kg/cm^2)

The amplitude of load and the initial load were varied as shown on Fig. 4-4. On this figure the moment has been expressed in terms of the unbalanced load on the right pan (see Fig. 4-1). This measure for the moment will be used several times below just as the movement of the contact point will be used as a measure for the angular deformation of the specimen.

Two more variables should be considered, namely.

4. Rate of testing (time)

5. Stress history of the sample

As to the rate of testing it should be noted that a certain creep was observed and the testing procedure was therefore designed in such a way that the sample was allowed to reach a stationary condition under each new loading before the corresponding deformation was recorded

If each of the 36 tests were carried out on fresh samples the stress history would be well defined, but this was not the case for the present tests where 18 tests were carried out successively on the samp sample. However, it can be shwn that the stress history is of little importance provided the sign of the moment changes between each test Consider Fig. 4-4 and imagine that three experiments are carried out:

Fig. 4-4 Test Schedule
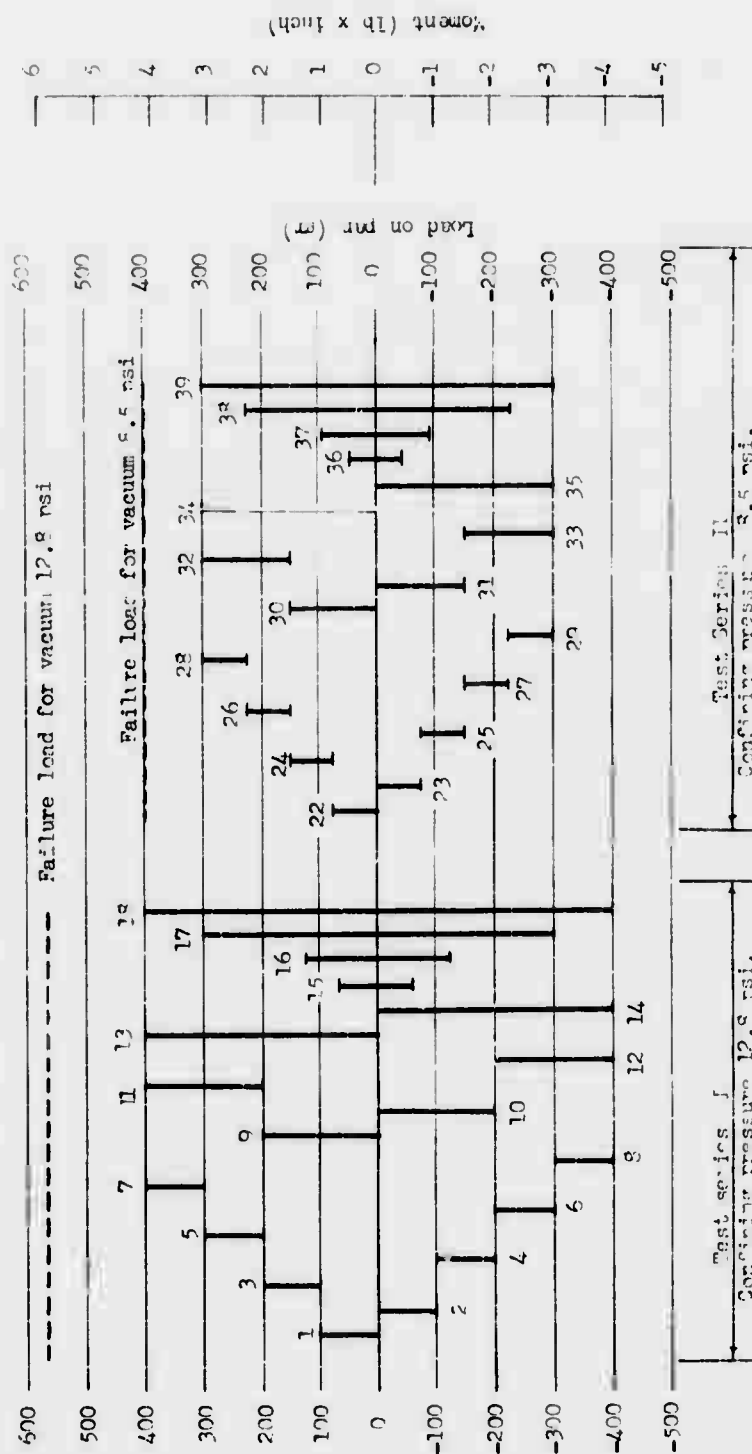
The vertical bars indicate the load range of the different tests

Exp. (a)   Test No. 1 on a fresh sample

Exp. (b)   Test No. 2 on a fresh sample

Exp. (c)   Test No. 2 on the sample used for Test No. 1

Exp. (a) and Exp. (b) must, because of symmetry, give the same result with opposite sign.   If Exp. (a) gives the same result (except for the sign) as Exp. (c) it can, therefore, be concluded that the stress history (Test No. 1) has no effect on the result of Exp. (c).   Both Exp. (a) and Exp. (c) were carried out.   A check on the results of Test No. 1 and Test No. 2 will show that, within the accuracy of the tests, they give exactly the same result with opposite sign.   This equivalence does not include the first loop which seems to be very dependent on the stress history.   A similar comparison can be made between Tests No. 13 and 14, etc.

It can, therefore, be concluded that all the tests gave approximately the same results as they would have given if they had been carried out on fresh samples.   This evidence is supported by the fact that no significant change in void ratio was observed when measurements were made between individual tests in each series.

During each test the loop was repeated 16 times but observations of the deformations were made only for loops Nos. 1, 2, 4, 8, 12 and 16.   A typical set of observations (Test No. 32) is shown in the upper part of Table 4-1.   The points referred to in this table are the points shown on the nth loop in Fig. 4-3.

Treatment of test results

For each test the results will plot approximately as Fig. 4-3, but due to the limited accuracy of the tests and the fact that the higher order loops will plot on top of each other, one will find that this type of plot is inconvenient in describing the observed load-deformation relationship.

Point	1	2	3	4	5	6	7	8	9	10	Mean of all points in nth loop	Position of nth loop
load on pan (gr)	180	210	240	270	300	270	240	210	180	150		
Reduced load (gr)	-45	-15	+15	+45	+75	+45	+15	-15	-45	-75		

Original observations (Readings on the micrometer in 10^{-4} inch)

	1	2	3	4	5	6	7	8	9	10	Mean of all points in nth loop	Position of nth loop
Loop 1	452	506	579	668	784	771	753	735	716	695	665.9	-96.0
Loop 2	712	730	750	767	799	786	770	750	732	711	750.7	-11.2
Loop 4	739	756	774	794	816	802	784	766	750	729	771.0	+9.1
Loop 8	755	773	791	810	832	814	798	780	751	742	784.6	+22.7
Loop 12	765	783	801	820	851	824	806	800	771	750	797.1	+35.2
Loop 16	773	790	808	827	848	832	813	796	778	757	802.2	+40.3
Mean of all loops	699.3	723.0	750.5	781.0	821.7	804.8	787.3	771.2	749.7	730.7	761.9	
Mean of last four loops	758.0	775.5	793.5	812.8	836.8	818.0	800.3	785.5	762.5	744.5	788.7	

Reduced observations (10^{-4} inch)

	1	2	3	4	5	6	7	8	9	10
Loop 1	-213.9	-159.9	-86.9	+2.1	+113.1	+105.1	+87.1	+69.2	+50.1	-29.1
Loop 2	-38.7	-20.7	-0.7	+16.3	+48.3	+35.3	+19.3	-0.7	-18.7	-39.7
Loop 4	-32.0	-15.0	+3.0	+23.0	+45.0	+31.0	+13.0	-5.0	-21.0	-42.0
Loop 8	-29.6	-11.6	+6.4	+25.4	+27.4	+29.4	+13.4	-4.6	-33.6	-42.6
Loop 12	-32.1	-14.1	+3.9	+22.9	+53.9	+26.9	+8.9	+2.9	-26.1	-47.1
Loop 16	-29.2	-12.2	+5.8	+24.8	+45.8	+29.8	+10.8	-6.2	-24.1	-45.2
Specific loop	-30.8	-13.3	+4.7	+24.0	+43.0	+29.2	+11.5	-3.3	-26.3	-44.3

TABLE 4-1. - Test Sheets for Test No. 32.

Thus, it is necessary to look for other means of presenting the test results. Examination of the data indicates that two factors are of importance, namely:

1. The shape of the nth loop

2. The position of the nth loop

The shape of the nth loop is completely described by its coordinates in relation to the coordinate axes II in Fig. 4-3. These axes have their origin in the center of gravity of the loop. The new coordinates are called reduced load and reduced deformation respectively and they are readily calculated for each point of the loop from the formulas

| Reduced load | = | Load on pan | - | Initial load |

| Reduced deformation | = | Observed deformation | - | Mean of observed deformation for all points in the loop |

The position of the nth loop in relation to the original axes is determined by the coordinates to the origin of axes II. However, as the first loop is affected by the stress history, we do not know the point of true zero deformation. The absolute position of the nth loop can, therefore, not be determined from the available test result. By choosing arbitrarily a system of coordinates (axes I in Fig. 4-3) which has its origin at the center of gravity for the entire set of observations we can, however, find the position of the nth loop relative to any other loop. Using the centers of gravity for the individual loops as reference points we have:

| Reduced position of nth loop | = | Mean of observations for nth loop | - | Mean of all observations |

These coordinates are shown in the last column of Table 4-1.

The histogram

On Fig. 4-5 is plotted what will be called a histogram for Test
No. 32. The histogram is a graph showing the reduced deformations
defined above as a function of the logarithm of the loop number. Each
line in the graph represents a certain reduced load (moment) and the
numbers shown on the first observations correspond to the numbers shown
on the nth loop on Fig. 4-3.

The entire system of lines gives a good picture of the variation
of the shape of the loops. Noting that a series of equal loops would
correspond to a system of parallel lines it can be concluded from the
histogram that as the loop number increases the shape of the loop approaches
a limit, this limiting loop will be called the specific loop. The reduced
coordinates to the specific loop can with good approximation be calculated
as the average of the reduced coordinates of the 4, 8, 12 and 16th loops.
Next to the histogram is shown the corresponding loop which was calculated
as an average of tests Nos. 32 and 33.

Coefficient of creep

The heavy curve shown on Fig. 4-5 is a plot of the reduced position
of the nth loop against the logarithm of the loop number.

For all 36 tests it was found that for $n > 2$ this curve plotted as
a straight line. This means that the absolute distance to the center of
gravity for the nth loop can be written as:

$$a_n = a_1 + C_{cr} \log n \tag{4-1}$$

where a_1 is a constant deformation which depends on the stress
history of the sample, and
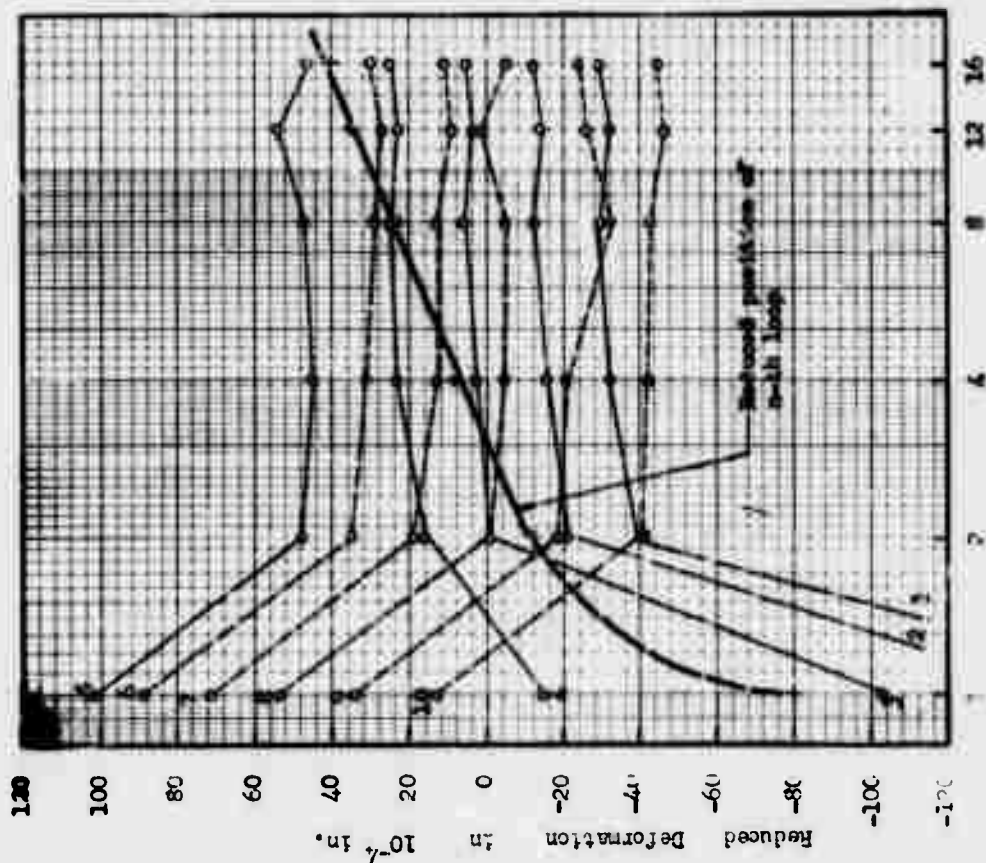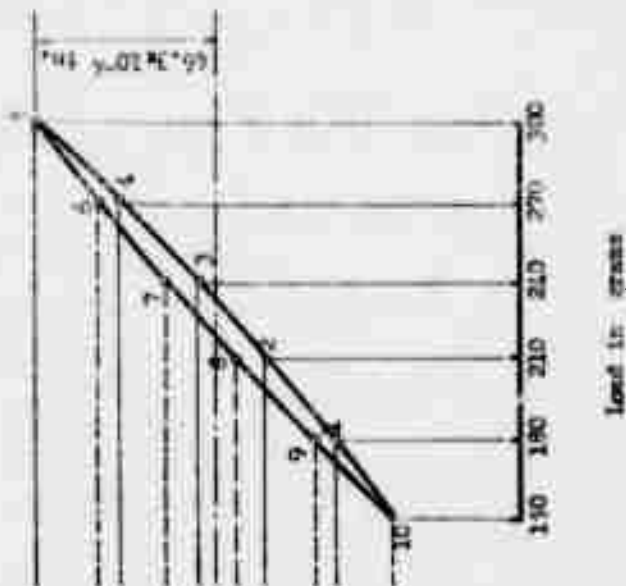
Fig. 4-5. - Histogram for test No. 32.

C_{cr} is a constant which can be calculated from the slope of the line. This constant will in the following be called the coefficient of creep. It has the dimension of deformation.

From Eq. (4-1) we see that the distance between the nth and the n + 1st loop is

$$a_{n+1} - a_n = C_{cr} \log \frac{n+1}{n} \qquad (4-2)$$

which together with the specific loop gives a good description of the behavior of the stress-strain relationship for large values of n. The result of each test is, therefore, reported as the numerical value of C_{cr} which is given in Table 4-10, and the reduced coordinates to the specific loop which are given in Tables 4-2 to 4-7.

Considerations of symmetry

The accuracy of the test results can be somewhat improved by making use of symmetry. Tests Nos. 1 and 2 give approximately the same result with opposite sign, which is not surprising as the main difference between the two tests is a change in the direction of the moment. Assuming that the symmetry exists, the accuracy of the test results can be improved by taking the average of the two tests. Similar considerations can be made for Tests Nos. 3 and 4 up to 13 and 14, and from 22 to 23 up to 34 and 35.

A study of the results also shows that all the specific loops are nearly symmetrical around their center of gravity. If it is assumed that this symmetry is exact, the test results can be improved once more by averaging the two sides of the loop. The above calculations were made for all the tests and the results are shown in Tables 4-2 to 4-7.

The specific loop

From Eq. (4-2) is is evident that for very large values of n there
is virtually no difference in the position of succeeding loops. The load-
deformation relationship can therefore be described as a simple repetition
of the specific loop, a situation which is very similar to the behavior of
a material under dynamic loading (see section II). Assuming that the
specific loop is equivalent to the dynamic hysteresis loop the specific
damping capacity was calculated for all tests using

$$p = \frac{\Delta W}{W} \qquad (2-13)$$

where ΔW is the area of the specific loop and W is the potential
energy at maximum amplitude. ΔW was readily calculated from the
coordinates to the specific loop and W was assumed to be equal to the
area of the triangle ABC shown on Fig. 4-3. The results of the calcula-
tions are shown in the summary Tables 4-8 and 4-9. In the same tables
are shown values of the logarithmic decrement calculated from formula (2-14).
The dynamic shear moduli have been calculated for all tests from the
formula

$$G = \frac{32}{\pi} \frac{M}{\Theta d^4} \qquad (4-3)$$

where Θ = the amplitude of deformation (rad./in.)

          M = the amplitude of moment (lbs./in.)

          d = diameter of specimen (in.)

The results of the calculations are shown in Tables 4-8 and 4-9. In the same tables are shown values of the velocity of the shear wave calculated from the formula

$$N_s = \sqrt{\frac{g\,G}{\gamma}}$$

(4-4

where g =   acceleration of gravity and

   γ =   unit weight of the sample

Discussion of test results

A description was given of the method whereby the load-deformation relationship for large loop numbers can be described by the coefficient of creep and the specific loop. It was also noted that due to the effect of stress history on the first loops, it is not possible to obtain any information about the absolute deformations from the available test results.

Assuming that the specific loop corresponds to the dynamic hysteresis loop, calculations were made for the dynamic properties of specific damping capacity, dynamic shear modulus, and the velocity of the shear wave.

In order to be able to compare these latter results with the results of dynamic tests several graphs were prepared.

Figure 4-6 shows the relationship between the relative amplitude of moment and damping. It appears from this graph that the relationship is independent of the confining pressure. It also appears that the damping depends on the initial load. The symmetrical tests (no initial load) showed a much higher damping than the asymmetrical tests. This is possibly due to a relaxation of prestrain effects when the direction of the moment is reversed. For the tests in which the direction of the moment was unchanged it was found that the damping increased with increasing initial load.
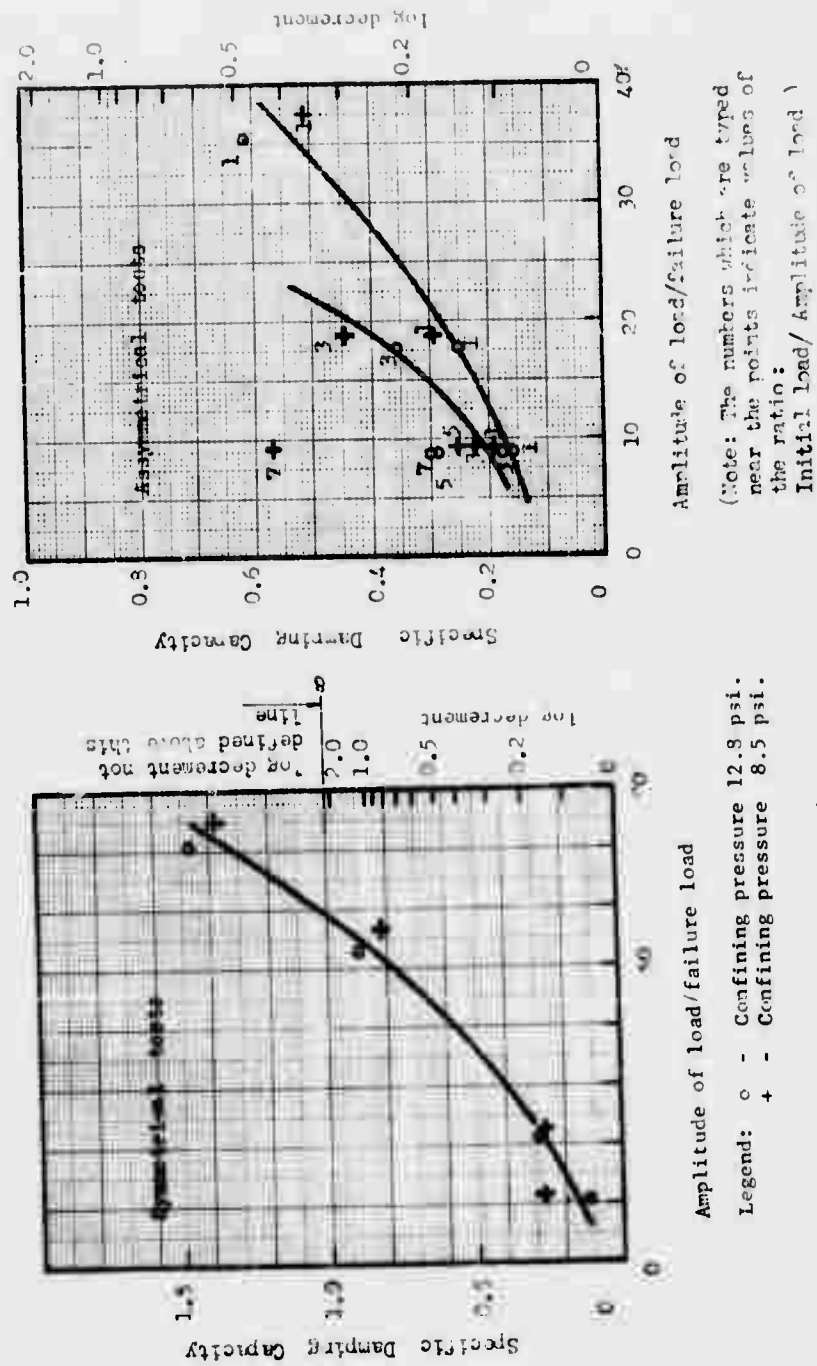
Fig. 4-6. - Relationship between damping and relative amplitude of load

(Note: The numbers which are typed near the points indicate values of the ratio:
Initial load/Amplitude of load)

Legend: o - Confining pressure 12.9 psi.
+ - Confining pressure 8.5 psi.

Figure 4-7 shows the variation of damping with amplitude of deformation. As could be expected the damping increases with amplitude and decreases with the confining pressure. Just as above a distinct difference between symmetrical and asymmetrical tests was found. A comparison between the results of the symmetrical tests and similar dynamic tests in the low amplitude range shows that the damping calculated from the present tests is of the same magnitude as the damping found from dynamic tests. No dynamic tests results are available for comparison with the asymmetrical tests. The variation of the calculated velocity of shear waves with amplitude of deformation is shown on Fig. 4-8. The values calculated from the symmetrical tests are 10% - 20% lower than the corresponding values measured in dynamic tests.

Figure 4-9 shows the relationship between the coefficient of creep and the initial moment. It is evident from this graph that the creep increases with increasing initial load and amplitude of moment.

Amplitude of deformation (radians per inch)

Amplitude of deformation (radians per inch)
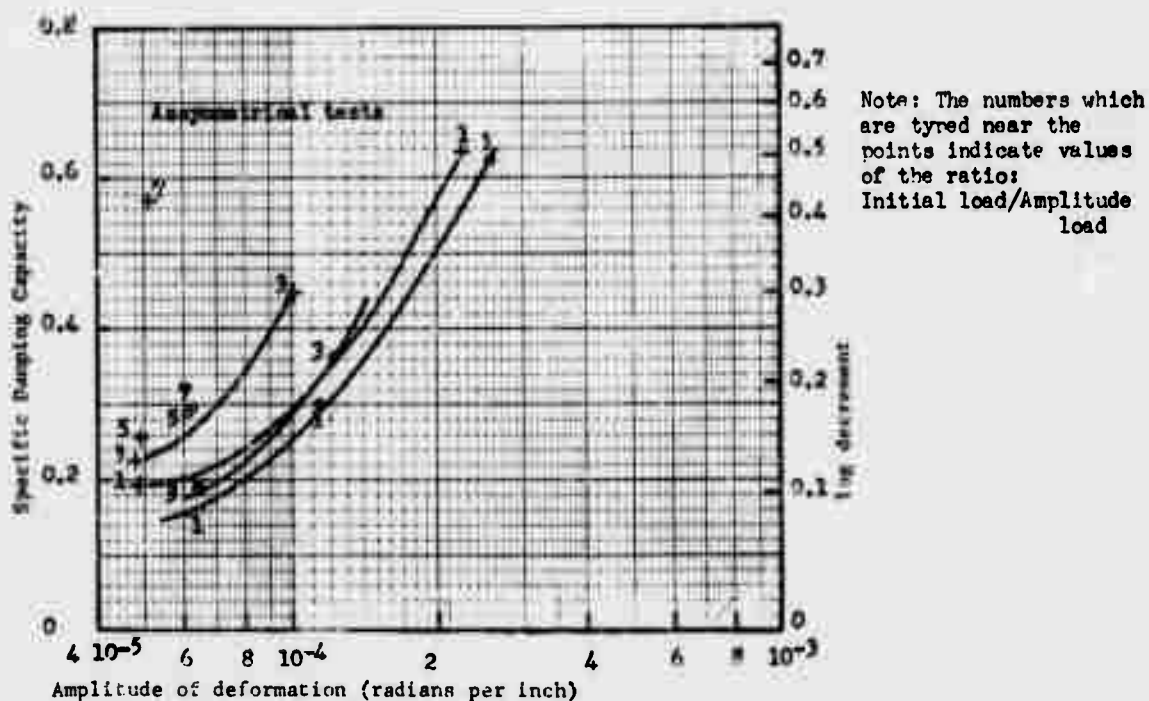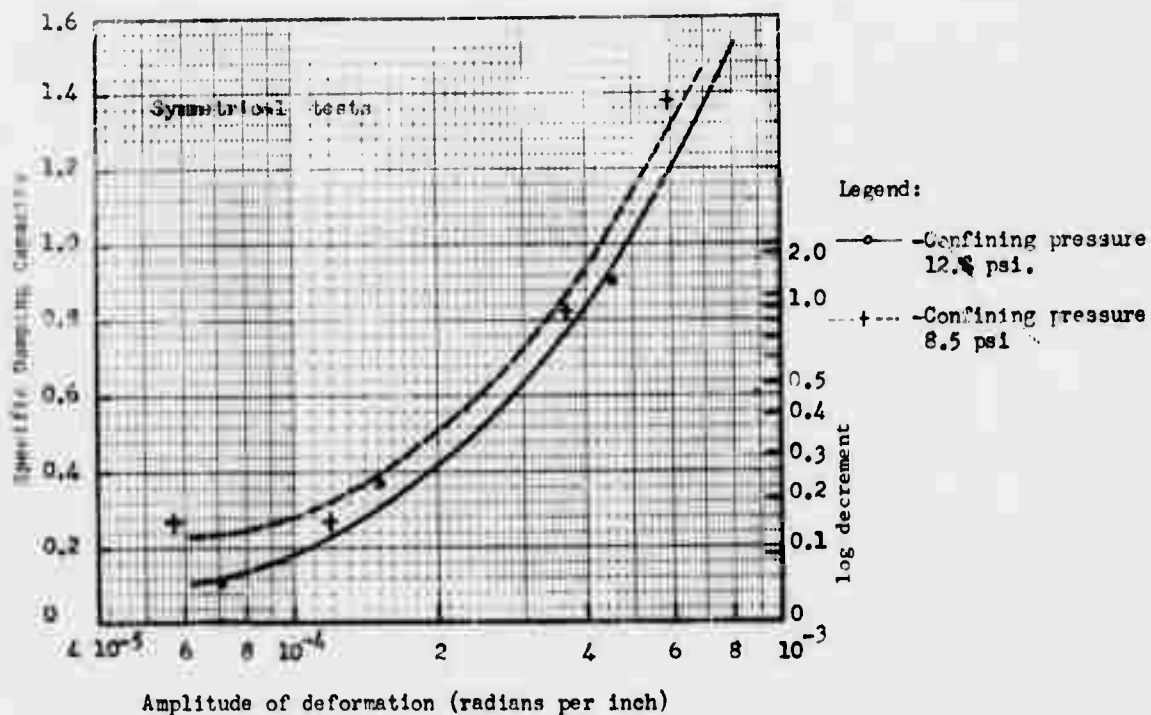
Fig. 4-7. - Relationship between damping and amplitude of deformation
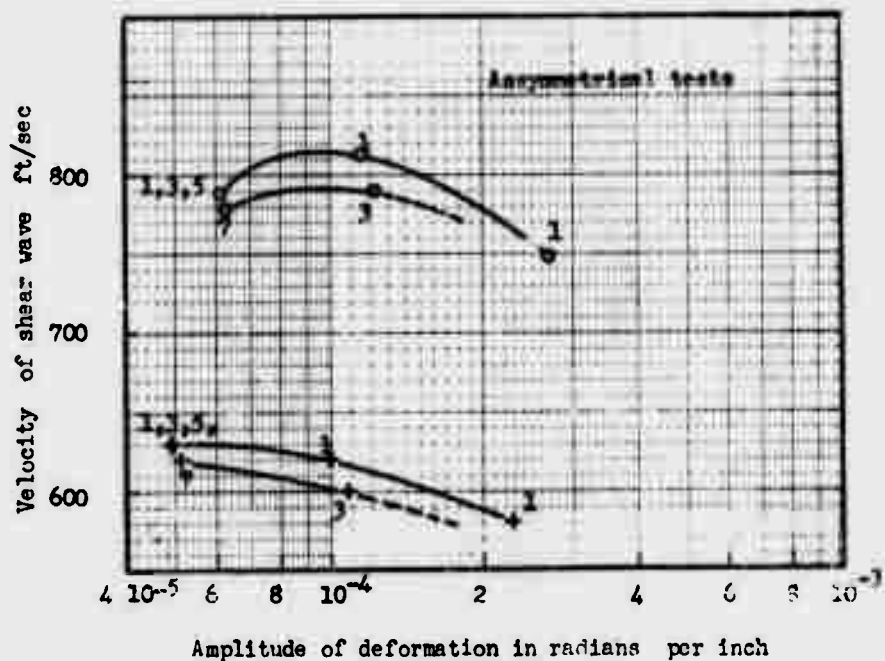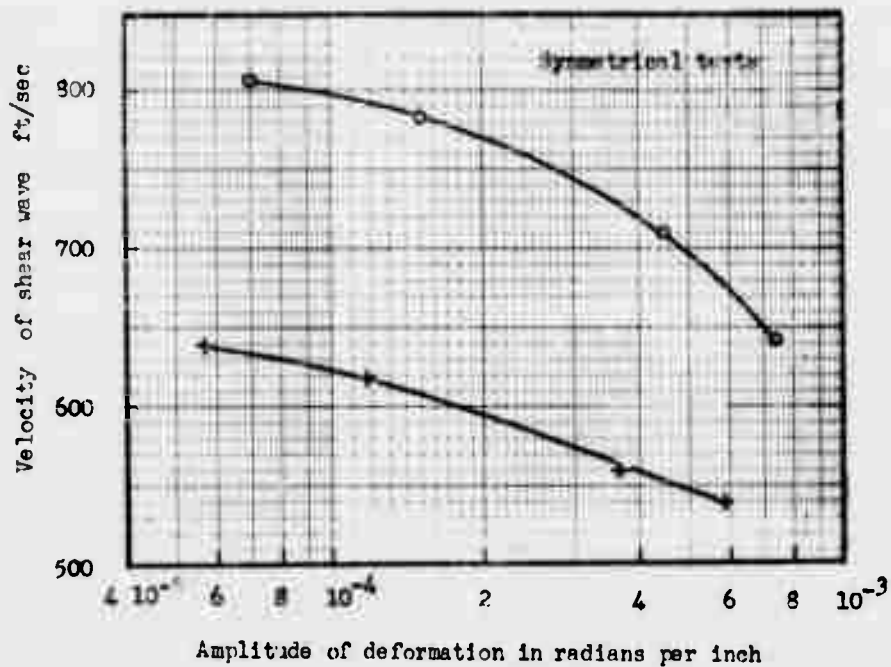
Fig. 4-8   Relationship between wave velocity and amplitude of deformation
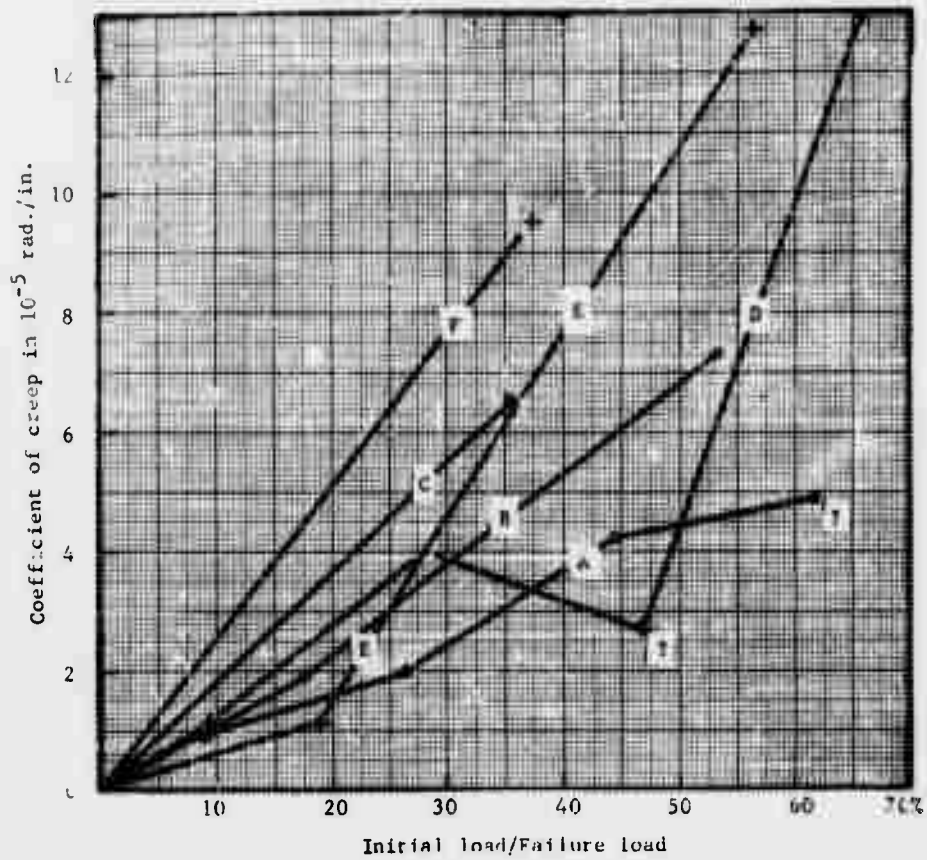
Curve	A	B	C	D	E	F
Confining pressure psi	12.8	12.8	12.8	8.5	8.5	8.5
Amplitude of moment in.-lb.	0.515	1.03	2.06	0.386	0.773	1.545

Points marked ? are uncertain.

Fig. 4-9. - Relationship between coefficient of creep and initial load.

Coordinates to points of specific loop as calculated from loops Nos. 4, 8, 12 & 16

Test No.	Rota-tion	Max. load gr.	Min. load gr.	Point 1	Point 2	Point 3	Point 4	Point 5	Point 6	Point 7	Point 8	Point 9	Point 10
				-30	-10	10	30	50	30	10	-10	-30	-50
Reduced load in grams													
1	pos.	100	0	-17.1	- 5.8	4.7	16.2	25.9	16.9	6.9	- 5.3	-16.3	-25.5
2	neg.	-	-	17.2	6.7	-4.6	-16.1	-27.6	-17.3	-6.6	4.9	15.9	25.9
3	pos.	200	100	-17.0	- 6.2	4.0	16.0	27.3	17.0	6.5	- 4.5	-16.5	-26.7
4	neg.	-	-	17.3	6.5	-5.0	-16.0	-26.7	-17.2	-6.7	5.0	15.5	25.5
5	pos.	300	200	-17.6	- 6.6	3.2	14.7	26.4	17.9	4.9	- 2.8	-16.6	-25.8
6	neg.	-	-	18.4	6.6	-4.1	-15.6	-28.1	-16.8	-6.1	3.4	15.2	26.9
7	pos.	400	300	-18.7	- 7.3	-3.2	15.5	27.5	18.5	7.0	- 4.0	-15.5	-29.2
8	neg.	-	-	17.9	6.7	-4.1	-16.1	-28.3	-17.8	-7.1	4.9	15.9	27.7
Assume that pos. and neg. rotation give the same specific loop													
1-2		100	0	-17.15	- 6.25	4.65	16.15	26.75	17.10	6.75	- 5.10	-16.10	-26.85
3-4		200	100	-17.15	- 6.35	4.50	16.00	27.00	17.10	6.60	- 4.75	-16.00	-26.60
5-6		300	200	-18.00	- 6.60	3.65	15.15	27.25	17.35	5.50	- 3.20	-15.90	-26.35
7-8		400	300	-18.30	- 7.00	3.65	15.80	27.90	18.15	7.05	- 4.45	-15.07	-26.95
Assume that the specific loop is symmetrical													
1-2		100	0	-17.13	- 6.50	4.88	16.13	26.80					
3-4		200	100	-17.13	- 6.48	4.63	16.00	26.80					
5-6		300	200	-17.63	- 6.05	3.38	15.53	26.30					
7-8		400	300	-18.23	- 6.53	4.05	15.75	27.43					

Note: The deformation is expressed in terms of the movement of the contact point (unit: 10^{-4} in).

TABLE 4-2. - Reduced coordinates for specific loops

Coordinates to points of specific loop as calculated from loops Nos. 4,8,12 & 13

Test No.	Rotation	Max. load gr.	Min. load gr.	Point 1	Point 2	Point 3	Point 4	Point 5	Point 6	Point 7	Point 8	Point 9	Point 10
				-60	-20	20	60	100	60	20	-20	-60	-200
Reduced load in grams													
9	pos.	200	0	-33.1	-13.1	8.2	28.9	50.4	31.2	12.9	-7.3	-26.1	-50.1
10	neg.	-	-	31.9	11.4	-7.6	-28.8	-50.6	-31.3	-12.5	8.2	28.9	50.2
11	pos.	400	200	-34.8	-13.8	7.2	29.4	53.2	33.7	13.7	-7.5	-29.3	-52.3
12	neg.	-	-	35.2	14.5	-7.0	-29.5	-54.0	-34.8	-13.8	7.5	29.2	53.6
Assume that pos. and neg. rotation give the same specific loop													
9-10		200	0	-32.50	-12.25	7.90	28.85	50.50	31.25	12.75	-7.85	-28.50	-50.15
11-12		400	200	-35.00	-14.15	7.10	29.45	53.60	34.25	13.75	-7.40	-29.25	-52.63
Assume that the specific loop is symmetrical													
9-10		200	0	-31.88	-12.50	7.88	28.68	50.10					
11-12		400	200	-34.63	-13.95	7.25	29.35	53.13					
				-120	-40	40	120	200	20	40	-40	-120	-200
Reduced load in grams													
13	pos.	400	0	-83.5	-38.5	8.5	61.3	121.5	82.3	37.5	-9.7	-61.2	-119.0
14	neg.	-	-	78.9	35.4	-11.3	-61.6	-118.3	-77.8	-34.1	11.9	61.2	115.7
Assume that pos. and neg. rotation give the same specific loop													
13-14		400	0	-81.20	-36.95	9.90	61.45	119.90	80.05	35.80	-10.80	-61.20	-117.35
Assume that the specific loop is symmetrical													
13-14		400	0	-80.63	-36.38	10.35	61.33	118.63					

Note: The deformation is expressed in terms of the movement of the contact point (unit 10^{-4} in.).

TABLE 4-3. - Reduced coordinates for specific loops

Point 1	Point 2	Point 3	Point 4	Point 5	Point 6	Point 7	Point 8	Point 9	Point 10	Point 11	Point 12	Point 13	Point 14	Point 15	Point 16
							Test NO. 15								
-40	-20	0	20	40	60	40	20	0	-20	-40	-60				
-21.3	-10.8	-0.6	9.9	20.2	31.2	20.9	11.2	0.7	-9.8	-20.3	-31.1				
-21.10	-11.00	-0.65	9.85	20.25	31.15	21.10	11.00	0.65	-9.85	-20.25	-31.15				
							Test NO. 16								
-80	-40	0	40	80	120	80	40	0	-40	-80	-120				
-45.40	-24.6	-3.9	18.9	40.9	65.3	45.1	24.6	3.3	-15.1	-41.1	-65.6				
-45.25	-24.60	-3.60	18.50	41.00	65.70	45.25	24.60	3.60	-15.50	-41.00	-65.70				
							Test NO. 17								
-200	-100	0	100	200	300	200	100	0	-100	-200	-300				
-151.8	-93.5	-32.3	34.2	108.5	200.0	150.5	94.5	31.2	-34.5	-108.5	-198.3				
-151.10	-94.00	-31.75	34.35	108.65	199.15	151.10	94.00	31.75	-34.35	-108.65	-199.15				
							Test NO. 18								
-300	-200	-100	0	100	200	300	400	300	200	100	0	-100	-200	-300	-400
-286.6	-226.6	-160.3	-86.1	-6.3	84.9	192.9	332.4	279.6	221.6	157.4	86.2	-1.7	-52.3	-186.1	-321.6
-283.10	-224.25	-158.85	-86.15	-2.30	83.60	189.50	327.00	283.10	224.25	158.85	86.15	2.30	-83.60	-189.50	-327.00

NOTE:

1st line indicates load (gr).

2nd line indicates deformation $(10^{-4}$ inch).

3rd line indicates deformation if symmetry is assumed.

Note: The deformation is expressed in terms of the movement of the contact point (units: 10^{-4} in.).

TABLE 4-4. - Reduced coordinates for specific loops

Coordinates to points of specific loop as calculated from loops Nos. 4,8,12 & 16

Test No.	Rotation	Max. load gr.	Min. load gr.	Point 1	Point 2	Point 3	Point 4	Point 5	Point 6	Point 7	Point 8	Point 9	Point 10
				-22.5	-7.5	7.5	22.5	37.5	22.5	7.5	-7.5	-22.5	-37.5
Reduced load in grams													
22	pos.	75	0	-14.1	-5.1	3.4	12.4	21.7	13.7	5.2	-4.1	-12.3	-20.8
23	neg.	-	-	11.7	5.2	-3.1	-12.1	-21.1	-15.1	-4.6	-4.2	12.7	21.7
24	pos.	150	75	-14.7	-5.0	3.3	12.3	21.0	13.3	4.5	-3.2	-12.2	-21.0
25	neg.	-	-	14.0	5.0	-3.7	-12.7	-21.5	-13.7	-5.5	4.0	12.5	21.0
26	pos.	225	150	-13.7	-5.7	3.1	11.6	20.6	13.8	5.6	-3.2	-1.9	-20.9
27	neg.	-	-	13.7	4.7	-3.5	-12.3	-22.3	-13.5	-5.3	4.2	12.7	21.5
28	pos.	300	225	-15.9	-6.9	2.4	11.9	22.6	14.6	6.3	-2.4	-12.1	-21.4
29	neg.	-	-	16.0	6.7	-2.3	-11.8	-23.3	-15.8	-6.5	2.7	-2.7	21.7
Assume that pos. and neg. rotation give the same specific loop													
22-23		75	0	-12.90	-5.15	3.25	12.25	21.40	14.40	4.90	-4.25	-12.50	-21.25
24-25		150	75	-14.35	-5.00	3.50	12.50	21.25	13.50	5.00	-3.60	-12.35	-21.00
26-27		225	150	-13.70	-5.20	3.30	11.95	21.45	13.65	5.45	-3.70	-12.30	-21.20
28-29		300	225	-15.95	-6.80	2.35	11.85	22.95	15.20	6.55	-2.55	-11.90	-21.55
Assume that the specific loop is symmetrical													
22-23		75	0	-13.65	-5.03	3.75	12.38	21.33					
24-25		150	75	-13.93	-5.00	3.55	12.43	21.13					
26-27		225	150	-13.68	-5.33	3.50	12.13	21.33					
28-29		300	225	-15.58	-6.68	2.45	11.88	22.25					

Note: The deformation is expressed in terms of the movement of the contact point (unit: 10^{-4} in.)

TABLE 4-5. - Reduced coordinates for specific loops

Coordinates to points of specific loop as calculated for loops Nos. 4,8,12 & 16.

Test No.	Rotation	Max. load gr	Min. load gr	Point 1	Point 2	Point 3	Point 4	Point 5	Point 6	Point 7	Point 8	Point 9	Point 10
Reduced load in grams				-45	-15	15	45	75	45	15	-15	-45	-75
30 pos.		150	0	-29.0	-11.5	6.3	24.8	44.0	29.3	10.3	- 6.7	-24.2	-42.5
31 neg.		-	-	27.4	11.6	-6.6	-24.6	-44.3	-27.1	-10.6	5.9	24.9	43.4
32 pos.		300	150	-30.8	-13.3	4.7	24.0	48.0	29.0	11.5	- 3.3	-26.3	-44.3
33 neg.		-	-	31.3	13.3	-5.5	-25.4	-47.7	-30.7	-12.4	6.1	25.1	45.3

Assume that pos. & neg. rotation give the same specific loop

Test No.		Max. load gr	Min. load gr	Point 1	Point 2	Point 3	Point 4	Point 5	Point 6	Point 7	Point 8	Point 9	Point 10
30-31		150	0	-28.20	-11.55	6.45	24.70	44.15	27.70	10.45	-5.30	-24.35	-42.95
32-33		300	150	-30.95	-13.30	5.10	24.70	47.85	29.85	11.95	-4.70	-25.70	-44.80

Assume that the specific loop is symmetrical

Test No.		Max. load gr	Min. load gr	Point 1	Point 2	Point 3	Point 4	Point 5
30-31		150	0	-27.95	-11.00	6.38	24.63	43.55
32-33		300	150	-30.40	-12.63	4.90	25.20	46.33

Test No.		Max. load gr	Min. load gr	Point 1	Point 2	Point 3	Point 4	Point 5	Point 6	Point 7	Point 8	Point 9	Point 10
Reduced load in grams				-90	-30	30	90	150	90	30	-30	-90	-150
34		300	0	-67.3	-32.0	7.0	50	100.7	66.5	30.0	8.3	-49.8	- 97.3
35		-	-	67.6	31.3	- 7.7	-50.9	-100.7	-66.2	-29.9	9.1	50.3	97.1

Assume that pos. & neg. rotation give the same specific loop

Test No.		Max. load gr	Min. load gr	Point 1	Point 2	Point 3	Point 4	Point 5	Point 6	Point 7	Point 8	Point 9	Point 10
34-35		300	0	-67.45	-31.65	7.35	50.45	100.70	66.35	29.95	- 8.70	-50.05	-97.20

Assume that the specific loop is symmetrical

Test No.		Max. load gr	Min. load gr	Point 1	Point 2	Point 3	Point 4	Point 5
34-35		300	0	-66.90	-30.80	3.03	50.25	98.95

Note: The deformation is expressed in terms of the movement of the contact point (unit: 10^{-4} in.)

TABLE 4-6. - Reduced coordinates for specific loops

Point 1	Point 2	Point 3	Point 4	Point 5	Point 6	Point 7	Point 8	Point 9	Point 10	Point 11	Point 12	Point 13	Point 14	Point 15	Point 16
								Test NO. 36							
30	15	0	-15	-30	-45	-30	-15	0	15	30	45				
16.3	9.8	1.6	-7.4	-15.7	-24.7	-17.9	-9.9	-1.7	7.6	16.3	25.3				
17.10	9.85	1.65	-7.50	-16.00	-25.00	-17.10	-9.85	-1.65	7.5	16.00	25.00				
								Test NO. 37							
60	30	0	-30	-60	-90	-60	-30	0	30	60	90				
35.80	20.1	2.6	-15.2	-33.4	-51.9	-36.2	-19.2	-1.9	14.1	32.8	51.8				
35.00	19.65	2.25	-14.65	-33.10	-51.35	-36.00	-19.65	-2.25	14.65	33.10	51.85				
								Test NO. 38							
150	75	0	-75	-150	-225	-150	-75	0	75	150	225				
118.1	73.9	24.6	-28.9	-88.4	-160.6	-118.4	-72.4	-23.6	28.6	88.1	159.5				
118.25	73.15	24.10	-28.75	-88.25	-159.60	-118.25	-73.15	-24.10	28.75	88.25	159.60				
								Test NO. 39							
225	150	75	0	-75	-150	-225	-300	-225	-150	-75	0	75	150	225	300
219.3	169.8	121.6	64.6	1.1	-70.2	-149.2	-259.7	-218.9	-170.9	-118.9	-62.2	-0.2	68.6	149.8	255.3
219.0	170.35	120.25	63.40	0.65	-69.40	-149.5	-257.5	-219.0	-170.35	-120.25	-63.40	-0.65	69.40	149.5	257.5

NOTE:

1st line indicates load (in).

2nd line indicates deformation (10^{-4} inch).

3rd line indicates deformation if symmetry is assumed.

Note: The deformation is expressed in terms of the movement of the contact point (unit: 10^{-4} in.).

Table 4-7   Reduced coordinates for specific loops

Test No.	Initial moment lb.-in.	Amplitude of moment lb.-in.	Initial Moment / Moment at failure %	Amplitude of moment / Moment at failure %	Amplitude of deformation 10⁻⁵ rad./in.	Shear modulus psi.	Velocity of shear wave ft./sec.	Specific damping capacity	Log decrement
1-2	0.515	0.515	8.8	8.3	6.10	14,300	790	0.156	0.085
3-4	1.545	0.515	26.5	8.8	5.10	14,300	790	0.178	0.098
5-6	2.575	0.515	42.2	8.8	6.19	14,300	790	0.288	0.170
7-8	3.605	0.515	61.9	8.8	6.24	14,400	780	0.289	0.171
9-10	1.030	1.030	17.7	17.7	11.5	15,700	810	0.250	0.141
11-12	3.090	1.030	53.1	17.7	12.1	14,900	790	0.361	0.224
13-14	2.06	2.06	35.4	35.4	27.0	13,300	750	0.611	0.342
15	0	0.618	0	10.6	7.09	15,300	800	0.113	0.056
16	0	1.236	0	21.2	15.0	14,500	780	0.283	0.166
17	0	3.090	0	53.1	45.3	12,000	710	0.893	1.13
18	0	4.12	0	70.8	74.4	9,800	640	1.473	not defined

Common data for test series I   confining pressure = 12.8 psi
void ratio = 0.501
diameter of sample = 1.557 in.

TABLE 4-8. - Summary of results from test series I

Test No.	Initial moment lb.-in.	Amplitude of moment lb.-in.	Initial moment at failure Moment at failure %	Amplitude of moment at failure %	Amplitude of defor- mation 10^{-5} rad./ in.	Shear modulus psi	velocity of shear wave ft./sec.	Specific damping capacity	Log decre- ment
22-23	0.386	0.386	9.38	9.38	4.88	13,700	630	0.192	0.107
24-25	1.159	0.386	28.13	9.38	4.83	13,900	630	0.224	0.147
26-27	1.931	0.386	46.88	9.38	4.88	13,700	630	0.252	0.145
28-29	2.704	0.386	65.63	9.38	5.09	13,200	620	0.570	0.422
30-31	0.773	0.773	18.75	18.75	9.95	13,500	620	0.293	0.173
32-33	2.318	0.773	56.25	18.75	10.6	12,600	600	0.447	0.296
34-35	1.545	1.545	37.5	37.5	22.6	11,800	580	0.637	0.510
36	0	0.464	0	11.25	5.71	14,100	640	0.272	0.159
37	0	0.927	0	22.5	11.9	12,500	620	0.261	0.151
38	0	2.318	0	56.25	36.5	11,000	560	0.823	0.870
39	0	3.090	0	75.0	58.9	10,100	540	1.378	not defined

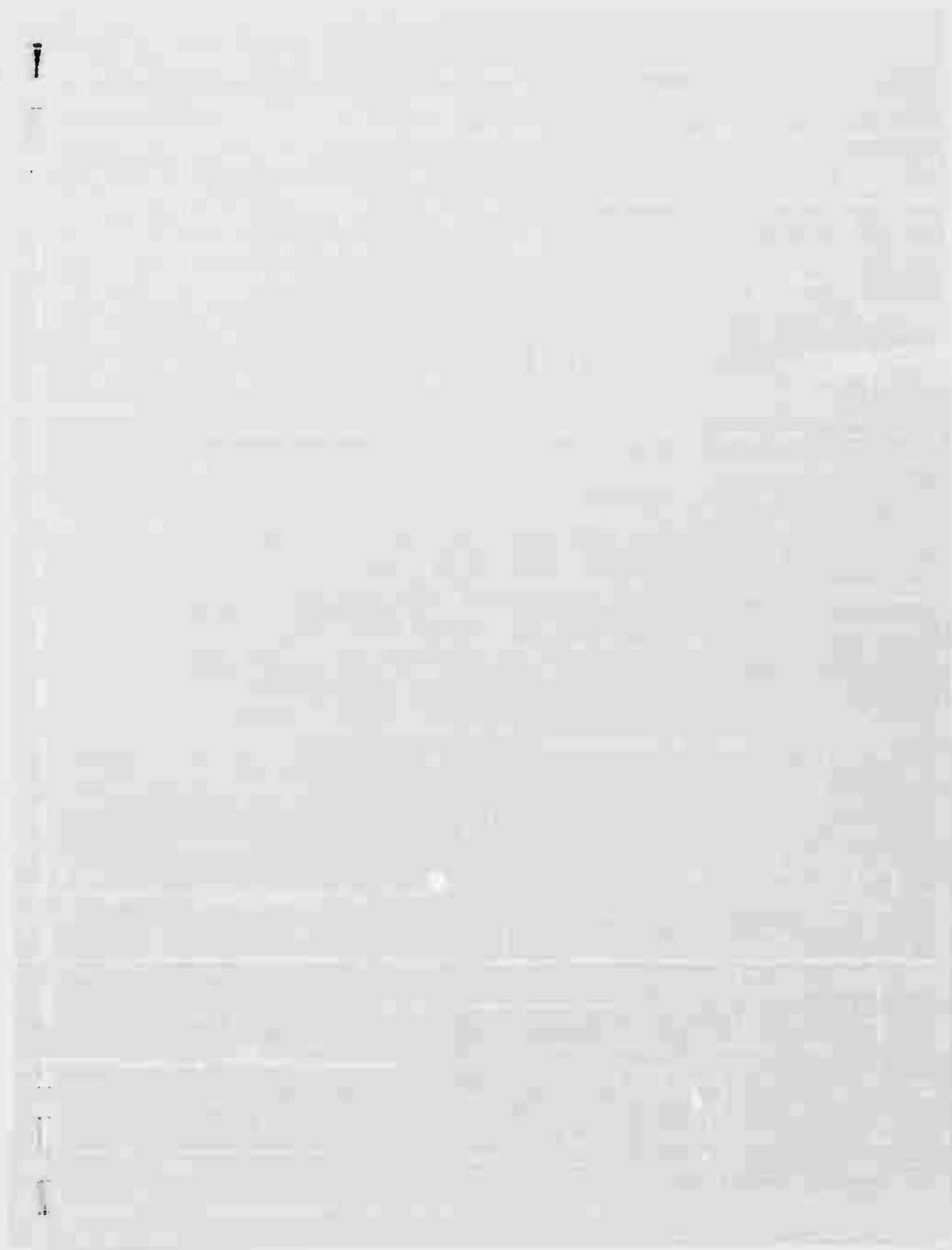Common data for test series II   confining pressure = 8.5 psi
                                  void ratio = 0.485
                                  diameter of sample = 1.557 in.

TABLE 4-9. - Summary of results from test series II

4-29

TEST NO.	INITIAL MOMENT in.-lbs.	AMPLITUDE OF MOMENT in.-lbs.	COEFFICIENT OF CREEP Assume symmetry		
			10^{-4} in	10^{-4} in	10^{-5} rad/in
1.	0.515	0.515	+ 5.0	3.8	0.9
2.			- 2.5		
3.	1.545	0.515	+ 9.5	8.8	2.0
4.			- 8.0		
5.	2.575	0.515	+18.5	18.6	4.2
6.			-18.7		
7.	3.605	0.515	+33.2	21.6	4.9
8.			-10.0		
9.	1.039	1.030	+ 9.8	8.3	1.9
10.			- 6.7		
11	3.090	1.030	+23.5	31.8	7.3
12.			-30.5		
13.	2.060	2.060	+36.4	28.3	6.5
14.			-20.2		
15.	0	0.618	No creep was observed tor		
16.	0	1.236			
17.	0	3.090	large loop numbers.		
18.	0	4.120			
22.	0.386	0.386	+ 6.8	4.9	1.1
23.			- 3.0		
24.	1.159	0.386	+10.6	17.5	4.0
25.			-24.4		
26.	1.931	0.386	+18.0	12.0	2.7
27.			- 6.0		
28.	2.704	0.386	+56.5	56.5	12.9
29.			-56.5		
30.	0.773	0.773	+ 6.2	5.3	1.2
31.			- 4.4		
32.	2.318	0.773	+52.6	55.6	12.7
33.			-58.6		
34.	1.545	1.545	+42.3	41.7	9.5
35.			+40.0		
36.	0	0.464	No creep was observed for		
37.	0	0.927			
38.	0	2.318	large loop numbers.		
39.	0	3.090			

Note: 12.8 psi vacuum (tests 1–18); 8.5 psi vacuum (tests 22–39).

Note: For definition see Equation (4-1)

TABLE 4-10. - Coefficients of Creep

V. CONCLUSIONS

The conclusions obtained from this study necessarily apply to granular soils which have been subjected to several load repetitions and have reached a relatively stable condition. This corresponds to construction conditions where the soil has been pre-vibrated or pre-compacted to eliminate the disastrous settlements which may accompany the first dynamic load application on loose granular soils.

From the steady state vibration tests on granular materials, the results for the Ottawa sand and glass beads gave results which should be typical for sands with rounded grains. A detailed discussion of these results is given in Section III-D and the more important conclusions are listed below:

1. Both the shear and compression wave velocities decrease as the amplitude of vibration is increased. This decrease may be as much as 10 to 15 per cent as the double amplitude is increased from 1×10^{-5} to 3×10^{-3} rad. in the shear tests or from 1×10^{-5} to 2.5×10^{-3} in. in the compression tests. The stresses developed at the maximum amplitudes were as high as 20 per cent of the failure stress in some tests.

2. The effects on wave velocities produced by changes of void ratio from the densest to the loosest condition is also about 10 to 15 per cent. Thus void ratio changes and changes of amplitude influence the wave velocities by comparable amounts.

3. The wave velocities are significantly affected by changes in the confining pressure as indicated on the summary Figs. 3-38 through 3-41. For confining pressures above 2000 lb./ft.^{2} the variation of wave velocity is with the 0.25 power of the confining pressure for the Ottawa sand and glass beads No. 2847. The variation was with the 0.21 power of pressure for the glass beads No. 0017. Both of these values are greater than the 0.167 power given theoretically for the relation between wave velocity and confining pressure.

4. For dry Ottawa sand the logarithmic decrement varies with about the 0.25 power of amplitude. Saturated Ottawa sand shows little variation of logarithmic decrement with amplitude. Therefore, the amount of damping contributed by the water apparently increases as the amplitude of vibration decreases. The variation of logarithmic decrement with amplitude for glass beads No. 2847 is with the 0.38 power for the dry condition and with the 0.15 power when saturated with water.

5. The damping determined from the decay of steady state vibrations in samples of rounded granular materials behaves like viscous damping. The values of logarithmic decrement varied from 0.02 to about 0.20 for the various materials and test conditions used.

6. The static torsion tests on dense Ottawa sand were run primarily to indicate the effect of amplitudes which approached the failure conditions. Figure 4-6 (p. 4-16) illustrates the variation of damping quantities with torsional loads up to 75 per cent of the failure load for the two confining pressures used. Large values of damping are associated with loads near failure.

7. The second purpose for the static damping tests was to evaluate
    the effects of stress history on the damping values. The tests
    using equal plus and minus torques (symmetrical tests) showed
    higher values of damping than for the tests using comparable
    torque magnitudes applied in one direction only (unsymmetrical
    tests). In the latter tests the damping characteristics could
    be described in terms of a specific loop, a shape of the hyster-
    esis loop, and a coefficient of creep, which relates the mean
    strain in the loop to the number of loop applications. This
    creep effect appeared to be continuous, varying almost linearly
    with the logarithm of the number of loops, and the creep rate
    increased with the torque amplitude.

8. Values of the logarithmic decrement obtained from the symmetrical
    static torsion tests were approximately the same as those obtained
    from the dynamic tests, for comparable test conditions.

9. Values of shear wave velocity computed using the hysteresis
    modulus from the static shear tests were 10 to 20 per cent lower
    than the corresponding values measured in the dynamic tests

Dynamic tests on the Novaculite No. 1250, a very fine-grained crushed
quartz, produced results which were somewhat different from those obtained
from the larger grained materials. The primary difference is that the wave
velocity and damping values obtained from laboratory tests are dependent
upon the stress history and upon the time the loading has been applied. The
wave velocity increases slightly as a particular confining pressure continues
to be applied to a specimen. However, it was also found that higher ampli-
tudes of vibration tend to destroy this time-dependent increase in velocity.
Further investigations are required in order to evaluate the time-dependent

increases in wave velocity (and decreases of damping) and the vibrational
energy required to destroy this gain.

For comparable conditions of confining pressure and amplitude of
vibrations, the Novaculite No. 1250 has a significantly lower value of
logarithmic decrement than that for the Ottawa sand. This is in line
with the test results for the glass beads No. 0017 which are considerably
lower than for the larger diameter glass beads or Ottawa sand. Thus the
value of logarithmic decrement seems to decrease as the average grain
size decreases.

Finally, it should be re-emphasized that the tests described herein
are concerned with the wave propagation and damping in granular materials
which are in a stable condition. Because the deformations are recoverable
when the stresses are below about 20 per cent of the failure stress, the
behavior of the material in this range has been termed "elastic" although
damping is definitely present. The order of magnitude of the logarithmic
decrement is generally below 0.2 for the test conditions used. This
defines a value of $\frac{c}{c_{cr}}$ = 0.03 if a steady state response is to be
considered. The damping due to dispersion of elastic waves in an ideal
medium can be estimated by procedures similar to that illustrated in
Section II-D. A value of R_{v}/c_{cr} , corresponding to c/c_{cr} , can
be expressed by

$$\frac{R_{v}}{c_{cr}} \approx \frac{0.91}{\sqrt{b}} \qquad \text{(for } \mu = 0.25)$$

where $b = m_{o}/\rho r_{o}^{3}$ for the oscillating footing. Thus a comparison can be
made between the material damping and dispersion damping for a given founda-
tion system.
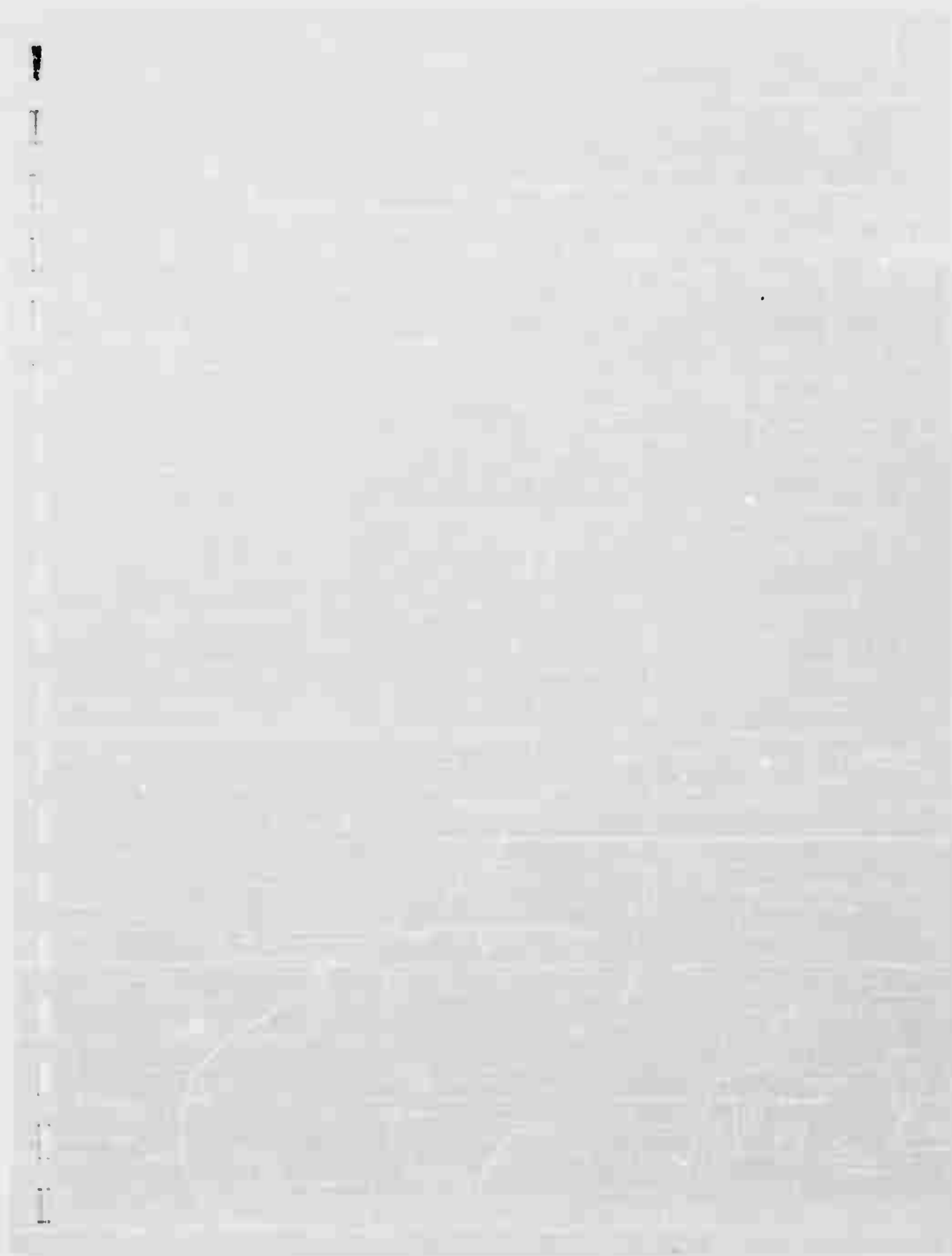
REFERENCES

Baron, M. L. and Matthews, A. T. (1961) "Diffraction of a Pressure Wave by a Cylindrical Cavity in an Elastic Medium," JAM Sept. pp. 347-354.

Bergstrom, S. G. and Linderholm, S. (1946) "A Dynamic Method for Determining Average Elastic Properties of Surface Soil Layers," Swedish Cement and Concrete Institute at the Royal Technical University, Stockholm. 44 pp.

Bernhard, R. K. (1957) "Microseismics," ASTM STP No. 206 Second Pacific Area Meeting Paper on Soils. pp. 83-102.

Biot, M. A. (1956) "Theory of Propagation of Elastic Waves in a Fluid Saturated Porous Solid," J. Acoust. Soc. Am. v. 28. pp. 168-191.

Biot, M. A. and Willis, D. G. (1957) "The Elastic Coefficients of the Theory of Consolidation," J. Appl. Mechanics. ASME v. 24, pp. 594-601.

Birch, F. and Bancroft, D. (1938) "Elasticity and Internal Friction in a Long Column of Granite," Bull. of the Seismological Society of America, v. 28, No. 4, October. pp. 243-254.

Birch, F. and Bancroft, D. (1940) "New Measurements of the Rigidity of Rocks at High Pressure," The Journal of Geology, v. XLVII. No. 7, Oct.-Nov. pp. 752-766.

Birch, F. and Bancroft, D. (1938) "The Effect of Pressure on the Rigidity of Rocks. I," The Journal of Geology, v. XLVI, Nos. 1 and 2. Jan.-Feb. and Feb.-Mar. pp. 58-87, 113-141.

Bornitz, G. (1931) "Uber die Ausbreitung der von Groszkolbenmaschinen erzeugten Bodenschwingungen in die Tiefe," J. Springer. Berlin.

Brandt, H. (1955) "A Study of the Speed of Sound in Porous Granular Media," J. Appl. Mech. v. 22, No. 4, Dec. pp. 479-486.

BRS (1955) "Vibration in Buildings," BRS Digest No. 78.

Crandell, F. J. (1949) "Ground Vibration Due to Blasting and Its Effect on Structures," J. Bost. Soc. C. E. April, 1949.

Demer, L. J. (1956) "Bibliography of the Material Damping Field," WADS Tech. Rep. 56-180. 92 pp.

Domzalski, W. (1956) "Some Problems of Shallow Refraction Investigations," Geophysical Prospecting, v. IV, No. 2, pp. 140-166.

Duffy, J. and Mindlin, R. D., "Stress-strain Relations of a Granular Medium," JAM Dec. 1957, p. 585.

Ewing, Wm., Jardetzky, W. S., and Press, F. (1957) "Elastic Waves in Layered Media," McGraw-Hill Book Co., 380 pp.

REFERENCES (continued)

Gassmann, F. (1951) "Elastic Waves through a Packing of Spheres" Geophysics
v. 16, No. 4, Oct. pp. 673-685.

Hamilton, E. L. (1956) "Low Sound Velocities in High Porosity Sediments,"
J. Acoust. Soc. Am. v. 28, 1956, pp. 17-19.

Hamilton, E. L., Shumway, G., Menard, H. W., Shipek, C. J. (1956)
"Acoustic and Other Physical Properties of Shallow-Water Sediments
Off San Diego," J. Acoustical Soc. Am., v. 28, 1956, pp. 1-15

Hara, G. (1935) "Theorie der akustischen Schwingungsausbreitung in
gekörnten Substanzen und experimentelle Untersuchungen an Kohle -
pulver," Elektrische Nachrichten-Technik. Heft 7, Band 12, July,
pp. 191-200.

Hardin, B. O. (1961) Discussion of paper by Richart (1960). J. Soil Mech.
and Found. Div. ASCE, April, pp. 157-158.

Hardin, B. O. (1961) "Study of Elastic Wave Propagations and Damping in
Saturated Granular Materials," Ph D. Dissertation. Dept. of Civil Eng.
Univ. of Fla., Aug. 1961.

Heukelom, W. and Foster, C. R (1960) "Dynamic Testing of Pavements," Proc.
Soil Mech. and Found. Div. ASCE, Feb. pp 1-28

Hsieh, T. K. (1962) "Foundation Vibrations," Proc. of the Institution of
Civil Engineers, June. v. 22, pp. 211-226.

Hvorslev, M. J. (1949) "Subsurface Exploration and Sampling of Soils for
Civil Engineering Purposes," Waterways Exp. Sta. (Obtained through
the Engineering Foundation, 29 W. 39th St., N. Y. 18, N Y.)

Iida, K. (1938) "The Velocity of Elastic Waves in Sand," Tokyo Imperial
University, Bulletin, Earthquake Research Institute. v. 16, pp. 131-144.

Iida, K. (1939) "Velocity of Elastic waves in a Granular Substance," Bull.
ERI, v. 17, pp. 783-807.

Iida, K. (1940) "On the Elastic Properties of Soil Particularly in Relation
to Its Water Content," Bull. ERI, v. 18, pp. 675-690.

Iida, K. (1939) "Determining Young's Modulus and the Solid Viscosity Coef-
ficients of Rocks by the Vibrations Method," Bull. ERI, v. 17, pp. 79-91.

Jensen, J. W. (1959) "Damping Capacity - Its Measurement and Significance,"
U. S. Dept. of the Interior. BuMines Report 5441.

Jones, R. (1958) "In-situ Measurement of the Dynamic Properties of Soil by
Vibration Methods," Geotechnic, v. 8, No. 1, Mar. pp. 1-21.

REFERENCES (continued)

Kessler, C. E., and Chang, T. S. (1957) "A Review of Sonic Methods for the Determination of Mechanical Properties of Solid Materials." Bulletin ASTM, Oct. 1957, pp. 40-46

Knopoff, L. (1952) "On Rayleigh Wave Velocities," Seismological Society of America, Bulletin, v. 42, pp. 207-308.

Knopoff, L. and MacDonald, G. J. F. (1958) "Attenuation of Small Amplitude Stress Waves in Solids," Review of Modern Physics, v. 30, No. 4, Oct. 1958, pp. 1178-1192

Lamb, H. (1904) "On the Propagation of Tremors Over the Surface of an Elastic Solid," Phil. Trans. Roy. Soc. London Series A, v. 208, pp. 1-42.

Laughton, A. S. (1957) "Sound Propagation in Compacted Ocean Sediments." Geophysics, v. 22, p. 233.

Leet, L. Don (1950) "Earth Waves," Harvard U. Press and J. Wiley, p 122.

Love, A. F. H. (1944) "The Mathematical Theory of Elasticity," 4th ed. Dover Publications, New York.

Matsukawa, E., and Hunter, A. N. (1956) "The Variation of Sound Velocity with Stress in Sand," Letter to the Editor. Proc. of the Physical Society. Sec. B, v. 69, part 8, No. 440 B, Aug. pp. 847-848.

Miles, J. W. (1960) "Motion of a Rigid Cylinder Due to a Plane Elastic Wave" J. Acoust. Soc. Amer. 32-12, pp. 1656-1659.

Miller, G. F., and Pursey, H. "On the Partition of Energy Between Elastic Waves in a Semi-Infinite Solid," Proc. Roy. Soc. London, v. 223, Series A, 1955, pp. 56-69.

Mindlin, R. D. (1949) "Compliance of Elastic Bodies in Contact," J. Appl. Mech., v. 16, pp. 259-262.

Mindlin, R. D., and Deresiewicz, H (1953) "Elastic Spheres in contact under Varying Oblique Forces," JAM, Sept. 1953, pp. 327-344.

Mintrop, L. (1911) "Uber die Ausbreitung der von den Massendrucken einer Grossgasmachine erzeuten Bodenschwingungen," Doctoral Dissertation - Gottingen, 32 pp.

Morse, P. M. (1952) "Acoustic Propagation in Granular Media," J. Acoust. Soc. of America, v. 24, No. 6, pp. 696-700.

Murphy, H. L. (1958) "Blast Loading on Structures," J. Struct. Div. Proc. ASCE Nov. 1958, Paper No. 1837, 11 pp.

Nasu, N. (1949) "Field Determination of the Elastic Property of Soil Layers I," Bull. ERI, v. 27, pp. 101-106.

REFERENCES (continued)

Nyborg, W. L., Rudnick, I., and Schilling, H. K. (1950) "Experiments on Acoustic Absorption in Sand and Soil." J. Acoust. Soc. Am. v. 22, No. 4, July, pp. 422-425.

Paterson, N. (1955) "Elastic Wave Propagation on Granular Media," Ph D. Dissertation, Univ of Toronto, Dept. of Physics.

Peselnick, and Outerbridge, W. F. (1961) "Internal Friction in Shear and Shear Modulus of Solenhofen Limestone Over a Frequency Range of 10^7 of Geophysical Research, v. 66, No. 2, Feb. pp. 581-588.

Pickett, G. (1945) "Equations for Computing Elastic Constants from Flexural and Torsional Resonant Frequencies of Vibration of Prisms and Cylinders," Proc. ASTM. v. 45. pp. 846-865. (pp. 864-865 disc.)

Pisarenko, G. S. (1962) "Vibrations of Elastic Systems Taking Account of Energy Dissipation in the Material," Technical Documentary Report No. WADD TR 60-582. Feb. Directorate of Materials and Processes. Aeronautical Systems Division. Air Force Systems Command. Wright Patterson Air Force Base, Ohio.

van der Poel, C. (1948) "Dynamic Testing of Pavements and Base Courses," Proc. 2nd ICSMFE. v. IV, pp. 157-163.

Proceedings of the Symposium on Vibration Testing of Roads and Runways held at Amsterdam, Koninklijke Shell-Laboratorium, April 20-24, 1959.

Rayleigh, L. (1885) "On Waves Propagated Along the Plane Surface of an Elastic Solid" Proc. of the London Mathematical Society, v. 17, pp. 4-11.

Ramspeck, A. and Müller, R. (1936) "Fortschritte der Baugrunduntersuchung," Z VDI, v. 80, p. 1125.

Reiher, H. and Meister, F. J. (1931) "Die Empfindlichkeit des Menschen gegen Erschutterungen," Forsch. Gebiete Ingenieurwesen, v. 2, No. 11, pp. 381-386.

Reissner, E. (1937) "Freie und erzwungene Torsionsschwingungen des elastischen Halbraumes," Ingenieur-Archiv, v. 8, part 4, Aug. pp. 229-245.

Reissner, E. (1936) "Stationäre, axialsymmetrische durch eine schuttelnde Masse erregte Schwingungen eines homogenen elastischen Halbraumes" Ingenieur-Archiv, v. 7, part 6, Dec. pp. 381-396.

Richart, F. E., Jr. (1960) "Foundation Vibrations," J. of Soil Mech. and Found. Div. ASCE, Aug. pp. 1-34.

Sato, Y. (1951) "Distribution of Surface Waves Generating No Rayleigh-Waves," Bulletin, Tokyo University, Earthquake Research Institute, v. 29, pp. 445-453.

REFERENCES (continued)

Seed, H. (1952) "Velocity of Elastic Waves Propagation in Media with Small
    Holes," Bull. ERI v. , pp. 189-190.

    . (1962) "Transmission of Intense Shock Waves into the Earth,"
    Oct. 195 . pp. 257-1262.

Shannon, W. L., Yamane, G., and Dietrich, R. J. (1959) "Dynamic Triaxial
    Tests on Sand," Proc. Mexico City Conf. Soil Mech.

Shumway, G. (1960) "Sound Speed and Absorbtion Studies of Mar. Sediments
    by a Resonance Method - Parts I and II," Geophysics, v. XXV, Nos. 2
    and 3, April and June, 1960, pp. 451-467 (Apr.) and 659-682 (June)

Smoots, V. A., Stickel, J. F., and Fischer, J. A. (1961) Discussion of the
    paper by Richart (1960). J. of the Soil Mechanics and Foundation Div.
    ASCE, April, pp. 158-163.

Steffens, R. J.(1952) "The Assessment of Vibration Intensity and its
    Application to the Study of Building Vibrations," National Building
    Studies. Special Report No. 19 DSIR BRS London.

Sung, T. Y. (1953) "Vibrations in Semi-Infinite Solids Due to Periodic
    Surface Loading," ASTM STP 156 Symposium on Dynamic Testing of Soils,
    pp. 35-64 disc. 64-68.

Taylor, D. W and Whitman, R. V. (1954) "The Behavior of Soils under Dynamic
    Loadings," - 3. Final Report on Laboratory Studies, Aug. MIT Dept. of
    Civil and Sanitary Engr. Soil Mechanics Lab.

Terzaghi, K. (1943) "Theoretical Soil Mechanics," J. Wiley and Sons, 510 pp.

Timoshenko, S. and Young, D. H. (1955) "Vibration Problems in Engineering,"
    D. Van Nostrand Col, Inc. 468 pp.

Ward, W. H., Samuels, S. G., and Butler, M. F. (1959) "Further Studies of the
    Properties of London Clay," Geotechnique, v. IX, No. 2, June, pp. 33-58.

Whitman, R. V., Roberts, J. E. and Mao, S. W. (1960) "One-Dimensional Com-
    pression and Wave Velocity Tests," MIT Report to WES.

Wilson, S. C. and Miller, R. P. (1961) "Discussion of the Paper by Richart,"
    (1960). J. Soil Mech. and Found. Div. ASCE, April, pp. 164-169.

Wilson, S. D. and Dietrich, R. J. (1961) "Effect of Consolidation Pressure
    on Elastic and Strength Properties of Clay," Proc. ASCE Research Conf.
    on Shear Strength of Cohesive Soils. Boulder, Colo. June.

Zwikker, C. and Kosten, C. W. (1949) "Sound Absorbing Materials," Elsevier,
    New York.